UNIVERSITÀ DEGLI STUDI DI MILANO

FACOLTÀ DI SCIENZE E TECNOLOGIE

DIPARTIMENTO DI CHIMICA

DOCTORAL SCHOOL OF CHEMICAL SCIENCES AND TECHNOLOGIES

PhD Course in Chemistry – XXIX cycle

MAGNETIC NANOPARTICLES FOR THE SYNTHESIS OF PHARMACEUTICALLY IMPORTANT MOLECULES

Coordinator: Prof. Emanuela Licandro

Advisor: Prof. Fabio Ragaini

PhD Thesis of:

Lilian M. S. Ansaloni

Matricola n. R10397

Academic Year 2015/2016

Dedication

To my dear husband for believing in my dream.

“A person who never made a mistake
never tried anything new”
Albert Einstein

Acknowledgements

I want to express my sincere gratitude to Prof. Fabio Ragaini for giving me the great opportunity to work in his research group and improve my scientific skills during this PhD thesis. I am grateful for the initial contact in 2013, the excellent project, and the special attention he paid to my bureaucratic issues when I was still in Brazil. Without this initial help, it would have been impossible to come to Italy. During these years in Italy, he has always been available, and I am especially grateful to him because instead of judging during various difficulties, he believed in me and in my determination to overcome the obstacles. I would like to thank him for his scientific advice and the chance to work under his supervision, which allowed me to conclude this work. For me, this was a great scientific and personal experience.

I am also grateful to Dr. Francesco Ferretti for helping me during my PhD; thanks for sharing your scientific knowledge, patience, support, and teaching over the years. I'll never forget!

I want to thank everyone who supported me during my work in Italy, especially Dario Formenti and Mohamed El-Atawy.

Thanks to the research group, Prof. Emma Gallo, Prof. Alessandro Caselli, and other students who have been part of my routine, Claudia Gatti, Daniela Carminati, Daniela Intrieri, Edoardo Barraco, Flavia Roncalli (in memory), Giorgio Tseberlidis, Roberta Gini, Stefano Ferrari, Abhijnan Sarkar, and especially Andrea Pichmeo, and all the other students involved.

Thanks to The University of Milan, especially to Prof. Emanuela Licandro, PhD program director, and to Dr. Egill Boccanera from the International Office.

I would also like to thank the technicians, Americo Costantino, Mario Rosa, and Pasquale Illiano for their help with analysis.

Special thanks go to my family, especially my dear parents. Thank you, my dear siblings, my in-laws, my cousins, my dear nephews, nieces, and friends, and all that endured my absence.

I also wish to thank my husband for everything he has done for me over these years, for his daily presence and unconditional support, both in the happy moments and the hard ones.

Thanks to Brazil, especially CAPES Process: BEX 5963-13-3 for a scholarship, which was essential for achieving my dreams and giving me the opportunity to broaden my scientific knowledge. Thanks to all the technicians and analysts from CAPES for their excellence over the years.

Finally, I would like to thank God for always being by my side.

Agradecimentos

Gostaria de expressar minha sincera gratidão ao Prof. Fabio Ragaini pela grande oportunidade de trabalhar no seu grupo de pesquisa e assim ajudar a aprimorar meus conhecimentos científicos.

Sou grata a ele desde 2013 pelo contato inicial, excelente projeto e especial atenção durante as minhas práticas burocráticas enquanto ainda estava no Brasil. Sem essa parte inicial não teria sido possível vir para Itália. Aqui na Itália durante todos os anos ele foi sempre disponível e sou especialmente grata porque ao invés de julgar algumas dificuldades ele foi capaz de acreditar em minha determinação para vencer os obstáculos. Gostaria de agradecer pelos seus conselhos científicos e pela possibilidade de trabalhar sob sua supervisão que me permitiu concluir este trabalho, foi uma grande experiência científica e pessoal.

Também dedico minha gratidão ao Dr. Francesco Ferretti, por ter me ajudado, por dividir seus conhecimentos científicos, paciência, apoio e ensinamentos ao logo dos anos. Jamais esquecerei!.

Quero agradecer a todos que me apoiaram durante o meu trabalho na Itália, especialmente Dario Formenti e Mohamed El-Atawy.

Obrigada ao grupo de pesquisa da Prof. Emma Gallo e do Prof. Alessandro Caselli e os estudantes que fizeram parte da minha rotina, Claudia Gatti, Daniela Carminati, Daniela Intrieri, Edoardo Barraco, Flavia Roncalli (in memory), Giorgio Tseberlidis, Roberta Gini, Stefano Ferrari, Abhijnan Sarkar e, especialmente, Andrea Pichmeo e todos os outros alunos envolvidos.

Obrigada a Universidade de Milão, especialmente a Prof. Emanuela Licandro diretora do Programa de Doutorado e ao Dr. Egill Boccanera do Escritório Internacional.

Gostaria também de agradecer aos técnicos, Américo Costantino, Mario Rosa, Pasquale Illiano, pelas ajudas durante as análises.

Faço um agradecimento especial à minha família, especialmente meus queridos pais, obrigado meus queridos irmãos, meus sogros, cunhados, primos, meus queridos sobrinhos, sobrinhas, amigos e todos os que suportaram a minha ausência.

Gostaria também de agradecer ao meu marido por tudo que ele fez por mim ao longo destes anos, a sua presença diária e apoio incondicional tanto nos momentos felizes e os difíceis.

Obrigada ao Brasil, especialmente a CAPES Processo: BEX 5963-13-3 pela bolsa concedida que foi essencial para alcançar meus sonhos e por ter me dado a oportunidade de ampliar meus conhecimentos científicos. Obrigada a todos os técnicos e analistas da CAPES pela excelência ao longo dos anos.

Finalmente, gostaria de agradecer a Deus por estar sempre ao meu lado.

List of Abbreviations

atm	atmosphere
dppp	1,3-bis(diphenylphosphino)propane
°C	degrees Celsius
Cat.	catalytic or catalyst
Conv.	Conversion
DCM	dichloromethane
DMF	*N*,*N*-dimethylformamide
DMSO	dimethyl sulfoxide
DNA	deoxyribonucleic acid
EDG	electron-donating group
EDTA	ethylenediaminetetraacetate
e.g.	for example or example given
Equiv.	Equivalent
EWG	electron-withdrawing group
Fe_3O_4	ferrite
FT-IR	Fourier transform infrared spectroscopy
g	gram
GC	gas chromatography
GC/MS	gas chromatography-mass spectrometry
h	hours
Lig.	ligand
LDA	lithium diisopropylamide
maghemite	γ-Fe_2O_3
MeCN	acetonitrile
4-MePhen	4-methyl-1,10-phenanthroline
4-MeO-Phen	4-methoxy-1,10-phenanthroline
4-OH-Phen	4-hydroxy-1,10-phenanthroline
mg	milligram
mL	milliliter

mmol	millimole
MNPs	magnetic nanoparticles
M.W.	molecular weight
nd	not detected
Neoc	neucuproine
NMR	nuclear magnetic resonance
$Pd(OAc)_2$	palladium(II) acetate
Phen	1,10-phenanthroline
ppm	parts per million
RT	room temperature
Sel.	selectivity
SPION	superparamagnetic iron oxide nanoparticles
Temp.	temperature
TEM	transmission electron microscopy
THF	tetrahydrofuran
TLC	thin-layer chromatography
PPh_3	triphenylphosphine
UNIMI	Università degli Studi di Milano
w/o	water-in-oil

Abstract

In recent years, the scientific community has been concerned with the development of ecofriendly strategies in several fields, including catalysis. Many studies have been performed that focus on the use of the special properties of ferrite nanoparticles. As a support, the small size of these particles allows their thorough dispersion in the reaction media, thus nearing the homogeneous environment of a soluble catalyst. At the same time, their magnetic properties allow easy recovery of the catalyst at the end of the reaction.

The synthesis of MNPs described in this work used a coprecipitation method that exhibited reproducibility because several parameters were controlled, such as temperature, pH, and component addition. In particular, owing to the possibility of aggregation, protection of the nanoparticles was carried out. Several acids described in the literature were examined, but owing to the possibility of improved catalytic properties, the MNPs were functionalized with 10-bromodecylphosphonic acid (protective layer), which bears a halogen in the ω-position to allow further modification.

The important feature of this work was demonstrated by several attempts to immobilize phenanthroline (4-MePhen and 4-OH-Phen) on the protective layer, and the success of these developed strategies is discussed. Immobilization was verified by IR spectroscopy following the formation of new complexes with molybdenum hexacarbonyl $Mo(CO)_6$.

$Pd(OAc)_2$ was then coordinated to phenanthroline immobilized on the protective layer, and finally catalytic tests were performed for strategic reactions that are interesting from the pharmaceutical point of the view, such as carbonylation and reductive cyclization reaction of *o*-nitrostyrenes to give indoles. The catalysis results obtained by employing these strategies were encouraging, but the recycling process was problematic, probably due to metal leaching during catalysis.

Oxidative Heck reactions were also performed using MNPs developed using these strategies. The results demonstrated the importance of tests in the homogeneous phase, which allowed the use of the best conditions with MNPs. Owing to the reagent employed (styrene), the catalysis results suggested the possibility of polymerization and so need future investigation.

General Introduction

Nanotechnology is a field of science that has undergone great growth in the last 20 years, especially in areas such as chemistry, pharmaceuticals, and biology, promoting innovation and technological progress.

Materials employed in nanotechnology have at least one dimension between 1 and 100 nanometers (nm) and usually contain from several hundreds to 10^5 atoms.[1] Many studies have demonstrated that several properties change completely in the nanometer regime, with the observation of low Curie temperatures, high magnetic susceptibilities, and high electrical conductivities, as well as the appearance of the superparamagnetism phenomenon.[2-4]

MNPs have various important applications in fields such as biomedicine,[5] environmental applications,[6] and catalysis.[7] Ferrite nanoparticles have been widely studied owing to their interesting magnetic properties and relatively low cost. In catalytic reactions, these materials have often been used as a support both for heterogeneous metallic catalysts and for heterogenized homogeneous catalysts. The use of ferrite nanoparticles in catalysis is attractive owing to their high surface area, high strength, and ease of recycling. Moreover, these MNPs are easily recovered, nontoxic, and widely available. This particular application is possible because MNPs have a very small size distribution.

The synthesis of ferrite nanoparticles requires several parameters to be controlled during the synthesis, such as pH value, type of salt used, ratio of ferric and ferrous ions, reaction temperature, and reaction temperature during the protective phase. Unfortunately, these nanoparticles tend to aggregate to achieve thermodynamic stability, resulting in a drastic reduction of the surface area. To prevent unwanted aggregation, the ferrite cores are coated with suitable capping agents able to interact with the nanoparticles by a functional group and allowing dispersion in an organic solvent. In general, these binders contain terminal phosphonic acid, polyethylene glycol, or carboxylic acid groups, or other molecules or complexes that can bind strongly to the surface of MNPs. The immobilization process is successful when a delicate balance of forces is achieved between the molecules to be grafted and the substrate surface.[8,9]

Phenanthroline is a very versatile compound that is commonly used in coordination chemistry. For years, our research group has examined applications of phenanthroline in catalysis.[10,11] Specifically, in this work, our strategy consisted of preparing ferrite nanoparticles capped with a suitable protective layer that makes them hydrophobic, functionalization of the nanoparticles by

covalently attaching a phenanthroline derivative, and finally coordination of palladium to test our strategy in organic synthesis reactions, such as cyclization of nitrostyrenes to indole groups and oxidative Heck reactions.

Cyclization of *o*-nitrostyrenes has long been known, but recently Davies and coworkers succeeded in obtaining the desired products under relatively mild conditions using palladium/phenanthroline complexes as catalysts.[12] Among the various compounds of pharmaceutical interest, indoles were chosen as the initial targets. Indeed, the indole skeleton is present in several pharmaceuticals, e.g., vincristine (anticancer), pindolol (antihypertensive), and indomethacin (anti-inflammatory).

Oxidative Heck reactions were used as another strategy to test our system because the synthesis conditions in the presence of dioxygen are less harsh when compared with the use of carbon monoxide in the synthesis of indoles, which makes these reactions attractive from the experimental point of view. The phenanthroline ligands are able to promote the interaction between palladium and dioxygen in a Pd(0)/Pd(II) redox cycle under open air.[13]

References

[1] B. Issa, I. M. Obaidat, B. A. Albiss, Y. Haik, *Int J Mol Sci*, **2013**, 14, 21266-21305.

[2] Y. Qiang, J. Antony, A. Sharma, J. Nutting, D. Sikes, D. Meyer, *J. Nanopart.Res*, **2006,** 8, 489-496.

[3] M. Knobel, W. C. Nunes, L. M. Socolovsky, E. DeBiasi, J. M. Vargas and J. C. Denardin, *J.Nanosc.Nanotechnol*, **2008**, 8, 2836-2857.

[4] W. Wu, Q. He, C. Jiang, *Nan Res Lett*, **2008,** 3, (11), 397-415.

[5] Murbe J, A. Recthenbach, J. Topfer, *Mater. Chem.Phys*, **2008**, 110, 426-433.

[6] Y. Sun, X. Li, X. J. Cao, W. Zhang, H. P. Wang, *Adv. Colloid Interface Sci*, **2006**, 120, 47-56.

[7] D. Wang and D. Astruc, *Chem. Rev*, **2014**, 114, (14), 6949-6985.

[8] B. Kaboudin, F. Kazemi and F. Habibi, *J. Iran. Chem. Soc*, **2015**, 12, 469-475.

[9] S. Laurent, D. Forge, M. Port, A. Roch, C. Robic, et al, *Chem Rev*, **2008,** 108, 2064-2110.

[10] F. Ragaini, F. Ventriglia, M. Hagar, S. Fantauzzi, S. Cenini, *Eur. J. Org. Chem*, **2009**, 2185-2189.

[11] F. Ferretti, F. Ragaini, R. Lariccia, E. Gallo, and S. Cenini, *Organometallics*, **2010**, 29, (6), 1465-1471.

[12] I. W. Davies, J. H. Simitrovich, R. Qu. Sidler, R. V. Gresham, C. Bazaral, *Tetrahedron*, **2005**, 61, (26), 6425-6437.

[13] P. A. Enquist, J. Lindh, P. Nilsson and M. Larhed, *Green Chem*, **2006**, 8, 338-343.

Chapter 1: Magnetic Nanoparticles and Their Preparation

Introduction

1.1 Magnetic materials

Magnetic materials can be classified into five main types: ferromagnetic, paramagnetic, diamagnetic, antiferromagnetic, and ferrimagnetic, according to the arrangement of their magnetic dipoles when an external magnetic field is applied.[1,2] Figure 1 shows schematic diagrams of these five different types of materials.

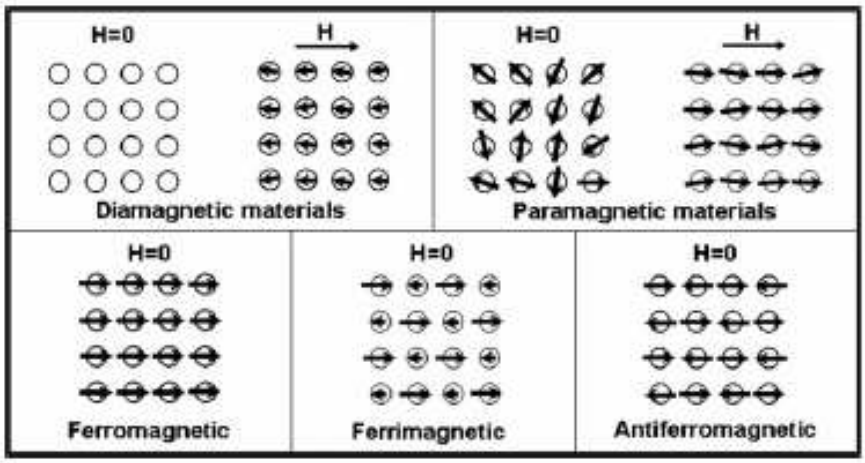

Figure 1: Schematic illustration of the five types of magnetic materials in the absence or presence of an external magnetic field (H).[1]

Ferromagnetism: Ferromagnetism occurs in materials that have permanent magnetization, resulting from the natural tendency to align the moments of atoms or molecules. The alignment is perfect in regions called domains. Ferromagnetic domains are small regions where dipoles are aligned parallel to each other. When a ferromagnetic material is in its demagnetized state, the magnetization vectors have different orientations and the total magnetization averages to zero.

An important feature of ferromagnetic materials is hysteresis. A hysteresis loop (induced magnetic flux density and the magnetizing force) is illustrated in Figure 2. When a large magnetic

field is applied, the spins become aligned with the field. The maximum magnetization value is called saturation. On the other hand, when the magnitude of the magnetic field decreases, spins cease to be aligned with the field and the total magnetization decreases. The loop represents the measurement of the magnetic flux of the material. A coercivity force occurs when an inverse magnetic field is applied to a material causing its flow to return to zero. Several years ago, Frenkel and Dorfman realized that particles of ferromagnetic materials with sizes below a critical value could exhibit different behavior and thus lead to high magnetization.[3]

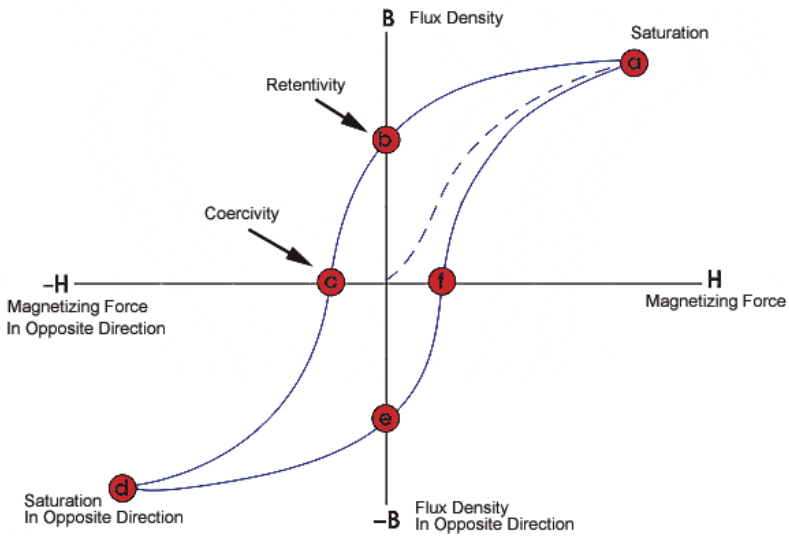

Figure 2: Illustration of a hysteresis cycle.[4]

Paramagnetism: Paramagnetism occurs in materials that have unpaired electrons. In paramagnetic materials, as the coupling between the magnetic moments is weak, it is subject to thermal changes around the alignment field. When a magnetic field is applied, the moments start to align, but only a small fraction of them are deflected into the field direction for all practical field strengths. Many salts of transition elements are paramagnetic. A ferromagnetic material becomes paramagnetic above their Curie temperature, when the thermal energy is enough to overcome the order of the magnetic moments.

Diamagnetism: Diamagnetism is associated with the magnetic dipole moments of electrons in atomic or molecular orbitals. Therefore, it is present to a greater or lesser degree in all substances.

However, in most cases, the intensity is very low and the presence of diamagnetism is masked by other phenomena. If a material does not have a magnetic dipole in the absence of an external field, but this condition changes in the presence of a magnetic field, it can be considered as a diamagnetic material. In a superconductor, the intensity of diamagnetism is so strong that the resulting magnetic field inside the sample is zero.

Antiferromagnetism: In antiferromagnetic materials, the interaction between the magnetic moments tends to result in the alignment of adjacent moments antiparallel to each other. Antiferromagnets have no net spontaneous magnetization, and their response to external fields at a fixed temperature is similar to that of paramagnetic materials.

Ferrimagnetism: Ferrimagnetism is a property exhibited by materials (such as Fe_3O_4 and γ-Fe_2O_3) whose atoms or ions tend to assume an ordered but nonparallel arrangement in a zero applied field below a certain characteristic temperature, known as the Neel temperature.

In bulk materials, magnetic properties are characterized using parameters such as coercivity (H) and susceptibility (χ), which depend on composition, crystallographic structure, vacancies, and defects. In the case of MNPs, the size and shape must also be considered to determine magnetic behavior.[5]

Owing to the small dimensions of MNPs, it is important to understand the superparamagnetic phenomenon. This phenomenon occurs when the dimensions of the magnetic domains generated by an external magnetic field are small. As a consequence, once the external magnetic field is removed, thermal fluctuations misalign the spins and no net magnetization remains.[6] This phenomenon can be understood from the plot shown in Figure 3. As the particle size decreases, multidomains (MDs) start to form a single domain (SD), with the diameter that coincides with the conversion of MDs to a SD represented as Ds. Each magnetic domain possesses independent directionality, which results in a decrease in the magnetic coercivity (Hc), which falls to about zero (remaining magnetization) for superparamagnetic particles at diameter Dp (Figure 3). This property of remaining magnetization prevents agglomeration.

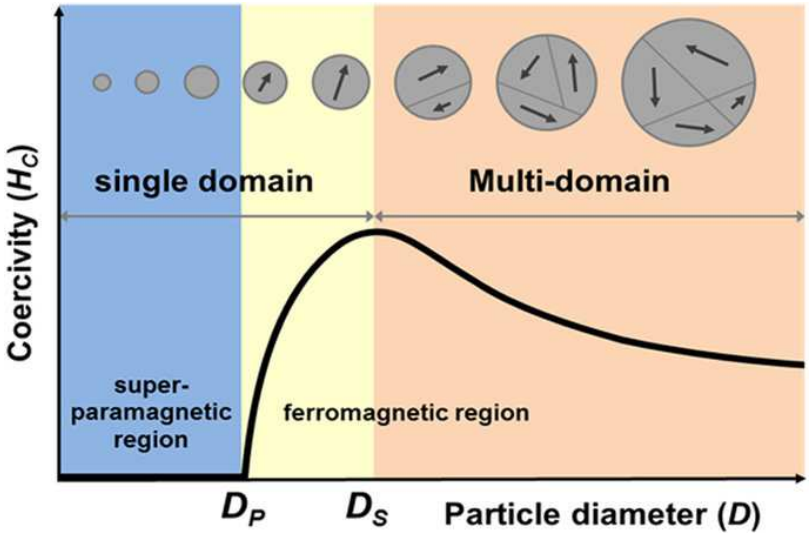

Figure 3: Plot of magnetic coercivity versus particle size.[2]

1.2 Fundamental features of MNPs

The literature,[7,8] including a recent review about MNPs in 2016,[3] explains the importance of parameters such as particle size, structure, shape, and composition for characterizing MNPs, as summarized in Figure 4.

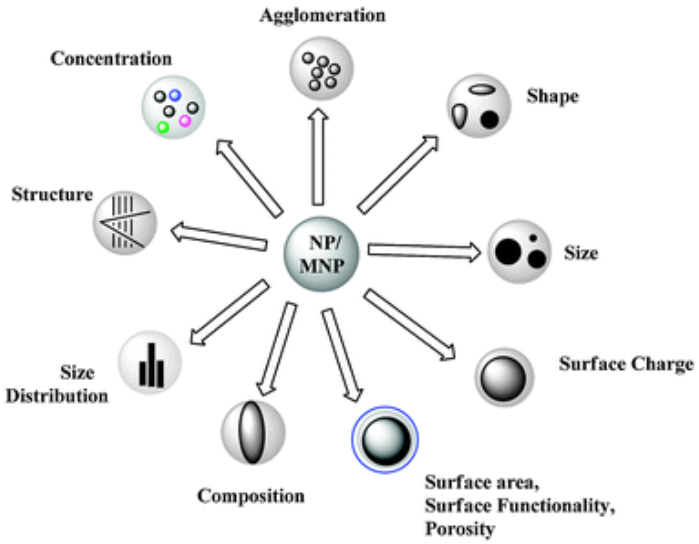

Figure 4: Important MNPs features.[8]

Briefly, the most prominent features are:

Size effects: Magnetic properties are highly dependent on the size of nanoparticles. When the size is below a certain critical value, the spins of free electrons within MNPs are aligned by

ferromagnetic coupling into only one direction, resulting in a single-domain magnet, as explained previously. In large magnetic particles, a multidomain structure is predominant. The presence of external magnetostatic energy is directly responsible for domain formation and increases with the interfacial area between domains.

Structure and shape effects: The crystalline structure determines the frontier size between multidomains and monodomains. Generally, a larger anisotropy constant results in larger coercivity. Spherical MNPs have no shape anisotropy owing to their isotropic structure, and they exhibit smaller coercivity.

Composition effects: In the ferrite Fe_3O_4 structure, O anions form a close-packed fcc structure, with Fe ions located at interstitial octahedral (O) or tetrahedral (T) sites. Composition control in MNPs is important not only for the magnetization value but also for the coercivity parameters.

Surface charge: A MNP surface can be positively or negatively charged depending on the pH. Consideration of this feature is very important during synthesis owing to the necessity of stabilizing the prepared material. Repulsion between nanoparticle with the same charge prevents agglomeration and the formation of larger aggregates.

1.3 Ferrite structure

Ferrite materials are characterized by the composition MFe_2O_4, where M = metal. When M = Fe, "magnetite" (common name for the mineral) or "ferrite" (common name for the synthesized compound) is obtained with the formula Fe_3O_4. The framework of oxygen atoms creates two types of coordination sites with tetrahedral and octahedral geometries (called A- and B-sites, respectively). In the case of metal cations tetrahedrally coordinated by oxygen, a spinel structure containing two sites for metal cations is obtained, and this configuration is expected to have 8 A-sites. In the case of octahedral coordination, a configuration with 16 B-sites is expected. The normal spinel configuration is obtained when the A-sites are occupied by M^{2+} cations and the B-sites are occupied by Fe^{3+} cations. On the other hand, if the A-sites are completely occupied by Fe^{3+} cations and the B-sites are randomly occupied by M^{2+} and Fe^{3+} cations, an inverse spinel structure is obtained. In the case of ferrite materials, magnetite Fe_3O_4, $NiFe_2O_4$, and $CoFe_2O_4$ have inverse spinel structures with eight formula units per unit cell. Fe^{3+} cations are located half in the

tetrahedral and half in the octahedral sites, while Fe^{2+} cations occupy the remaining octahedral sites, as shown in Figure 5.[9]

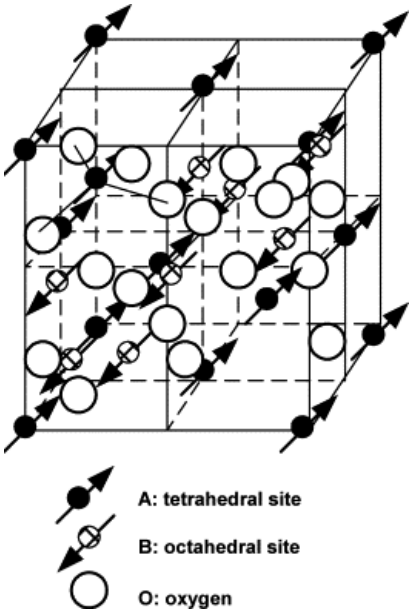

Figure 5: Schematic view of a partial unit cell and ferrimagnetic ordering of a spinel ferrite structure.[9]

1.4 Applications of MNPs

In biomedicine, MNPs and (SPION or Fe_3O_4) have several uses, e.g., as potential materials for drug delivery,[10,11] gene delivery,[12] biosensors,[13] hyperthermia,[14] and contrast agents for magnetic resonance imaging.[15] In the case of biomedical applications, high saturation magnetization (M_S) of the MNPs is desirable to exploit the magnetic properties. Figure 6 shows the application of MNPs as targeted drug carriers.

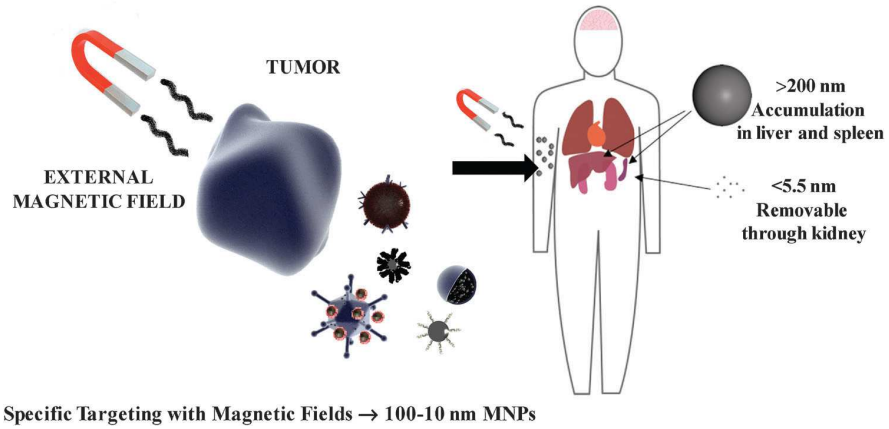

Figure 6: Biomedical applications of MNPs.[5]

In environmental applications, MNPs can be used for remediation and water treatment owing to the possibility of selective removal of the hazardous metal ions from complicated matrices. MNPs have an excellent ability to remove high concentrations of organic compounds. The most widely used MNPs in such applications are nano zero-valent iron (nZVI), magnetite (Fe_3O_4), and maghemite (γ-Fe_2O_3) nanoparticles.[16]

In catalysis applications, MNPs can be used in several reactions because they possess special characteristics that allow for recycling and reuse, as shown in Figure 7. Thus, MNPs have become a very attractive tool in catalysis. Several years ago, catalysis studies were focused on achieving good activities and selectivities, but in recent years, "green chemistry" has become an important factor to be considered to address ecological and economical demands. Several uses of MNPs in catalysis have been described in recent reviews,[17] including their use in organic chemistry in reactions such as Suzuki coupling, Heck, Sonogashira coupling, Stille coupling, hydroformylation,[18] hydrogenation,[19] and polymerization reactions.[20]

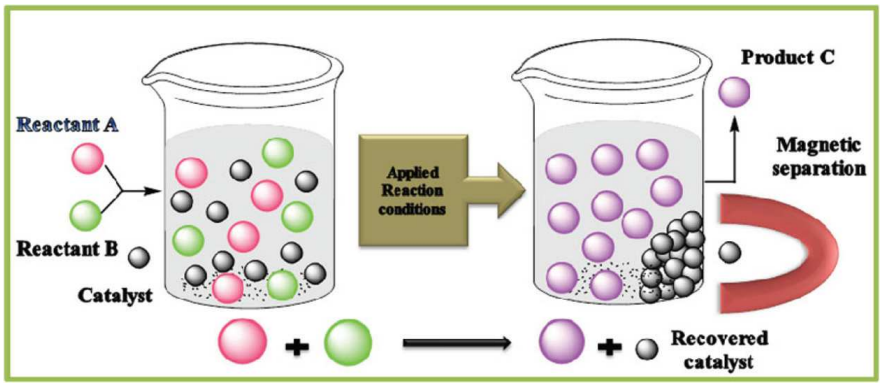

Figure 7: Catalytic applications of MNPs.[17]

1.5 Synthesis of MNPs

Successful preparation of MNPs is directly related to several factors, including control of the size, shape, agglomeration, composition, and surface chemistry of the nanoparticles, as explained previously. There are several protocols in the literature for the synthesis of MNPs, such as microemulsion,[21,22] thermal decomposition,[23,24] coprecipitation,[25-27] template-mediated synthesis,[28] sonochemical technique,[29] and continuous flow reaction.[30] The most common methods are described in the following sections.

1.5.1 Microemulsion

Microemulsion as a general concept refers mixtures of oil, water, and surfactant, which can be employed in the preparation of MNPs using a single-phase system. In this case, an appropriate surfactant needs to be chosen. Surfactant molecules decrease the interfacial tension between the two components: water and oil (W/O). However, even in the presence of surfactants, preventing aggregation in this procedure usually requires several washing processes and further stabilization. By controlling the water content, type of solvent, and concentration of surfactant in solution, the nanoparticle dimensions can be tuned. Surfactants that have been employed in the literature include dioctyl sodium sulfosuccinate[31] and sodium dodecyl sulfate.[32] The disadvantage of this synthesis procedure is that surfactant present in the final medium, even in the smallest quantities, canalter the properties of the final material.

1.5.2 Thermal decomposition

The synthesis procedure is based on the thermal decomposition of organometallic precursors at high temperatures in organic solvents in the presence of surfactants.Surfactants that have been employed include oleic acid, oleylamine, and hexadecylamine. Heyon[33] used this route to synthesis MNPs by employing $Fe(CO)_5$ at 100 °C in the presence of oleic acid. In other study, Sun and Zeng[34] reported the thermal decomposition of $Fe(acac)_3$ at 265 °C in diphenyl ether in the presence of surfactants such as oleic acid and oleylamine. Lee et al.[35] prepared polyvinylpyrrolidine-coated iron oxide nanoparticles by thermal decomposition of $Fe(CO)_5$. Although the thermal decomposition method has the advantages of producing highly monodisperse particles with a narrow size distribution, the resulting MNPs exhibit lower dissolution abilities in polar solvents.

1.5.3 Coprecipitation

The most common method for obtaining Fe_3O_4 or Fe_2O_3 is coprecipitation. This method consists of mixing ferric and ferrous ions in a 1:2 molar ratio in highly basic solutions at RT or at elevated temperatures. In this synthetic procedure, ferric and ferrous hydroxides are precipitated by the addition of a base (NH_4OH or NaOH) to a solution of Fe^{3+} and Fe^{2+} inorganic salts (eq. 1).

$$Fe^{++} + 2Fe^{+++} + 8OH^- \longrightarrow Fe_3O_4 + 4H_2O$$

(Eq.1)

Success in this method depends on the type of salt used (e.g., chlorides, sulfates, nitrates, and perchlorates), the ratio of ferric and ferrous ions, the reaction temperature, the pH value, the ionic strength of the media, and other reaction parameters (e.g., stirring rate and dropping speed of basic solution), as discussed in detail in the following sections.

1.6 Protection methods

MNPs have a high energy associated with their superficial area and, for this reason, have a tendency to agglomerate. This behavior is not desirable in several applications, including catalysis. Another problem concerns the interaction of MNPs with dioxygen under atmospheric conditions. In the case of oxidation, the formation of a thin layer of oxides leads to a loss or decrease of several properties. For this reason, the MNP synthetic procedure must afford nanoparticles with long-term stability. Strategies in the literature concerning the use of protection agents involve surfactants, polymers, or an inorganic layer, such as silica or carbon.[36]

Silica is the most popular inorganic coating material for MNPs because it is easy to functionalize. Moreover, it has several advantages including improving the stability of MNPs in solution, avoiding agglomeration of MNPs, and improving the biocompatibility of MNPs.

In the case of polymers, two processes exist for coating MNPs: in situ polymerization or grafting of polymers onto MNPs via coordination, hydrophobic interactions, or electrostatic interactions. Other alternatives include the encapsulation of MNPs in various solid supports, such as mesoporous materials, graphene, or carbon nanotubes, and oxidation of a pure single-metal or nonmetal shell, such as gold, silver, platinum, palladium, iron, or carbon.

Figure 8 shows several possibilities for the protection of MNPs. In the case, of catalysis applications, several studies demonstrated the use of a coating with strategies targeted at performing catalytic reactions. For example, for a Sonogashira reaction, Zolfigol et al.[37] employed a silica coating and then functionalized the coated MNPs with palladium complexes. Naeimi et. al[38] functionalized the surface of silica-coated MNPs with sulfonic acid and then employed this nanocomposite to synthesize 1,8-dioxooctahydroxanthene derivatives. Seidi and coworkers[39] employed a functionalized poly(ionic liquid) to coat Fe_3O_4 nanoparticles, which were then used for the deprotection of acylals.

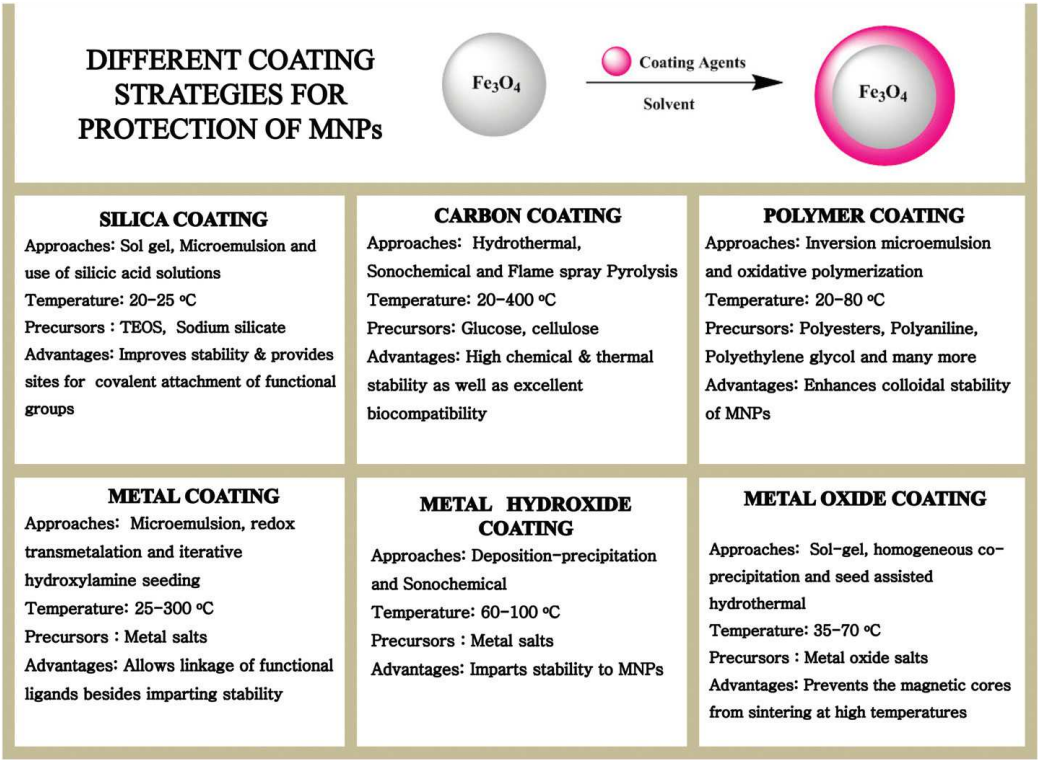

Figure 8: Protective strategies developed for stabilizing MNPs.[17]

Results and Discussion

1.7 Synthesis and protection of ferrite MNPs

Ferrite nanoparticles with diameters of less than 20 nm are not readily available in large amounts or at a reasonable cost. For these reasons, we developed a procedure for the synthesis and subsequent protection of such nanoparticles to avoid aggregation and facilitate the functionalization step.

The synthetic procedures reported in most papers attempt to control the size of nanoparticles by controlling the rate of the nucleation and growth steps (a kinetic approach: nucleation speed vs. particle growth speed). This method is based on carrying out the chemical reaction in a monophasic aqueous medium under an inert atmosphere, which allows both the nucleation and growth of iron hydroxide nuclei to be controlled. In the absence of stabilizing factors, the formation of massive particles and aggregation are always favored. The classical model of burst nucleation and growth proposed by LaMer and Dinegar is depicted in Figure 9.

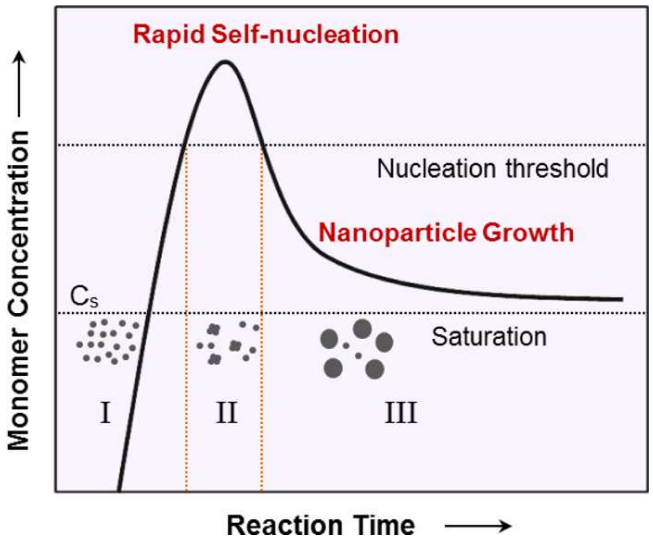

Figure 9: LaMer model of nucleation and growth processes for monodisperse MNPs.[3]

This process can be explained as a balance of the three phases. The first phase consists of the formation of nuclei when the concentration of monomers increases. Burst nucleation in phase II starts to form nuclei, resulting in a rapid decrease of the monomer concentration. When the

concentration falls to a level below the nucleation threshold in phase III, no new nuclei form and growth begins. During syntheses employing the kinetic nucleation speed approach, the process of nucleation and growth, precise control of the parameters involved, such as stirring speed and the presence of impurities, is required to avoid aggregation and maintain a uniform rate of growth.

A different approach has been reported in which the nanoparticle size is controlled by the solution pH. The particle size is influenced by the precipitation pH, with particles becoming smaller with increasing pH. This phenomenon is the result of surface tension and electrostatic repulsion. Every ferrite nanoparticle is negatively charged (deprotonated) to a certain extent, depending on the solution pH. As fusing two negatively charged particles results in a lower total surface area, this would cause increased electrical repulsion between the charges on the particles. Thus, there are two opposing tendencies. On one side, larger particles are thermodynamically more stable than smaller ones; on the other, negative charge is best distributed over many small particles than over a few larger ones. Balancing these two tendencies results in nanoparticles that are small at higher pH and increasingly large as the pH is lowered. In this case, the size control mechanism is a "thermodynamic approach" (a trade-off between surface tension and electrostatic repulsion), as it results in an equilibrium situation and does not depend on the rate of addition or any reaction involved.

Our research group decided that this approach would allow easier promotion of reproducible results and scale up. Changing the solution pH, even after the nanoparticles have been prepared, results in a change in their dimension, but the process is very slow and takes a longer time than required for our standard work up procedure. According to the literature, working at a pH between 12 and 13 should provide particles with diameters of 2 nm, but under these conditions, we obtained reproducible particles with average diameters of 2.8–4 nm, as demonstrated by TEM analyses. In our procedure, after their synthesis, the particles are separated by centrifugation, washed until the pH of the solution is 10, and then dispersed in water.

Control of the pH is also important during the capping stage with carboxylic acids. Indeed, the interaction between carboxylate ions and the ferrite surface is ionic and, to be effective, needs positively charged particles. For this reason, it is necessary to work at a slightly acidic pH to allow efficient coordination of the acid to the particle surface. In general, our research group works with aqueous solutions at pH 5–6 that are left under stirring.[40] Our group has introduced a new protocol for the protection of the nanoparticles in which a biphasic medium water/chlorinated organic solvent is employed and the particles pass into the organic phase over a time that depends on the

identity of the acid used. During acidification, the ferrite isoelectric point (pH_{pzc}) must be exceeded without protonating the carboxylate anions.

Different isoelectric points are reported in several studies at pH 6,[41] 6.3,[42] 6.8,[43] 7.2,[44] or even 7.9.[45,46] Thus, it should be considered that the magnetite origin (e.g., natural or heated at high temperature after RT synthesis) is not negligible, as small changes could have a significant effect. For example, the particles reported in ref. [46], for which pH_{pzc} = 7.9 was measured, were synthesized as reported in ref. [41], but for the latter pH_{pzc} = 6 was measured. There are some minor differences in the two preparations, as the particles were washed with a solution of NaCl in the former case[46] and with a solution of $NaClO_4$ in the latter.[41] The particles obtained using this strategy disperse very well in organic solvents. Nevertheless, chloride ions can coordinate iron effectively. As the interaction between ferrite and carboxylate ions is ionic, the presence of ions on the surface could neutralize superficial positive charges and inhibit the interaction with carboxylate ions. We can approximate that for each superficial chloride ion there is one less bound carboxylate ion. In fact, by destroying particles with HNO_3, precipitating chloride by addition of $AgNO_3$, and quantifying it gravimetrically, we found that chloride ions account for 1.06% of the particle weight. As the amount of absorbed carboxylic acid on the same particles is 24.45% (w/w), the molar acid/chloride ratio is 3.10, which means that there is one chloride ion for every three carboxylic acid molecules. Therefore, the presence of chloride ions has a negative and nonnegligible effect.

To minimize the presence of chloride ions, the procedure was modified to use $Fe(ClO_4)_2$ and $Fe(NO_3)_3$ as starting materials and to acidify with $HClO_4$, as shown in eq. 2. Maintaining the same synthetic procedure, the use of new reagents did not result in any change in the nanoparticle dimensions. In addition, in the washing procedure to promote particle separation, we used $NaClO_4$. This addition was necessary during the washing procedure owing to an increasing difficulty in nanoparticle separation with successive washing steps, likely owing to a variation in the concentration of ions in solution. Indeed, in this synthesis stage, particles are negatively charged and have the tendency to repel each other. Ions act to shield this repulsion among particles, but washing steps remove counterions, inducing particles repulsion and making separation more difficult. Therefore, addition of $NaClO_4$ during the washing procedure provides a certain amount of ions to shield the nanoparticle charge, avoiding repulsion. Chloride must also be avoided in this case to prevent its coordination on the particle surface.

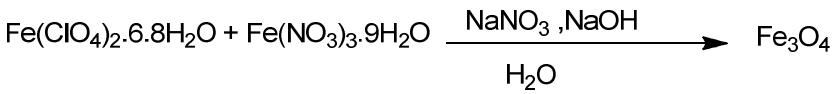

(Eq.2)

As an alternative to carboxylic acids, phosphonic acids can also be employed. In this case, acidification by another acid is not required, apparently because the phosphonic acid is acidic enough to protonate ferrite.

In my synthesis, the ferrite nanoparticles were prepared in aqueous solution by coprecipitation of $Fe^{II}(ClO_4)_2$ and $Fe^{III}(NO_3)_3$ salts by addition of NaOH, at controlled pH and ionic strength conditions. The dispersion was then treated with a solution of protecting agent (10-bromodecylphosphonic acid) in dichloroethane and methanol. In my thesis, we solved the problem of the low solubility of phosphonic acid in dichloroethane by adding a small quantity of methanol to increase the polarity minimally. This was an interesting factor to resolve, as the protection level of the obtained nanoparticles was increased.

Particle protection was performed without acidifying with 1.17 M $HClO_4$ (10.9%). Moreover, we found that the amount of phosphonic acid bound to the particles was larger (2.5 times higher) than the amount of bound carboxylic acid in previous experiments. Thus, the influence of the amount of acid employed on the level of particle protection was investigated by varying the phosphonic acid/Fe^{II} molar ratio between 1.0 and 1.6. When the molar ratio was over 1.2, the amount of bound phosphonic acid decreased, but adding more (molar ratio of 2) or less (molar ratio of 0.5) phosphonic acid was not effective. Therefore, the best molar ratio of phosphonic acid was found to be 1:1.2.

1.8 Protection of ferrite nanoparticles

Ferrite nanoparticles do not exhibit good stability under ambient conditions, as shown in eq. 3. Oxygen causes the oxidation of iron ions, affecting the desired stoichiometric ratio of Fe^{II}/Fe^{III}. Oxidation turns magnetite into maghemite (Fe_2O_3), resulting in a general loss magnetism and decreased dispersibility of the nanoparticles. Moreover, if nanoparticles are left unprotected, they show a tendency to aggregate. For these reasons, the protection procedure must be carried out in the shortest time possible after nanoparticle synthesis. Further, coprecipitation and all other stages are performed under an inert atmosphere to avoid the formation of byproducts.

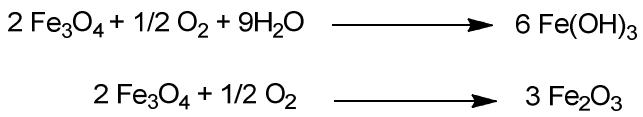

(Eq.3)

The available protection strategies described previously consist of grafting or coating nanoparticles with organic species, including surfactants or polymers, or with an inorganic layer, such as silica or carbon. In our group, particle protection is generally performed using 11-bromoundecanoic acid in dichloroethane. Several important tests were performed using this acid, as described in the following sections.

1.8.1 Temperature effect during protection

In a previous mater thesis, it was found that temperature has an influence on the amount of carboxylic acid that can bind to particles. Increasing the temperature of the protection reaction from RT to 40 °C increased the amount of bound acid from 22.3% to 25.4%. However, increasing the temperature further (60 and 75 °C) did not result in any significant improvement.

1.8.2 pH effect during protection

After acidification with $HClO_4$, the amount of absorbed carboxylic acid depends on the pH. As the pH is close to the ferrite zero point charge, small differences could be important.

Table 1. Amount of 11-bromoundecanoic acid as a percentage of total particle weight (experiments performed on a single batch of nanoparticles).

Final pH	Acid %
8.11	21.8
6.62	19.1
3.08	17.9
1.89	17.3

Table 2. Amount of 11-bromoundecanoic acid as a percentage of total particle weight (same as Table 1, but operating on a different batch of nanoparticles).

Final pH	Acid %
7.95	20.2
7.74	18.2
7.48	17.9
6.8	21.7

At pH values of about 7–8, small changes do not have a statistically significant effect.

1.8.3 Effect of amount of carboxylic acid

The amount of carboxylic acid used in the protection step is in large excess with respect to the final amount of bound acid. If the process is in equilibrium, variations in the initial amount of carboxylic acid could affect the final amount absorbed on the particles. In a previous mater thesis, tests were performed by varying the molar ratio between the acid and the amount of $Fe(ClO_4)_2$ used for the synthesis.

Table 3. Amount of 11-bromoundecanoic acid as a percentage of total particle weight.

Molar ratio RCOOH/Fe^{II}	Acid %
0.3	22.5
0.6	20.6
1.0	21.5

These data show that the amount of acid used for the protection step has not effect on the final amount of bound acid.

1.8.4 Synthesis of 10-bromodecylphosphonic acid

Some recent studies indicate that phosphonic acids improve the magnetic properties of nanoparticles.[47-49] The acid used in the protection of nanoparticles in my thesis was synthesized in two steps: the first[50] (eq. 4) is the synthesis of diethyl 10-bromodecylphosphonate (Arbuzov

reaction) using 1,10-dibromodecane and triethyl phosphite, and the second[51] (eq. 5) is the hydrolysis of the reaction mixture containing phosphonate to give 10-bromodecylphosphonic acid (69.7% overall yield, m.p. 80–85 °C).

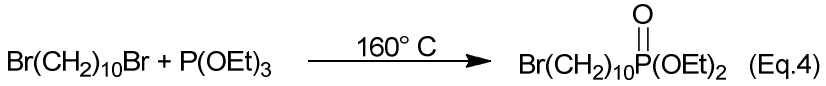

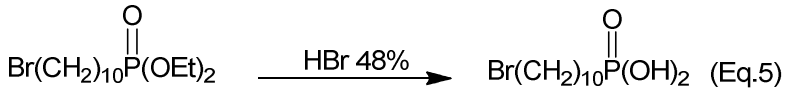

After the synthesis of phosphonate, we analyzed the reaction mixture to check if the reaction was complete. The ^{31}P NMR spectrum showed only one signal at 32.6 ppm, which is very close to one value reported in the literature (δ = 32.8 ppm),[49] but different by 1 ppm from another reported value (δ = 31.7 ppm).[48]

The ^{31}P NMR spectrum of the free acid showed one signal at 37.9 ppm, which is about 1 ppm higher than the literature value (δ = 36.4 ppm).[50] Elemental analysis gave the following experimental values: C% 40.68 and H% 7.49 (calculated values: C% 39.88 and H% 7.36).

The particle protection process was performed with 10-bromodecylphosphonic acid in dichloroethane and methanol without acidifying with $HClO_4$ because the acidity of the phosphonic acid was high enough to obtain pH 6 in the aqueous phase which is sufficient to allow the particles to pass into the organic phase.

1.8.5 Comparison of phosphonic acid and carboxylic acid

The amount of phosphonic acid bound to the particles as a protecting agent was larger than the amount of bound carboxylic acid. Thus, the particle protection process was performed with different molar ratios of 10-bromodecylphosphonic acid in dichloroethane. The amounts of organic acid for about 100 mg of particles, the amounts of organic acid calculated for 100 mg of ferrite, and the molar ratios between the phosphonic and carboxylic acids (mmol of phosphonic acid for 100 mg of ferrite and mmol of carboxylic acid for 100 mg of ferrite) are shown in Tables 4 and 5. In all cases, the molar ratio between the phosphonic and carboxylic acids is over 1 for the same type of nanoparticles. This result means that the amount of phosphonic acid bound to the particles is more than the amount of bound carboxylic acid.

During the protection step with 11-bromoundecanoic acid, it is necessary to acidify the aqueous suspension of particles with $HClO_4$ to obtain pH 6–7, allowing the organic acid to bind to the ferrite nuclei. On the other hand, the acidity of the phosphonic acid is high enough to reach pH 6 in the aqueous phase and allow the particles to pass into the organic phase. In fact, acidification with $HClO_4$ did not result in a significant increase in the amount of phosphonic acid bound to the particles. We tested different amounts of acid by varying the molar ratio between 1.0 and 1.6 with respect to the Fe^{II} salt, and we found that increasing the molar ratio to more than 1.2 decreased the amount of bound phosphonic acid (Table 5). However, adding more (molar ratio of 2) or less (molar ratio of 0.5) phosphonic acid was not efficient. Thus, the best molar ratio of phosphonic acid to Fe^{II} for the particle protection process is 1.2.

Table 4. Synthesis and protection at RT.

21EZ	%	mg acid	mmol	mg ferrite[a]	mg particles
Carboxylic acid[b]	20.7	20.800	0.0784	79.800	100.6
For 100 mg of ferrite		26.065	0.0983		
Phosphonic acid 2[b]	54.9	54.900	0.1823	45.200	100.1
For 100 mg of ferrite		121.460	0.4033		
Molar ratio phosph. ac./ carb. ac.				4.104	
Phosphonic acid 3	50.9	50.900	0.1690	49.300	100.2
For 100 mg of ferrite		103.245	0.3428		
Molar ratio phosph. ac./ carb. ac.				3.488	
Phosphonic acid 4	38.9	38.900	0.1292	61.300	100.2
For 100 mg of ferrite		63.458	0.2107		
Molar ratio phosph. ac./ carb. ac.				2.144	

[a]Calcd. Based on the amount of particles and that of acid found on the particles. [b] Acidified with 0.07 mL of $HClO_4$ 1.17 M (10.9%).

Table 5. Synthesis and protection at 25 °C.

35EZ	%	mg acid	mmol	mg ferrite[a]	mg particles
Phosphonic acid 1	40.8	41.000	0.1546	59.600	100.6
For 100 mg of ferrite		68.792	0.2284		
Molar ratio phosph. ac./ carb. ac. [b]				2.078	
Phosphonic acid 2	50.5	50.800	0.1687	50.800	101.6
For 100 mg of ferrite		100.000	0.3320		
Molar ratio phosph. ac./ carb. ac. [b]				3.021	
Phosphonic acid 3	37.7	38.200	0.1268	63.000	101.2
For 100 mg of ferrite		60.635	0.2013		
Molar ratio phosph. ac./ carb. ac. [b]				1.832	
Phosphonic acid 4	26.5	26.600	0.0883	73.900	100.5
For 100 mg of ferrite		35.995	0.1195		
Molar ratio phosph. ac./ carb. ac. [b]				1.087	

[a]Calcd. Based on the amount of particles and that of acid found on the particles. [b]mmol of carboxylic acid (from Table 4).

1.9 Particle characterization

To characterize the nanoparticles, TEM analyses were carried out on nanoparticles that were synthesized, protected (23EZ, 27EZ), and dispersed in dry CH_2Cl_2. TEM micrographs are presented in Figures 10 and 11. TEM analyses were also carried on a batch of unprotected ferrite particles and on particles from the same batch that were protected by 11-bromoundecanoic acid (8EZ) (Figures 12 and 13). Partial aggregation was observed in this case, probably because the particles were synthesized about one month before the measurement, but the particles size is the same before and after protection. The particles size is in the range of 2.8–4 nm.

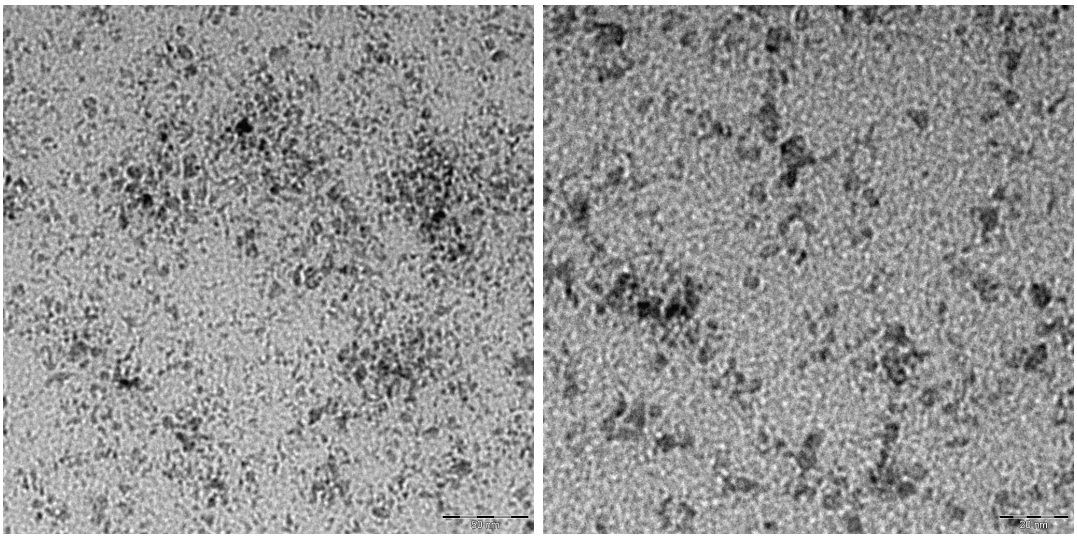

Figure 10: Particles 23EZ (left: image2 and right: image13).

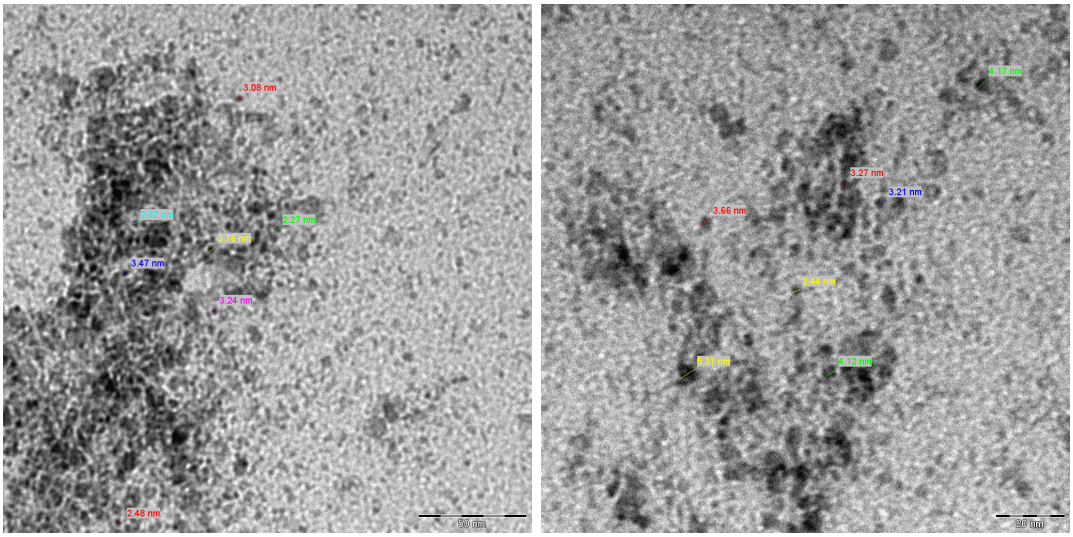

Figure 11: Particles 27EZ (left: image21_misure and right: image24).

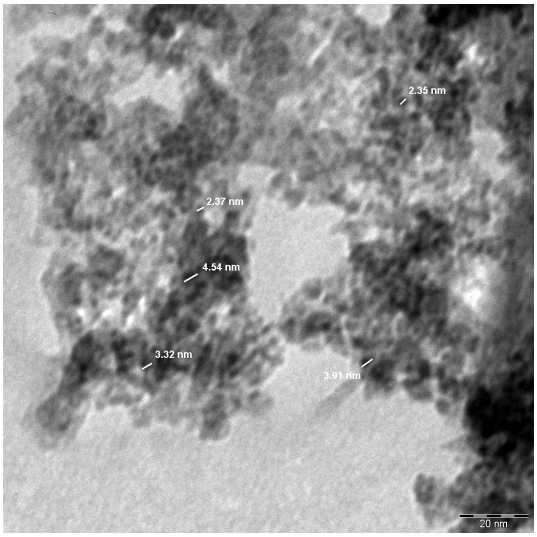

Figure 12: Particles 8EZ (after synthesis) (Image7misure).

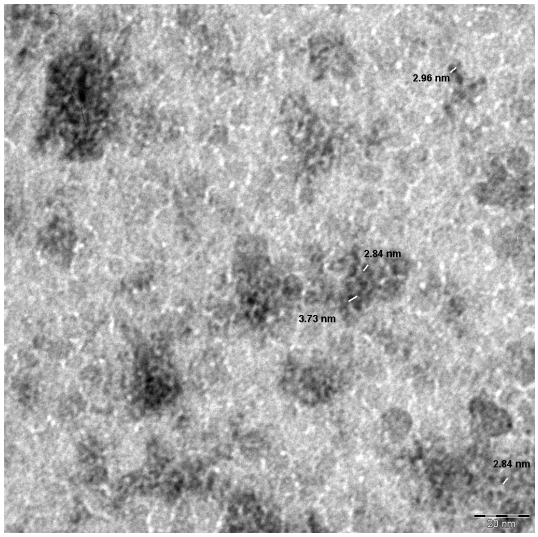

Figure 13: Particles 8EZ (after protection) (Image11misure).

Figure 12 represents unprotected particles from an aqueous suspension stored at basic pH for a month. The particles were dispersed a little bit after sonication. Some drops of the solution were diluted with degassed milli-Q water and then sonicated. A yellow solution with a solid was formed, and the purified solution was used for the TEM analysis.

Figure 13 represents particles protected with 11-bromoundecanoic acid, dried in vacuo, and stored under a N_2 atmosphere for a month. The particles were dispersed in CH_2Cl_2 by sonicating for 1 h, and the obtained orange solution was used for the TEM analysis.

X-ray diffraction analyses carried out on the same particle samples (8EZ, 23EZ, and 27EZ) (Figures 14–17) showed that the particle sizes are below 4 nm. However, the broadness of the peaks does not allow more precise quantification of the particle sizes.

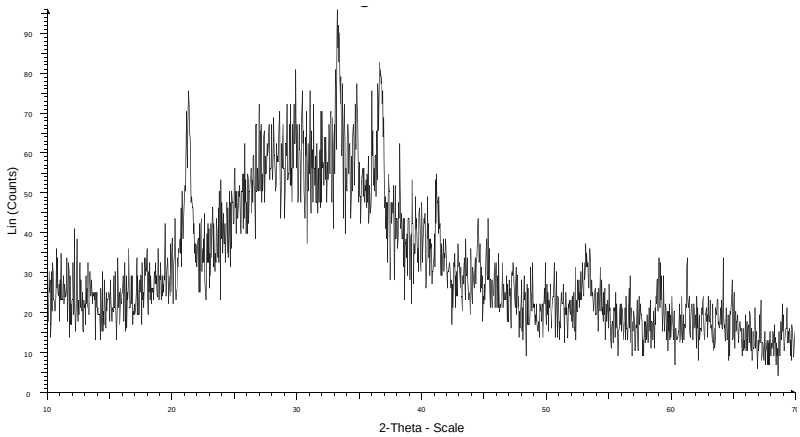

Figure 14: Particles 8EZ after synthesis.

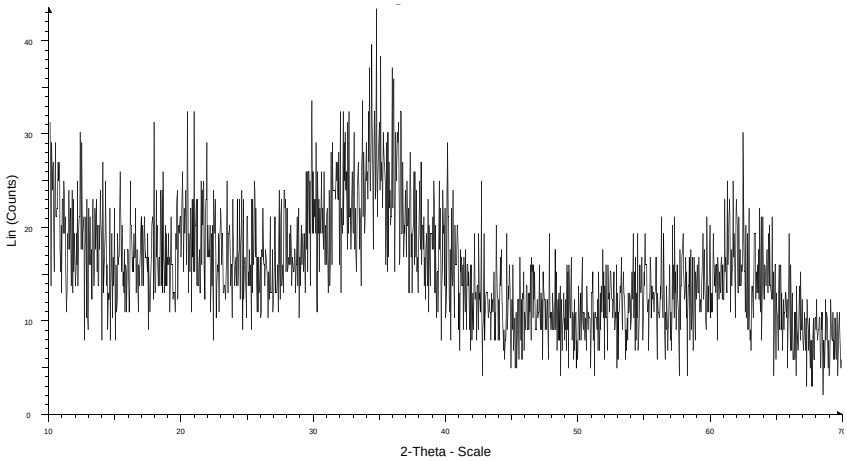

Type: 2Th/Th locked - Start:10.000° - End 70.000° - Step 0.040° - Step time: 2 s - Temp.: 25°C (Room) - Time Started: 0 s - 2-Theta: 10.000° - Theta: 5.000° - Chi: 0.00° - Phi: 0.00°

Figure 15: Particles 8EZ after protection.

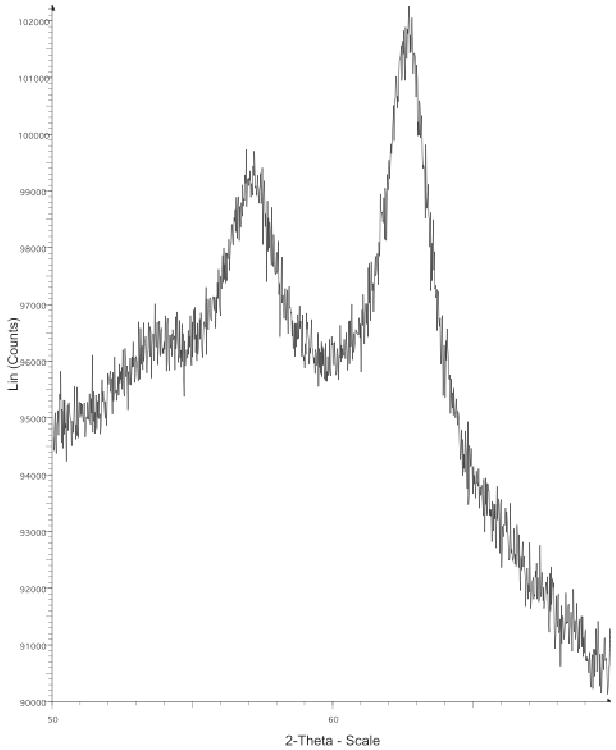

locked - Start:50.000° - End 69.900° - Step 0.021° - Step time: 1670.4 s -Temp.: 25°C (Room) - Time Started: 0 s – 2-Theta: 50.000° - Theta: 25.000° - Chi: 0.00° - Phi: 8.00°

Figure 16: Particles 23EZ.

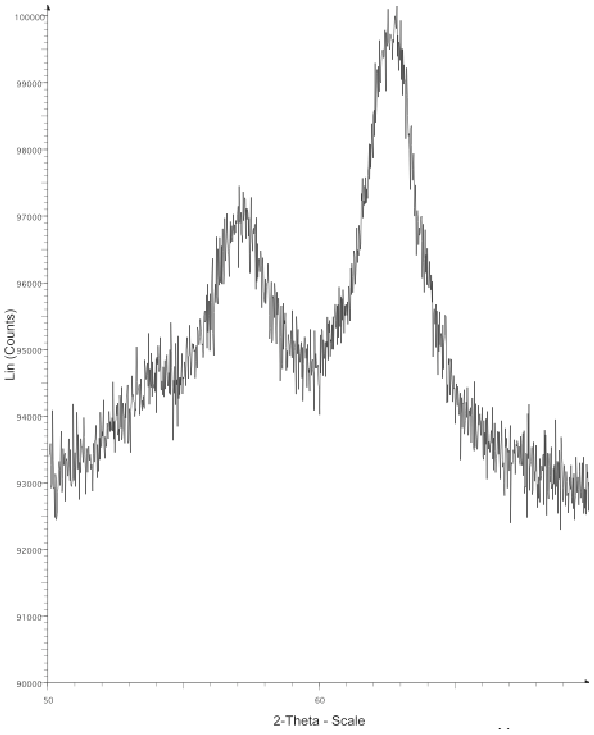

Figure 17: Particles 27EZ.

Experimental Section

1.10 Instrumentation

^{1}H NMR and ^{31}P NMR spectra were recorded on a Bruker AC 300 FT or Avance Bruker DPX 300 spectrometer operating at 300 MHz or on a Bruker DPX 400 spectrometer operating at 400 MHz. Elemental analyses were recorded on a PerkinElmer 2400 CHN elemental analyzer. IR spectra were recorded on a Varian Scimitar FS-1000 or Perkin Elmer Spectrum BX spectrophotometer using a 0.48 nm or 0.10 mm liquid sampling cell with CaF_2 windows. The products were analyzed by gas chromatography (Shimadzu GC-2010 equipped with a SUPELCO EQUITY^{TM}-5ms column). TEM analyses were performed on 300 mesh formvar/carbon copper grids or 300 mesh carbon copper grids using an EFTEM Leo912ab transmission electron microscope (Zeiss) at 80 kV. Digital images were acquired using an Esivision CCD-BM/1K system. Quantification of palladium in catalysts was performed on a PerkinElmer PinAAcle 900T atomic adsorption spectrometer. Degassed milli-Q water was obtained by sonication of milli-Q water under a N_2 atmosphere.

Gas chromatography (fast)

Shimadzu GC-2010

Column: SUPELCO EQUITY^{TM}-5ms, 10 m × 0.1 nm × 0.1 μm film thickness capillary column

Carrier (He) linear velocity: 32.6 cm/s

Air flow: 400.0 mL/min

Hydrogen flow at the detector: 40.0 mL/min

Makeup gas (N_2) flow: 30.0 mL/min

Split ratio: 10.0

FID temperature: 270 °C

Oven temperature program

Rate (°C/min)	Temperature (°C)	Hold Time (min)
	130.0	0.0
8.0	150.0	0.0
60.0	195.0	5.0

80.0	250.0	1.0

PTV injector program

Rate (°C/min)	Temperature (°C)	Hold Time (min)
	190.0	7.0
80	250.0	2.0

GC-MS

Shimadzu GC-17A, Shimadzu GCMS-QP5050

Column: SUPELCO SLB^{TM}-5ms, 30 m × 0.25 mm × 0.25 μm film thickness capillary column

Carrier pressure (He): 28.7 kPa

Injection port: 250 °C

Detector temperature: 260 °C

Oven temperature program

Rate (°C/min)	Temperature (°C)	Hold time (min)
-	60.0	4.50
25.0	120.0	2.00
7.0	240.0	5.0
15.0	270.0	10.00

Pressure program

Rate (°C/min)	Temperature (°C)	Hold time (min)
-	28.7	4.50
5.2	43.7	2.0
1.7	72.5	5.00
3.0	79.4	10.00

1.11 Solvent purification

Most of the solvents used in the experimental procedures were dried and distilled under a N_2 atmosphere immediately before use. Various drying agents were used, depending on the solvent.

CH_2Cl_2	Magnesium/$Mg(OCH_3)_2$
MeOH	CaH_2
DMSO	Na
$(CH_2)_2Cl_2$	
$CHCl_3$	
DMF	
n-heptane	

1.11.1 Standard amounts for nanoparticle synthesis

Solution (A)

The required concentration of $NaNO_3$ was 3 M ($2.28 \cdot 10^{-1}$ mol = 19.382 g) in 76 mL of degassed milli-Q water and the required pH was 13. The quantity of NaOH needed to obtain this pH was $7.60 \cdot 10^{-3}$ mol = 0.304 g, so the final concentration of NaOH was 0.1 M.

Solution (B)

The equivalents of NaOH necessary for the synthesis were two for each Fe^{II} ion, three for each Fe^{III} ion, and 3.2 to maintain pH 13 when adding solutions B and C to solution A. Thus, the total equivalents of NaOH were 8.2 ($6.23 \cdot 10^{-2}$ mol = 2.492 g) in 12 mL of degassed milli-Q water (the final amount of water must equal the volume of solution C).

Solution (C)

The solution was prepared with the following components in 7.6 mL of degassed milli-Q water:

Concentration of Fe^{II} salt of 1 M = $7.60 \cdot 10^{-3}$ mol = 2.868 g

Concentration of Fe^{III} salt of 2 M = $1.52 \cdot 10^{-2}$ mol = 6.141 g

Concentration of $NaNO_3$ of 3 M = $2.28 \cdot 10^{-2}$ mol = 1.938 g

Owing to the presence of hydrated iron salts, the volume of the solution became 12 mL. Solutions (B) and (C) were added dropwise into solution (A) at the same time and at the same rate using a sirynge pump.

1.12 General procedures

1.12.1 General procedure for nanoparticle synthesis

All procedures were performed under a N_2 atmosphere. For the synthesis step, the operating temperature was 30 °C.

Solution (A)

In a Schlenk flask equipped with a magnetic stirring bar, $NaNO_3$ and NaOH were dissolved in degassed milli-Q water, as reported in section (1.11.1).

Solution (B)

In a Schlenk flask equipped with a magnetic stirring bar, NaOH was dissolved in degassed milli-Q water, as reported in section (1.11.1).

Solution (C)

In a Schlenk flask equipped with a magnetic stirring bar, $Fe^{II}(ClO_4)_2 \cdot 6.8H_2O$, $Fe^{III}(NO_3)_3 \cdot 9H_2O$, and $NaNO_3$ were dissolved in degassed milli-Q water, as reported in section (1.11.1).

Elemental analysis of purchased $Fe(ClO_4)_2 \cdot nH_2O$, as found on the Aldrich site, allowed us to determinate that the composition was $Fe(ClO_4)_2 \cdot 6.8H_2O$.

In the early synthesis attempts, we found that the chemicals for Solution (C) could not be mixed/prepared very long before use. In particular, when mixing $Fe^{III}(NO_3)_3 \cdot 9H_2O$ with $Fe^{II}(ClO_4)_2 \cdot 6.8H_2O$ or even with $NaNO_3$, we observed some type of redox reaction releasing a nonnegligible amount of NOx gases. Such a process may change the oxidation state of iron, probably by oxidizing Fe^{II} to Fe^{III}, and affect the correct stoichiometry for the synthesis.

The best way to avoid this side reaction is to prepare Solution (C) using the following procedure: weigh salts and place them in the Schlenk flask in the sequence $Fe(NO_3)_3 \cdot 9H_2O$, $NaNO_3$, and finally $Fe(ClO_4)_2 \cdot 6.8H_2O$. After the last addition, immediately add the necessary amount of water. The side reaction occurred when the salts were in direct contact with each other, but no visible reaction was observed in solution. Moreover, to avoid any problems, it is better to prepare the solution immediately before use.

Solution (B) and (C) were then loaded in two syringes and slowly added to solution (A), under stirring, over 30 min using a syringe pump. During this process, a black precipitate was instantly formed. While maintaining vigorous stirring, the suspension was divided with a graduated pipette into four 30 mL centrifuge tubes with screw caps. After the synthesis, the solution pH was still 13.

The nanoparticles were separated by centrifugation at 2750 rpm and washed four times with degassed milli-Q water. The washing procedure, as described in the next paragraph, was repeated until the solution reached pH 10.

1.12.2 General procedure for nanoparticle washing

All operations were performed in a wide-mouth (diameter of 9 cm) Schlenk tube under a N_2 atmosphere. The nanoparticle washes were carried out in 30 mL centrifuge tubes closed with a screw cap to always maintain a N_2 atmosphere. Every solution of dispersed nanoparticles was centrifuged to promote the separation of the liquid phase (aqueous solvent) from the solid one (nanoparticles). Following removal of the liquid phase with a pipette, the new washing solvent (10 mL of degassed milli-Q water) was added to the nanoparticles. The suspension was stirred for 15 min, sonicated for 15 min (to improve nanoparticle dispersion), and then centrifuged until complete separation occurred. At the fourth washing step, it was necessary to add 1 mL of a 0.24 M solution of $NaClO_4$ (0.3371 g/10 mL) to reduce nanoparticle aggregation. Otherwise, the nanoparticles could not be separated from the solution. If the addition $NaClO_4$ is not necessary, something has gone wrong in the synthesis process.

1.12.3 General procedure for nanoparticle protection

All manipulations were performed under a N_2 atmosphere. For the protection step, the operating temperature was 40 °C. In a Schlenk flask, the organic acid (10-bromodecylphosphonic acid, 11-bromoundecanoic, or others) was dissolved in a mixture of dichloroethane (40 mL) and methanol (2 mL). This solution was added in equal parts to the four centrifuge tubes containing nanoparticles. A biphasic system formed, with the nanoparticles initially remaining in the upper aqueous phase. For protection with 10-bromodecylphosphonic acid (or generally with phosphonic acids), we found that it was better not to acidify the aqueous phase owing to the high acidity of these kinds of acids. Higher amounts of phosphonic acid linked to the nanoparticles were obtained without acidification. In this case, prolonged stirring was sufficient to cause migration of the nanoparticles from the aqueous phase to the organic layer. After stirring the samples overnight, the aqueous phase was removed and the organic layers of the four samples were washed with degassed milli-Q water (10 mL each time) until the washing solution appeared clear and colorless (3–4 washes). The nanoparticles were then precipitated with degassed MeOH (10 mL) and washed four times with degassed MeOH (10 mL each time). The MeOH washing solution was evaporated in vacuo and the resulting residue (organic acid) weighed. The washing procedure was repeated until the amount of washed protecting agent was equal to or less than 6 mg per tube. Finally, the nanoparticles were dried in vacuo. The nanoparticles must be black before the protection phase and dark brown after protection.

1.12.4 General procedure for quantitative determination of protective organic acids on the particles by their destruction

Approximately 100 mg of nanoparticles were chemically degraded by sonicating and stirring in 8 mL of 6 M HCl until a clear yellow solution was obtained. The organic acid was extracted with CH_2Cl_2 (4 × 10 mL). The combined organic phases were dried over Na_2SO_4 and the solvent was evaporated in vacuo. The solid obtained was then analyzed by quantitative gravimetric determination.

1.12.5 General procedure for GC analysis of protecting layers on the particles

Long-chain carboxylic acids must be silanized for GC analysis. The silanization was performed by adapting a literature procedure.[51] In a test tube, the organic acid (10 mg) was dissolved in dry MeCN (1 mL) and naphthalene (10 mg) was added as an internal standard. Then, 20 µL of BSA (*N*,*O*-bis(trimethylsilyl)acetamide) and 1 µL of TMCS (trimethylchlorosilane) were added to the solution. TMCS works as a catalyst (5% of the amount of BSA). The solution was vigorously stirred for 30 s and then heated at 70 °C for 40 min. The solution was diluted with CH_2Cl_2 to achieve a naphthalene concentration of 0.1 mg/mL, and 1 µL of the diluted solution was injected into the gas chromatograph.

1.13 Preparation of Fe_3O_4 nanoparticles protected by organic acid

1.13.1 Synthesis of Fe_3O_4 nanoparticles protected by 10-bromodecylphosphonic acid

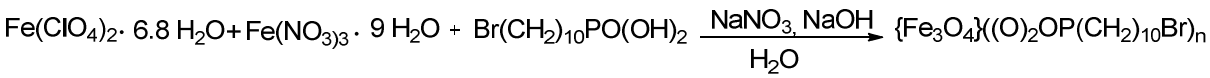

	Reagent	M.W. (g•mol^{-1})	g	V(mL)	M (mol/L)	mmol	Molar ratio
A	$NaNO_3$	84.99	19.3833		3.00	228.0	30.0
	NaOH	40.00	0.3114		0.102	7.78	1.02
	H_2O			76			
B	NaOH	40.00	2.4991		5.20	62.47	8.23
	H_2O			12			
C	$Fe^{II}(ClO_4)\cdot 6.8H_2O$	377.39	2.8668		1.00	7.59	1.00
	$Fe^{III}(NO_3)_3\cdot 9H_2O$	404.00	6.2036		2.02	15.35	2.02
	$NaNO_3$	84.99	1.9398		3.00	22.82	3.00
	H_2O			7.6			

The nanoparticles were synthesized, protected, and washed, as described in the general procedure.

Tube	Reagent	M.W. (g•mol^{-1})	g	V(mL)	mmol	Molar ratio
1,2,3,4	$Br(CH_2)_{10}PO(OH)_2$	301.16	2.7492		9.12	1.2*
	MeOH(degassed)			2		
	$(CH_2)_2Cl_2$ (degassed)			40		

*Calculated on 1 of Fe^{II} moles.

The nanoparticles were washed as reported in the general procedure and dried in vacuo.

A small amount of nanoparticles were treated to determinate the achieved protection level:

Tube	Amount of MNPs used for the analysis (g)	Acid recovered (g)	Protection level (%)
1	0.1032	0.0590	57.17
2	0.1033	0.0569	55.08
3	0.1012	0.0573	56.62
4	0.1042	0.0597	57.29

The percentages obtained were similar, with an average protection level of **56.54%**. The total amount of nanoparticles protected by 10-bromodecylphosphonic acid that we obtained was **2.4158 g**.

Phosphonic acid showed poor solubility in dry dichloroethane, forming a dispersion. For this reason, we decided to mix dichloroethane with the minimum amount of MeOH capable of solubilizing the protecting agent. Tests were carried out by varying the amount of MeOH in the range of 20–2000 µL. The best amount was found to be 2 mL of MeOH in 40 mL CH_2Cl_2.

1.13.2 Synthesis of 10-bromodecylphosphonic acid

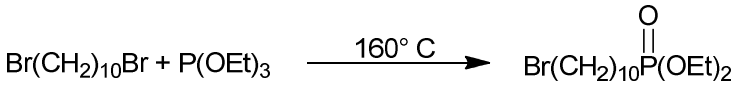

Reagent	MW ($g \cdot mol^{-1}$)	g	mol	Molar ratio	V [mL]	d[g/mL]
$Br(CH_2)_{10}Br$	300.07	60.012	$2.00 \cdot 10^{-1}$	3.63	45	1.335
$P(OEt)_3$	166.16	9.160	$5.51 \cdot 10^{-2}$	1.00	9.5	0.969

The reaction was performed under a N_2 atmosphere. In a Schlenk flask, 1,10-dibromodecane and triethylphosphite were heated at 160 °C for 4 h. The completion of the reaction was checked by TLC (silica gel, 1:1 CH_2Cl_2/hexane, stained by I_2 vapor). The ^{31}P NMR spectrum of the reaction mixture showed only one signal at 32.6 ppm.

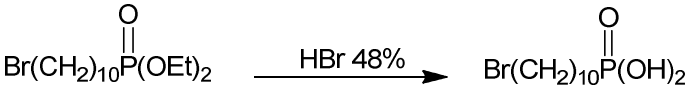

Reagent	MW ($g \cdot mol^{-1}$)	g	mol	Molar ratio	V [mL	d[g/mL]
$Br(CH_2)_{10}P(O)(OEt)_2$			$5.51 \cdot 10^{-2}$*	1.00		
HBr 48%	80.98		$1.93 \cdot 10^{-1}$	3.50	22.4	1.45
$Br(CH_2)_{10}P(O)(OEt)(OH)$	329.47	11.5554	$3.50 \cdot 10^{-2}$	1.00		
HBr 48%	80.98	22.867	$2.82 \cdot 10^{-1}$	4.00	15.8	1.45

*It was supposed that $P(OEt)_3$ reacted completely.

The reaction was performed under a N_2 atmosphere. First, 22.4 mL of 48% HBr was added to the above reaction mixture, which was then heated to reflux for 20 h. The HBr solution was evaporated under vacuum and then 90 mL of hexane was added under stirring to eliminate excess 1,10-dibromodecane. The formed suspension was then centrifuged. The obtained solid was washed with hexane (6 × 15 mL) and then dried in vacuo, affording 11.5554 g.

The ^{31}P NMR spectrum showed two signals instead of one: 37.4 ppm (10-bromodecylphosphonic acid) and 35.7 ppm ($Br(CH_2)_{10}P(O)(OEt)(OH)$). Thus, the hydrolysis was repeated by considering all of the obtained solid as the monophosphonic acid.

In a Schlenk flask, 15.8 mL of 48% HBr was added to 11.5554 g of product and then heated to reflux for 24 h. The ^{31}P NMR spectrum of the reaction mixture in $CDCl_3$ showed one signal at 37.9 ppm. The phosphonic acid was extracted with 400 mL of CH_2Cl_2, dried over Na_2SO_4, and filtered using a cannula. Rotary evaporation and drying in vacuo afforded 11.5684 g ($3.84 \cdot 10^{-2}$, 69.70% overall yield, m.p. 80–85 °C).

Elemental analysis for $C_{10}H_{22}BrO_3P$: calcd. C% 39.88, H% 7.36; found C% 40.68, H% 7.49.
^{31}P NMR (162 MHz, $CDCl_3$, 300 K) δ 37.9 ppm. (figure 18)
^{1}H NMR (400 MHz, $CDCl_3$, 300 K) δ 7.55 (bs, 2H, –OH), 3.42–3.49 (t, 2H, $–CH_2Br$, J = 6.9 Hz), 1.89–1.82 (m, 2H, $–CH_2CH_2Br$), 1.75–1.28 (m, 16H) ppm.(figure 19)
^{13}C NMR (100 MHz, $CDCl_3$, 300 K) δ 34.10 (s), 32.97 (s), 30.60 (s), 29.48 (s), 29.37 (s), 29.13 (s), 28.86 (s), 28.30 (s), 25.35 (d, J = 144.3 Hz), 22.16 (s) ppm. (figure 20)

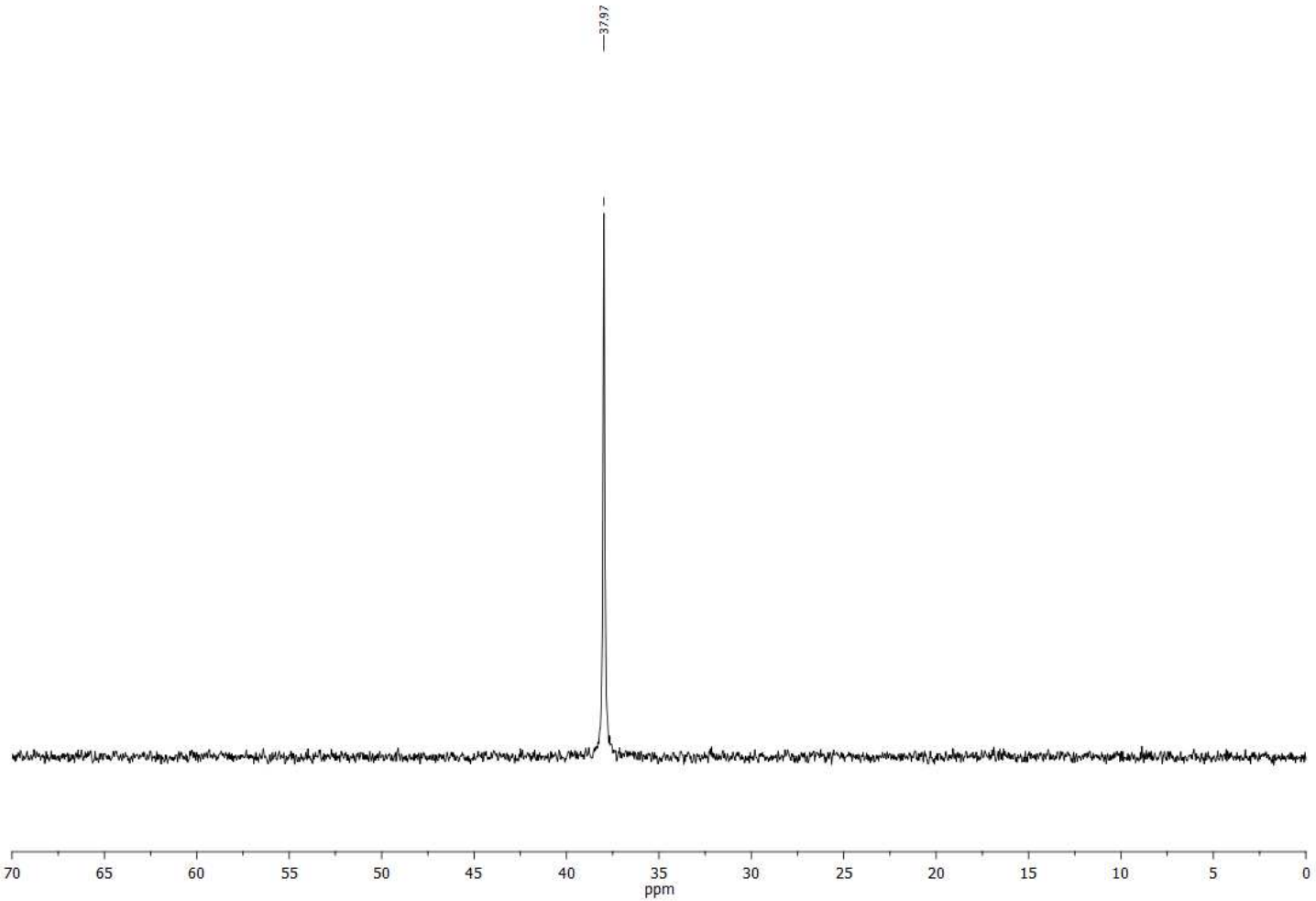

Figure 18: ^{31}P NMR (162 MHz, $CDCl_3$, 298 K) spectrum of 10-bromodecylphosphonic acid.

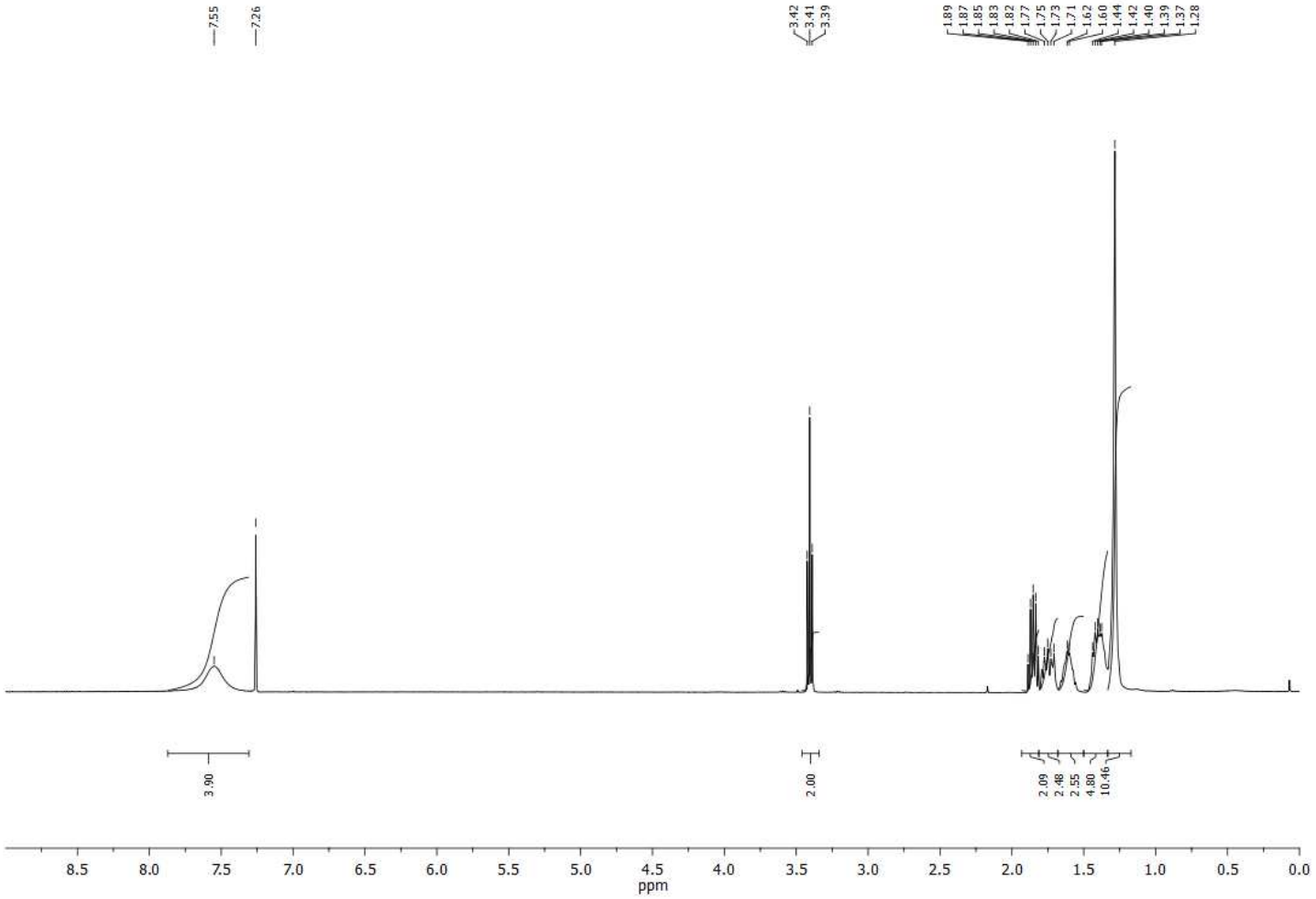

Figure 19: ^{1}H NMR (400 MHz, $CDCl_3$, 298 K) spectrum of 10-bromodecylphosphonic acid.

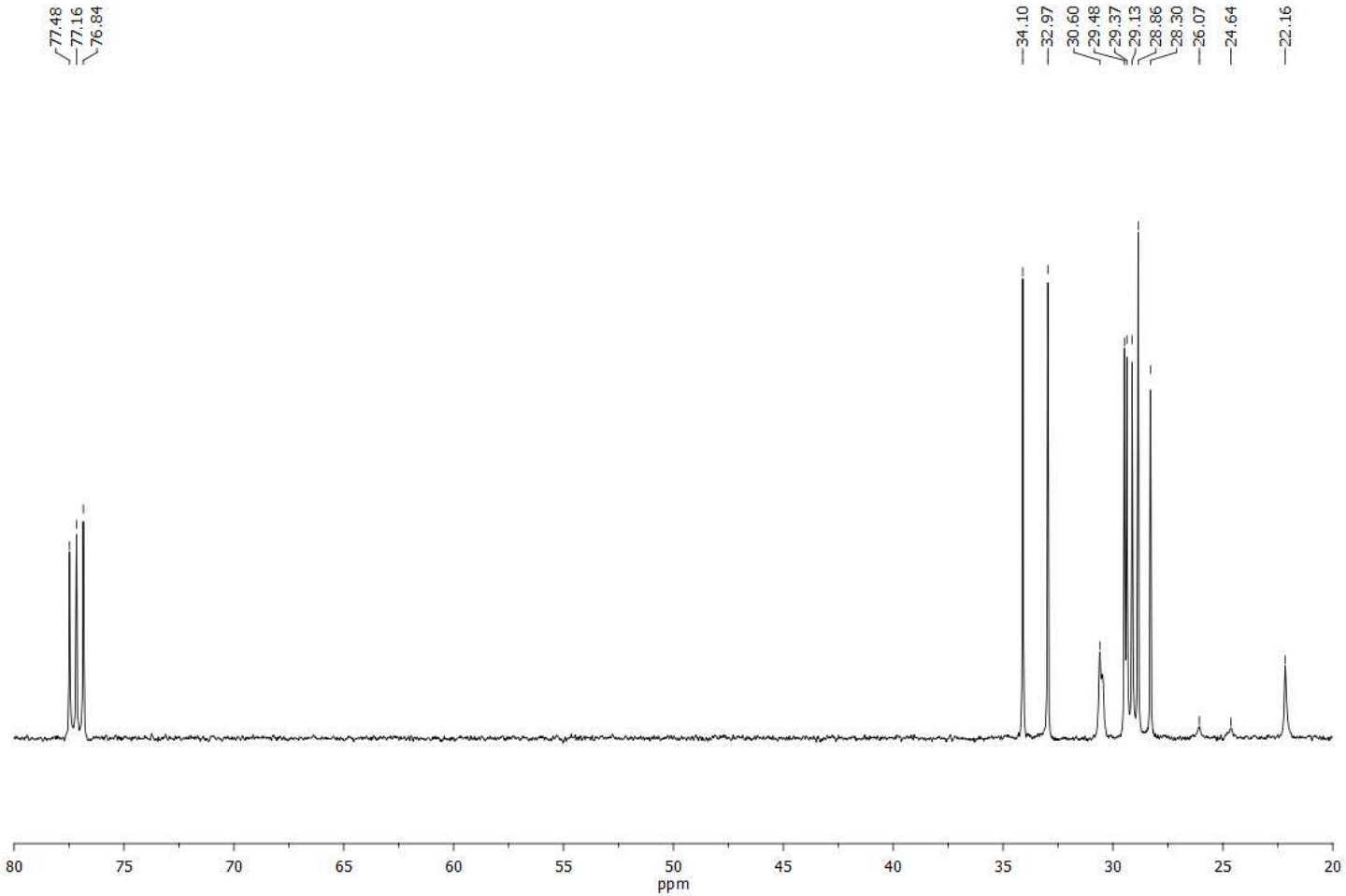

Figure 20: ^{13}C DEPT (100 MHz, $CDCl_3$, 298 K) spectrum of 10-bromodecylphosphonic acid.

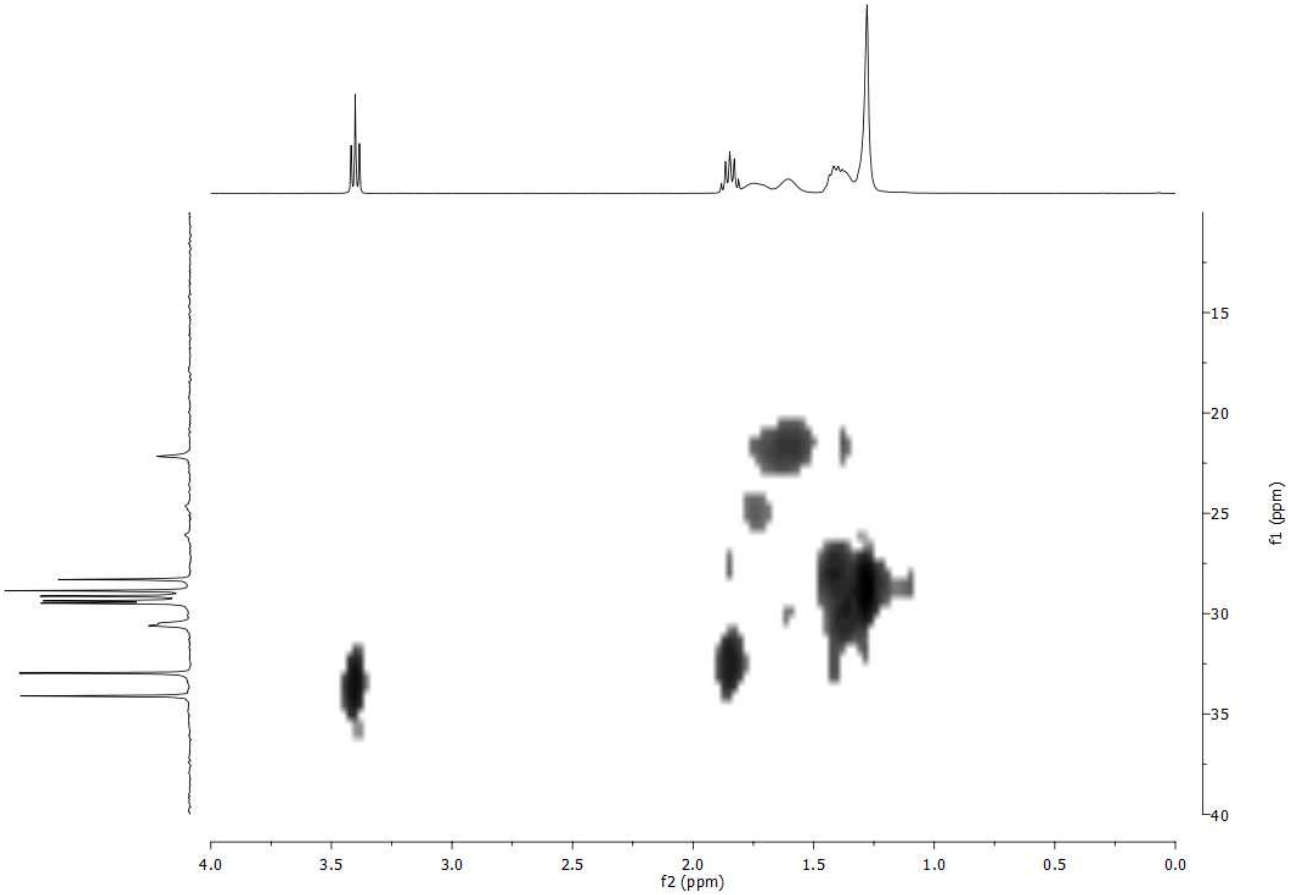

Figure 21: ^{1}H-^{13}C HSQC (300 MHz, $CDCl_3$, 298 K) spectrum of 10-bromodecylphosphonic acid.

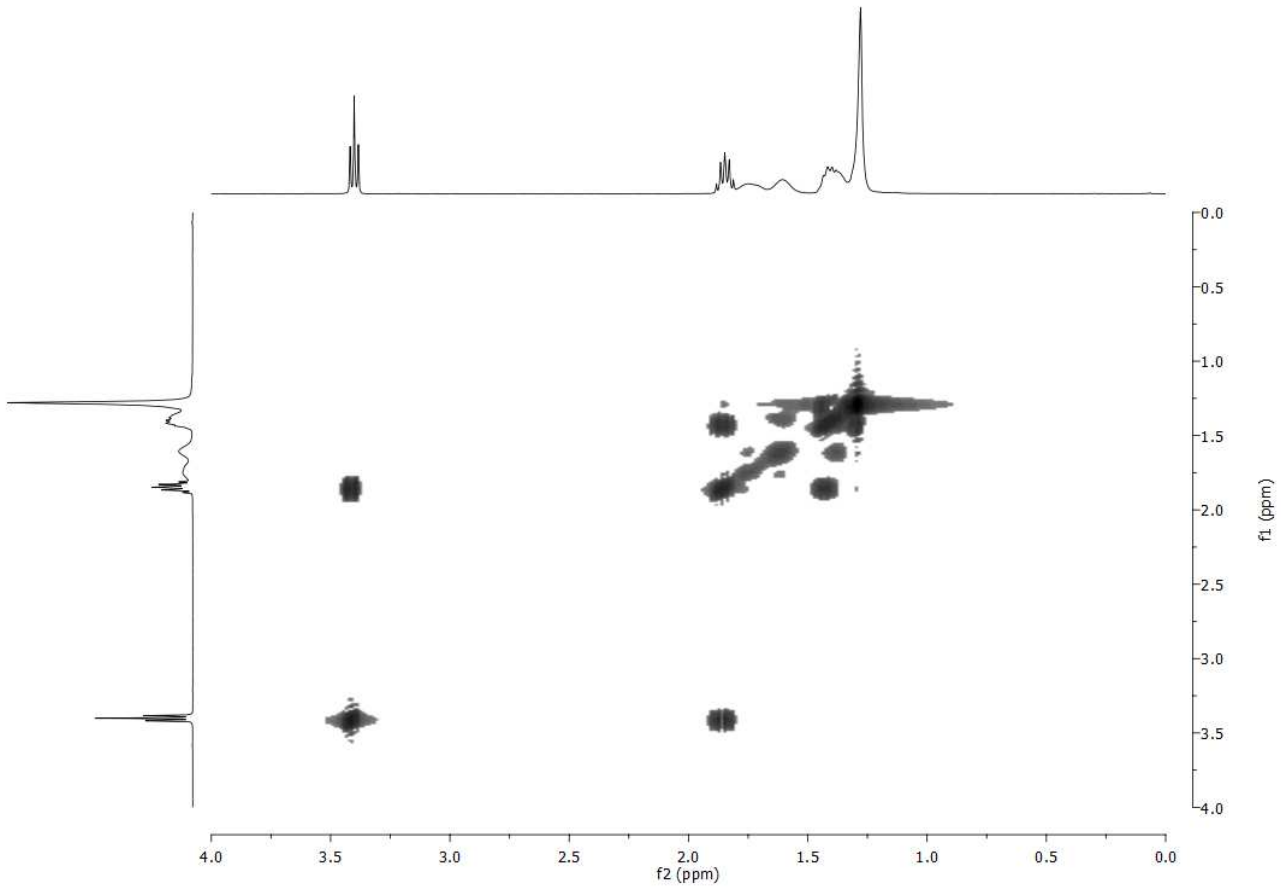

Figure 22: ^{1}H-^{13}C COSY (300 MHz, $CDCl_3$, 298 K) spectrum of 10-bromodecylphosphonic acid.

References

[1] U. Jeong, X. Teng, Y. Wang, H. Yang, Y. Xia, *Adv. Matter*, **2007**, 19, 33-60.

[2] J.S. Lee, J.M Cha, H.Y. Yoon, J.K. Lee, Ha Lee, Y.J.Kim, , Sci Rep 5, **2015**, 12135.

[3] Wu Liheng, A Mendoza-Garcia, Li Qing, and Sun Shouheng, *Chem. ev*, **2016**, 116(18), 10473-10512.

[4] Figure adapted from: https://www.nde-ed.org/ EducationResources/CommunityCollege/ MagParticle/Physics/HysteresisLoop.htm.

[5] M. Colombo, S. Carregal-Romero, M. F. Casula, L. Gutiérrez, M. P. Morales, IB Böhm, J. T. Heverhagen, D. Prosperi, W. J. Parak, *Chem.Soc.Rev*, **2012**, 41, 4306-4334.

[6] M. Faraji, Y. Yamini and M. Rezaee, J. *Iran. Chem. Soc*.7, (1), **2010**, 1-37.

[7] K. M. Krishnan, *IEEE Trans. Magn*, **2010**, 46, 2523-2558.

[8] Manoj B. Gawande, Paula S. Branco and Rajender S. Varma, *Chem. Soc. Rev.* **2013**, 42, 3371-3393.

[9] D. S. Mathew, R. S. Juang, *Chem. Eng. Journal*, **2007**, 129 51-65.

[10] R. Gómez-Sotomayor, S.Ahualli, Jl Viota, K. Rudzka, A.V. Delgado, *J Nanosci Nanotechnol*, **2015** ,15(5),3507-14

[11] K. Nejati-Koshki K, M. Mesgari M, E. Ebrahimi, F. Abbasalizadeh, S. Fekri Aval, A. AKhandaghi, A.Abasi M, Akbarzadeh, *J Microencapsul*, **2014**,31(8),815-23

[12] McBain S. C, Yiu H. H, Dobson J, **2008**, 3(2),169-180

[13] S. H. Gee, Y. K. Hong, D. W. Erickson, M. H. Park and J. C. Sur, *Appl. Phys*, 2003, 93, 7560-7562.

[14] Q. L. Jiang, S. W. Zheng, R. Y. Hong, S. M. Deng, L. Guo, R. L. Hu, B. Gao, M. Huang, L. F. Cheng, G. H. Liu, Y. Q. Wang, *Appl. Surf. Sci*, **2014**, 307, 224-233.

[15] Li. Xiao, Ji. Li, D. F. Brougham, E. K. Fox, N. Feliu, A. Bushmelev, A.Schmidt, N. Mertens, F. Kiessling, M. Valldor, B. Fadeel, and S. Mathur, *ACS Nano*, **2011**, 5 (8), 6315-6324.

[16] L. Sun, C.Zhang, L. Chen, J. Liu, H. Jin, H. Xu, L. Ding, *Anal.Chem.Acta*, **2009**,638,162-168.

[17] R. K. Sharma, S. Dutta, S. Sharma, R. Zboril, R. S. Varma and M. B. Gawande, *Green Chem*, **2016**, 18, 3184-3209.

[18] R. Abu-Reziq, H. Alper, D. S. Wang, M. L. Post, *J. Am Chem. Soc*, **2006**, 128, 5279-5282.

[19] D. Guin, B. Baruwati, S. V. Manorama, *Org. Lett*, **2007**, 9, 1419-1421.

[20] S.J. Ding, Y.C. Xing, M. Radosz, Y.Q. Shen, *Macromolecules*, **2006**, 39, 6399-6405.

[21] T. Wang, D. La Montagne, J. Lynch, J. Zhuang and Y. C. Cao, *Chem. Soc. Rev*, **2013**, 42, 2804-282.

[22] A. K. Ganguli, T. Ahmad, S. Vaidya and J. Ahmed, Pure Appl. Chem, 2008, 80, 2451-2477.

[23] N. Perez, F. L. Calahorra, A. Labartaac and X. Batlle, *Phys.Chem*. **2011**, 13, 19485-19489.

[24] C. X. Guo, S. Huang and X. Lu, *Green Chem*, **2014**, 16, 2571-2579.

[25] C. Pereira, A. M. Pereira, C. Fernandes, M. Rocha, R. Mendes, M. P. F. García, A. Guedes, P. B. Tavares, J. M. Grenèche, J. P. Araújo and C. Freire, Chem. Mater, **2012**, 24, 1496-1504.

[26] Y.Zhao, Qui Z, Huang. J, *Chinese J.Chem.Eng*, **2008**, 16 (3), 451-455.

[27] Y.S.Kang,S.Risbud, J.F.Rabolt, and P.Stroeve, *Chem.Mat*,**1996**,8,2209-2211.

[28] F. Guignard and M. Lattuada, *Langmuir* **2015**, 31, 4635-4643.

[29] G. Marchegiani, P. Imperatori, A. Mari, L. Pilloni, A. Chiolerio, P. Allia, P. Tiberto and L. Suber, *Ultrason.Sonochem*, **2012**, 19, 877-882.

[30] T. Togashi, S. Takami, K. Kawakami, H. Yamamoto, T. Naka, K. Sato, K. Abee and T. Adschiria, *J. Mater. Chem*, **2012**, 22, 9041-9045.

[31] F. R. Li, W. H. Yan, Y. H. Guo, H. Qi and H. X. Zhou, Int. J. Hyperthermia, **2009**, 25, 383.

[32] N. Moumen and M. P. Pileni, Chem. Mater, **1996**, 8, 1128.

[33] T.Heyon, Chem. Commun, **2003**, 927–934

[34] S. Sun and H. Zeng, J. Am. Chem. Soc, **2002**, 124, 8204

[35] H.Y Lee,N.H. Lim, J.A Seo, S.H Yuk, B.K Kwak, G .Khang, et al, J Biomed Mater Res. **2006**,79B,142–50.

[36] V. V. Makarov, S. S. Makarova, A. J. Love, O. V. Sinitsyna, A. O. Dudnik, I. V. Yaminsky, M. E. Taliansky and N. O. Kalinina, Langmuir, **2014**, 30, 5982-5988.

[37] M.A Zolfigol,V.Khakyzadeh,A.R Moosavi-Zare, A. Rostami, A.Zare, N.Iranpoor, M.H, Beyzavi, R.Luque, Green Chem. **2013**, 15, 2132–2140

[38] H. Naeimi, Z.J.Nazifi, Nanopart. *Res.* **2013**, *15*, 2026

[39] A. Pourjavadi, S.H.Hosseini,M. Doulabi,S.M.Fakoorpoor, F.Seidi,. *ACS Catal.* **2012**, *2*, 1259–1266.

[40] K. S. Wilson, J. D. Goff, J. S. Riffle, L. A. Harris, T. G. St Pierre, *Polym Adv Technol*, **2005**, 16, 200-211.

[41] Z.-X. Sun, F.-W. Su, W. Forsling, P.-O. Samskog, *J Colloid Interface Sci*, **1998**, 197, 151-159.

[42] N. Marmier, A. Delisée, F. Fromage, *J Colloid Interface Sci*, **1999**, 211, 54-60.

[43] P. H. Tewari, A. W. McLean, *J Colloid Interface Sci*, **1972**, 40, 267-272.

[44] L. Vayssières, C. Chanéac, E. Tronc, J. P. Jolivet, *J Colloid Interface Sci*, **1998**, 205, 205-212.

[45] T. J. Daou, S. Begin-Colin, J. M. Grenèche, F. Thomas, A. Derory, P. Bernhardt, P. Legaré, G. Pourroy, *Chem Mater*, **2007**, 19, 4494-4505.

[46] E. Illés, E. Tombácz, *Colloid Surf A: Colloid Surf A Physicochem Eng Asp*, **2003**, 230, 99-109.

[47] T. J. Daou, J. M. Grenèche, G. Pourroy, S. Buathong, A. Derory, C. Ulhaq-Bouillet, B. Donnio, D. Guillon, S. Begin-Colin, *Chem Mater*, 2008, 20, 5869-5875.

[48] Y. Catel, M. Degrange, L. Le Pluart, P.-J. Madec, T.-N. Pham, L. Picton, J Polym Sci Pol Chem, **2008**, 46, 7074-7090.

[49] K. Ohashi, S. Kosai, M. Arizuka, T. Watanabe, Y. Yamagiwa, T. Kamikawa, M. Kates, Tetrahedron, **1989**, 45, 2557-2570.

[50] M.-Y. Tsai, Y.-T. Sun, J.-C. Lin, *J Colloid Interface Sci*, **2007**, 308, 474-484.

[51] E. M. Chambaz, E. C. Horning, *Anal. Biochem*, **1969**, 30, 7-24.

Chapter 2: The Ligand and Its Immobilization

Introduction

2.1 Phenanthroline

1,10-Phenanthroline (Phen) is a bidentate ligand for transition metal ions commonly used in coordination chemistry. The Phen ligand, which behaves as a weak base in aqueous solution, is electron-poor and a relatively poor σ-donor. Owing to its low σ-donor ability, Phen is very stable. The important structural features of Phen are its planarity, rigidity, and hydrophobicity. The 1,10-isomer is the most basic phenanthroline isomer, which can be attributed to intramolecular bonds between hydrogen and both nitrogen atoms that stabilize the conjugate acid. Scheme 1 shows some isomers of phenanthroline.

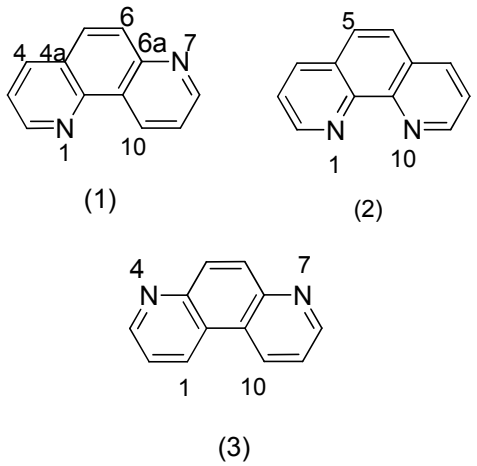

Scheme 1: Various phenanthroline isomers (1) 1,7-, (2) 1,10-, and 4,7-phenanthroline.

The first phenanthroline isomer (1,7-isomer) was synthesized by Skraup and Vortmann in 1882.[1] However, 2-methyl-1,10-phenanthroline was the first *ortho*-phenanthroline reported, as synthesized nine years later by Blau.[2] In nature, there are a few examples of naturally occurring phenanthrolinic skeletons,[3] such as in marine animals (Scheme 2).

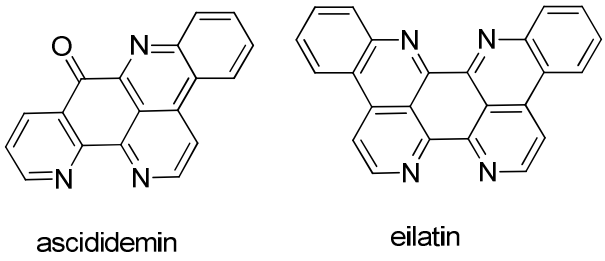

ascididemin eilatin

Scheme 2

There are many derivatives of Phen, but few are commercially available. Generally, the synthesis of substituted phenanthrolines is difficult and gives low yields. The classical method for the preparation of phenanthroline derivatives is the Skraup reaction. This reaction was first applied to the formation of quinoline, which was prepared by heating a mixture of aniline, nitrobenzene, glycerol, and sulfuric acid, but this reaction has the disadvantage of proceeding violently. Besides sulfuric acid, hydrochloric and phosphoric acids can also be employed, but afford lower yields. As an oxidizing agent, arsenic acid is apparently the best, but its toxicity discourages its use.

In my thesis, we performed the synthesis of two phenanthrolines, the first being 4-MePhen. The first synthesis of 4-MePhen was published by Case.[4] In this synthesis, 8-aminolepidine and glycerol were reacted in the presence of diarsenic pentoxide but the yield was low at 15%. Over the subsequent years, other processes have been employed, but yields of less than 50% still presented a problem. Bernhard and coworkers[5] synthesized 4-MePhen in 51% yield using 8-aminoquinoline and methylvinylketone in the presence of sodium iodide as a catalyst,[6] as shown in Scheme 3.

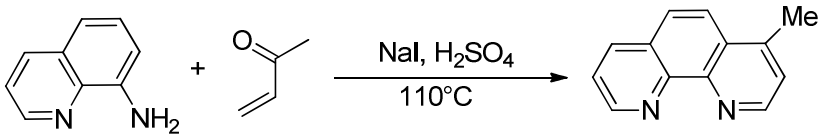

Scheme 3

The results of this synthesis demonstrated that the product was impure, and separation by chromatography on silica was required. For several years, our research group has studied phenanthrolines as ligands in catalysis. This previously reported synthesis was repeated by our group, but the synthesized phenanthroline was still very impure. For this reason, a purification method was developed using a zinc complex, which will be discussed later.

The second phenanthroline derivative used in this thesis was 4-OH-Phen. The synthesis was performed in our research group by adapting the procedure reported in the literature.[7] Both 4-MePhen and 4-OH-Phen could be immobilized on the protective layer of the MNPs and finally tested in catalysis.

Results and Discussion

2.2. Synthesis of 4-MePhen

In this synthesis, we employed methyl vinylketone and 8-aminoquinoline in H_2SO_4 with 3-nitrobenzenesulfonic acid as an oxidant (Scheme 4). The use this oxidant instead of NaI was motivated by the search for a reagent that affords a product with higher purity. The synthesized phenanthroline derivative was still impure (figure 29,30), but fewer colored impurities were present, as judged by the color of the product. In any case, purification of the product is still required.

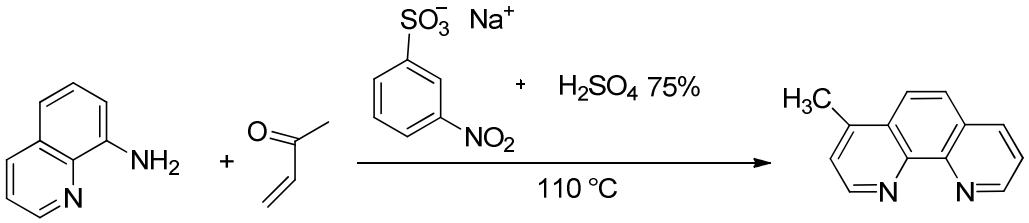

Scheme 4

The purification method developed in our research group involves the formation of a complex with zinc chloride (Scheme 5). The first important feature of this process was finding an appropriate solvent. In this case, we required a solvent in which both $ZnCl_2$ and the phenanthroline derivative have good solubility, but the complex is insoluble. The choice of a suitable solvent is very important, for example, methanol has too a low polarity to dissolve zinc chloride efficiently.

Further, polar and aprotic solvents, such as DMF and DMSO, could not be used because they strongly coordinate zinc, leading to its deactivation. Among the available solvents, ethylene glycol was found to be the solvent of choice, affording the complex with an acceptable degree of purity.

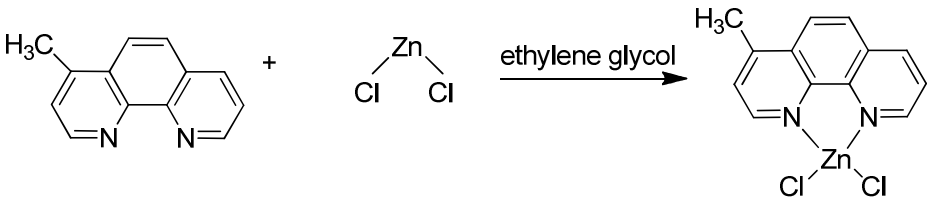

Scheme 5

After formation of the complex, we performed two crystallizations, again using ethylene glycol. The free ligand was then obtained by treating the complex with aqueous ammonia (Scheme 6). The advantage of this process is that $[Zn(NH_3)_4]^{2+}$ is formed, which is soluble in the water phase, without forming any intermediate insoluble species, allowing recovery of the ligand by extraction with CH_2Cl_2. The final product (figure 31,32) is suitable for immobilization on the protective layer.

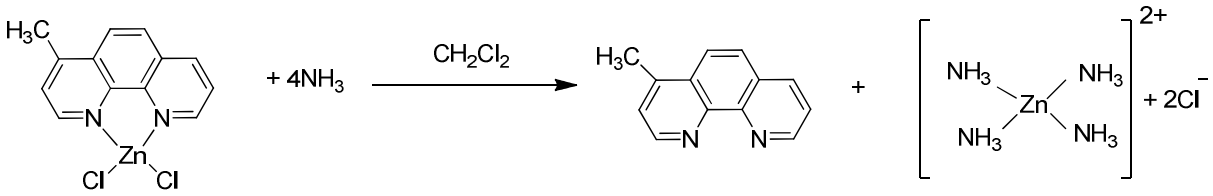

Scheme 6

^{1}H NMR (300 MHz, $CDCl_3$, 300 K): δ = 9.22 (dd, $^3J_{H,H}$ = 4.3 Hz and $^4J_{H,H}$ = 1.7 Hz, 1H, H9), 9.09 (d, $^3J_{H,H}$ = 4.5 Hz, 1H, H2), 8.28 (dd, $^3J_{H,H}$ = 8.1 Hz and $^4J_{H,H}$ = 1.8 Hz, 1H, H7), 8.04 (d, $^3J_{H,H}$ = 9.1 Hz, 1H, H5), 7.85 (d, $^3J_{H,H}$ = 9.1 Hz, 1H, H6), 7.64 (dd, $^3J_{H,H}$ = 4.3 and 8.1 Hz, 1H, H8), 7.50 (d, $^3J_{H,H}$ = 4.5 Hz, 1H, H3), 2.81 (s, 3H, CH_3) ppm.

2.3 Immobilization of 4-MePhen on the protective layer

Immobilization of 4-MePhen on the protecting layer (Scheme 7) was achieved by adapting a reaction previously reported for the free ligand.[8] The methyl group at the 4 can be lithiated with LDA and then alkylated.

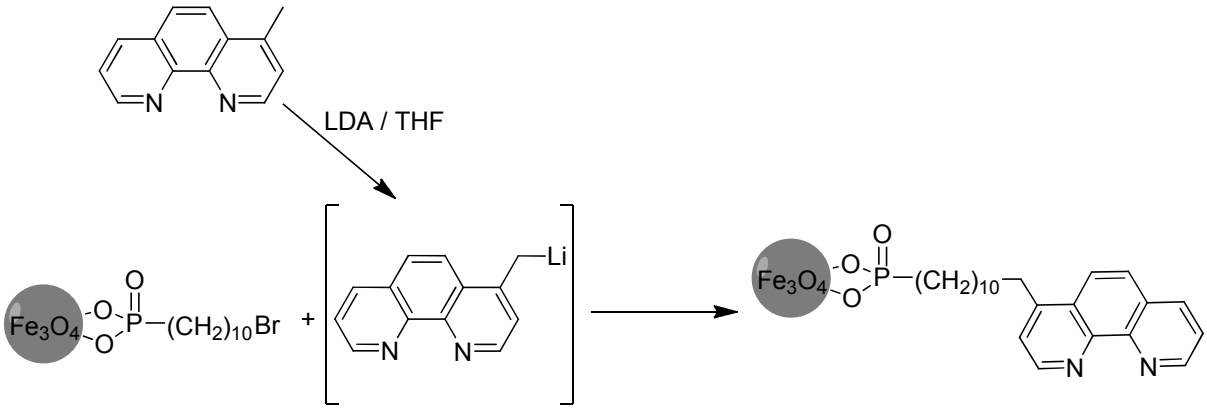

Scheme 7

During this thesis, we initially changed the immobilization procedure systematically according to the conditions given in Table 6 because the initial attempt gave a low amount of immobilized phenanthroline on the protective layer of MNPs. Among the many attempts, the procedure that produced the best results was synthesis V (Table 6). In this synthesis, the nanoparticles were initially placed in a sonication bath for 14 h to prevent aggregation; principally, sonication acts to stabilize the nanoparticles, suggesting a physical process. During the various attempts, we showed the importance of the sonication time for successful immobilization owing to increased dispersion. This procedure was also performed with freshly synthesized MNPs to exclude the interpretation that aggregation of nanoparticles synthesized a long time previously led to the poor results.

In the literature, functionalization as a consequence of a reaction is usually taken for granted and no tests are carried out to check that functionalization actually occurs or if secondary reactions also occur. As phenanthroline forms strong complexes with iron, we were worried about the possibility of this ligand being coordinated to the nanoparticle surface. The first attempt to verify the success of immobilization was performed using the procedure for quantification of the MNPs by destruction; however, it was not possible to use the same methodology because of problems with the formation of a red solution and undissolved material during the destruction with HCl. When we carry out the same procedure without phenanthroline, the obtained solution was yellow and no

precipitate appeared. We attributed these observations to the possible formation of ferroin. Other methods for verifying immobilization were tested, such as complexation with EDTA, potassium fluoride, or thiocyanate, but the results were not conclusive because iron/phenanthroline complexes could form after the reactions.

Thus, to verify that immobilization actually occurred, we synthesized a Mo carbonyl complex on the protected MNPs, Mo(4-MePhen)$(CO)_4$, recorded the IR spectrum, and compared the spectrum with that of a monomeric complex prepared from 4-MePhen under otherwise identical conditions. The complex was prepared by adapting a literature procedure for the corresponding complex of unsubstituted phenanthroline.[9]

The IR spectrum of the complex with MNPs recorded in dry toluene (Figure 23) showed four bands at 2011 (w), 1900 (s), 1886 (m), and 1845 (m) cm^{-1}. The bands in the carbonyl region were very intense, demonstrating the formation of the monomeric complex (Scheme 8). The spectrum of the nanoparticles after functionalization with phenanthroline and reaction with $Mo(CO)_6$ in dry toluene was also recorded (Figure 24). The intensity of the absorption bands was lower owing to limited dispersibility, but the spectrum clearly showed four bands at 2009 (w), 1899 (s), 1877 (m), 1839(m) cm^{-1}. Taking into account that small differences in the frequencies are expected owing to the different environment around the complex and that the intensity pattern is the same for the two spectra, a comparison of these spectra proves that phenanthroline is bound to the nanoparticles in a way that allows further coordination to the nitrogen atoms, as desired (Scheme 9).

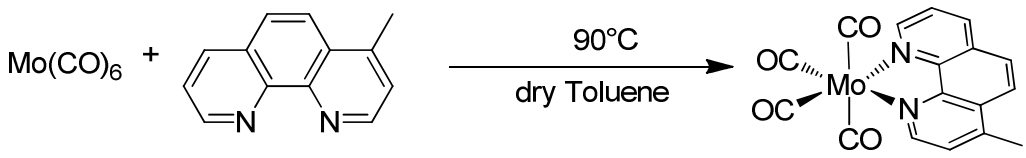

Scheme 8

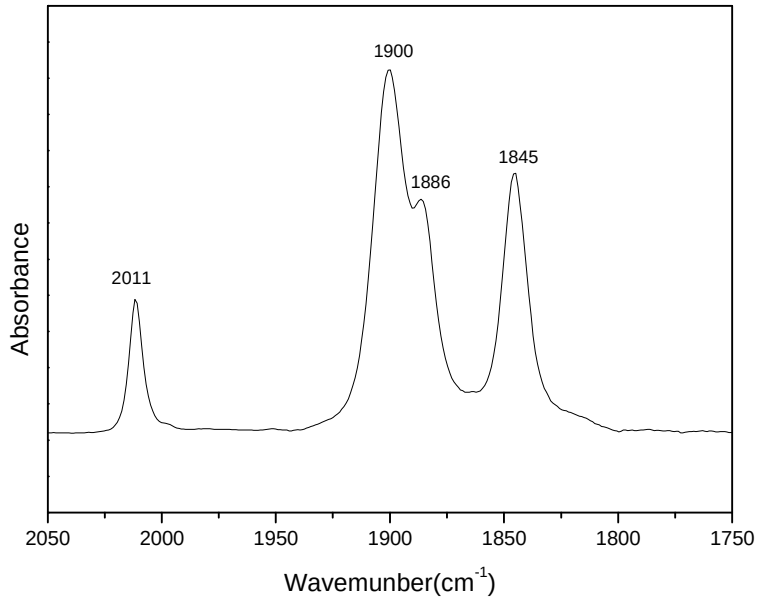

Figure 23: IR spectrum of monomeric complex Mo(4-MePhen)$(CO)_4$ in toluene.

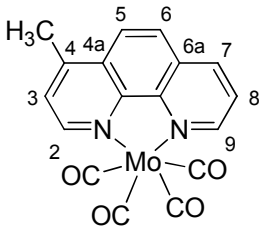

^{1}H NMR (300 MHz, $CDCl_3$) δ 9.48 (d, *J* = 4.6 Hz, 1H, H9), 9.31 (d, *J* = 5.1 Hz, 1H, H2), 8.41 (d, *J* = 8.1 Hz, 1H, H7), 8.13 (d, *J* = 9.0 Hz, 1H, H5), 7.97 (d, *J* = 9.1 Hz, 1H, H6), 7.73 (dd, *J* = 8.1, 5.0 Hz, 1H, H8), 7.57 (d, *J* = 5.1 Hz, 1H, H3), 2.90 (s, 3H, CH_3) ppm. Attribution of the ^{1}H NMR signals is based on the correspondence with those of the free ligand. (figure 33)

^{13}C NMR (75 MHz, $CDCl_3$) δ 223.34 (C), 205.46 (C), 153.29 (CH), 152.79 (CH), 146.27 (C), 136.57(CH), 130.09 (C), 129.93 (C), 126.93 (CH), 125.73 (CH), 124.46 (CH), 123.77 (CH), 19.46 (CH_3) ppm. Signals corresponding to the carbonyl carbons could not be detected. (figure 34)

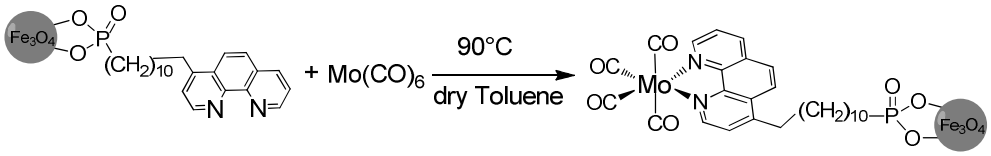

Scheme 9

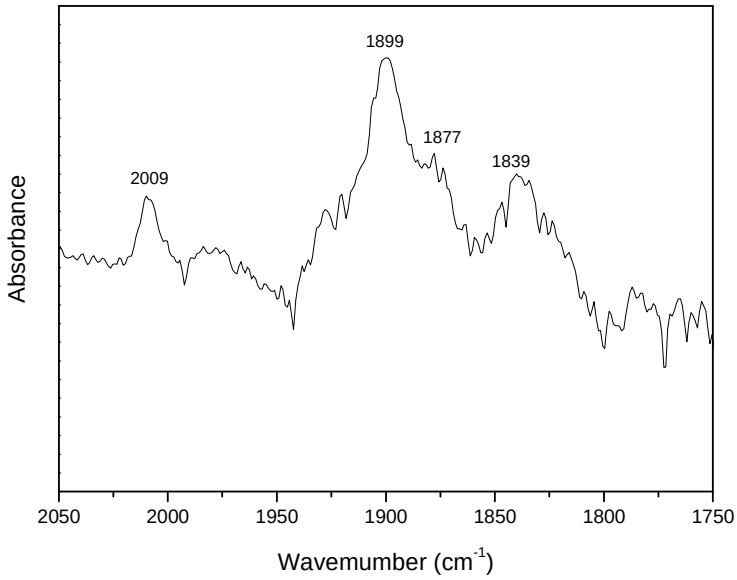

Figure 24: IR spectrum of the Mo complex with 4-MePhen immobilized on the protective layer of MNPs in toluene.

In an attempt to obtain a more defined spectrum for the supported particles, we recorded an ATR spectrum of the Mo carbonyl complex with the MNPs to verify the success of the immobilization (Figure 25). Although the spectrum is less defined than that in solution, it show signals at 2013(w), 1899(s), 1868(m), and 1830 (m) cm^{-1}, which again support efficient immobilization.

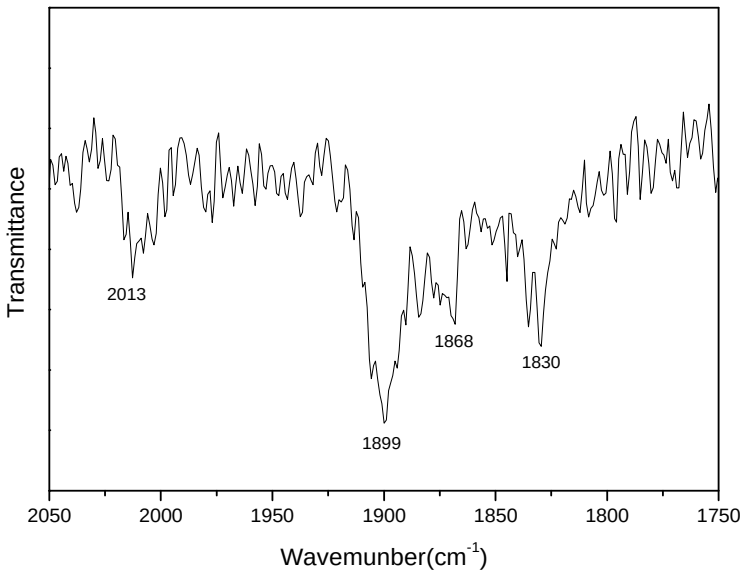

Figure 25: ATR spectrum of the Mo complex with 4-MePhen immobilized on the protective layer of MNPs.

Having clarified that phenanthroline was effectively bound to the nanoparticles, we turned to the problem of quantifying the extent of immobilization. Among the various existing techniques, we found that it was possible to use elemental analysis to quantify the amount of nitrogen present following immobilization, as the only source of nitrogen is 4-MePhen in the sample. We used this technique as an indication of the success of immobilization by comparing the value predicted for complete substitution of all bromine atoms by phenanthroline with the experimental values. Calculations allowed us to conclude that only about 45% of the bromine atoms were functionalized and the others were most likely unchanged, as summarized in Table 6.

Table 6. Attempts to immobilize 4-MePhen on the protective layer.

Synthesis		% C		% H		%N	
	Ligand	Calculated	Found	Calculated	Found	Calculated	Found
I	**4-MePhen**[a]	42.41	25.44	4.81	4.29	4.30	0.13
II	**4-MePhen**[a]	42.41	25.11	4.81	4.33	4.30	0.19
III	**4-MePhen**[a]	42.41	30.22	4.81	4.44	4.30	1.48
IV	**4-MePhen**[a]	42.41	32.89	4.81	4.47	4.30	2.26
V	**4-MePhen**[a]	42.41	31.97	4.81	4.40	4.30	2.28
VI	**4-MePhen**[b]	42.41	31.39	4.81	4.27	4.30	2.04

a) In the syntheses I-V a 1.5 excess of 4-MePhen with respect to the estimated bromine content in the protective layer was used.
b) In synthesis VI a 3.0 excess of 4-MePhen with respect to the estimated bromine content in the protective layer was used..

In synthesis VI (Table 6), we tested the immobilization process with a three-fold excess of 4-MePhen with respect to the protective layer under the same conditions as the other attempts. These conditions were expected to result in about twice the extent of immobilization achieved in synthesis V. However, the immobilization unfortunately did not have the expected result. The conditions for immobilization are extremely delicate and any small changes interfere dramatically with the results, making reproducibility difficult. Although only approximately 50% immobilization was achieved, as demonstrated in synthesis V, we proceeded to test these nanoparticles in catalysis.

We also considered a different way of attaching phenanthroline to the nanoparticle surface by taking advantage of a substitution reaction between a bound alkyl bromide and a phenolate anion. For this reason, we synthesized 4-OH-Phen, in the hope that a better functionalization level could be achieved.

2.4 Synthesis of 4-OH-Phen

4-OH-Phen was prepared by adapting the literature procedure.[7] 8-Aminoquinoline was initially treated with Meldrum's acid in triethyl orthoformate (first step) to give an adduct that cyclizes to 4-OH-Phen on refluxing in diphenyl ether (second step) (Scheme 10). The synthesis procedure is faster in comparison with that of 4-MePhen and moreover, no purification is needed. The obtained product can be used directly for immobilization on the protective layer.

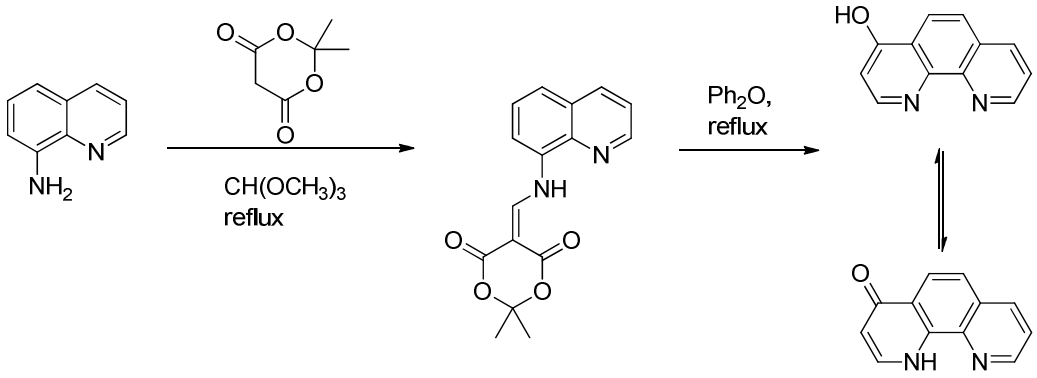

Scheme 10

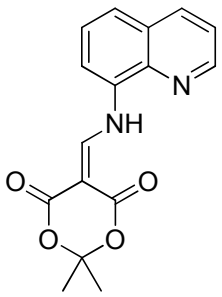

First Step: ^{1}H NMR (300 MHz, $CDCl_3$, 300 K) δ 12.86 (br d, $^{3}J_{H,H}$ = 14.9 Hz, 1H, NH), 9.02 (dd, $^{3}J_{H,H}$ = 4.2 Hz and $^{4}J_{H,H}$ = 1.6 Hz, 1H, H2), 8.94 (d, $^{3}J_{H,H}$ = 14.9 Hz, 1H, H-olefinic), 8.23 (dd, $^{3}J_{H,H}$ = 8.3 Hz and $^{4}J_{H,H}$ = 1.6 Hz 1H, H4), 7.73–7.69 (m, 2H, H5 and H7), 7.61 (ps t, $^{3}J_{H,H}$ = 7.8 Hz, 1H, H6), 7.56 (dd, $^{3}J_{H,H}$ = 8.3 and 4.2 Hz, 1H, H3), 1.80 (s, 6H, CH_3) ppm.

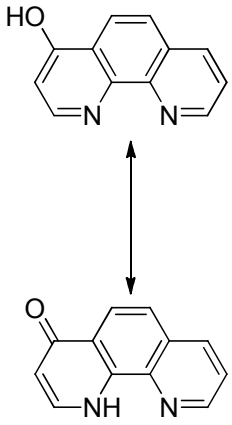

Second Step: ^{1}H NMR (300 MHz, $CDCl_3$, 300 K) δ 10.47 (br, 1H, NH), 8.93 (dd, $^{3}J_{H,H}$ = 4.3 Hz and $^{4}J_{H,H}$ = 1.6 Hz, 1H, H9), 8.42 (d, $^{3}J_{H,H}$ = 8.9 Hz, 1H, H5), 8.28 (dd, $^{3}J_{H,H}$ = 8.2 Hz and $^{4}J_{H,H}$ = 1.6 Hz, 1H, H7), 7.85 (dd, $^{3}J_{H,H}$ = 7.5 and 5.8 Hz, 1H, H2), 7.67 (d, $^{3}J_{H,H}$ = 8.9 Hz, 1H, H6) overlapping with 7.64 (dd, $^{3}J_{H,H}$ = 8.2 and 4.3 Hz, 1H, H8), 6.57 (dd, $^{3}J_{H,H}$ = 7.5 Hz and $^{4}J_{H,H}$ = 1.6 Hz, 1H, H3) ppm.

2.5 Immobilization of 4-OH-Phen on the protective layer

The immobilization (Scheme 11) was performed according to a procedure adapted from the literature.[10]

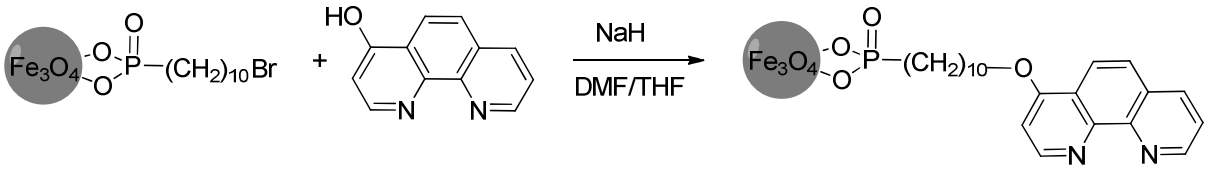

Scheme 11

As for the 4-MePhen immobilization procedure, we carried out several attempts to immobilize 4-OH-Phen on MNPs. Even the initial results realized better substitution efficiency than that achieved with the methylated phenanthroline. The first attempt was performed using sodium hydride and 4-OH-Phen in a DMF/THF solvent mixture, as reported in the literature.[9] The MNPs were first put in

a sonication bath for 8 h, and then transferred to an equilibrated dropping funnel and slowly dropped into a solution containing the phenanthroline. In the second attempt, the influence of temperature was tested. After addition of the reagents, the reaction was heated and, as a result, the amount of bound phenanthroline doubled, but the results were still below the expectations.

We returned to the initial idea on the importance of sonicating the nanoparticles, and the best conditions confirmed the importance of this physical process. Immediately after addition of MNPs to 4-OH-Phen, we placed the reaction flask in a sonication bath overnight. This procedure differs with respect to previous attempts, even with 4-MePhen, in that only the nanoparticles had been sonicated in those cases. The best results (Table 7, synthesis V) confirmed the success of the immobilization process.

To verify the success of this immobilization process, we used the same procedures as previously described. We synthesized a Mo carbonyl complex on the protected MNPs, recorded the IR spectrum, and compared the obtained spectrum with that of a monomeric complex prepared from 4-MeO-Phen under otherwise identical conditions (Scheme 12). The bands in the carbonyl region were very intense, demonstrating the formation of the monomeric complex (Scheme 12). The spectrum of the monomeric complex in dry toluene (Figure 26) showed four bands at 2011 (w), 1898 (s), 1883 (m), and 1843 (m) cm^{-1}. Similar to other verifications, the bands in the carbonyl region were very intense, demonstrating the formation of the monomeric complex. The spectrum of the complex with the protected MNPs in dry toluene (Figure 27) showed four bands at 2008 (w), 1895 (s), 1869 (m), and 1829(m) cm^{-1}. The similarity between these spectra again proves that the phenanthroline is bound to the nanoparticles in a way that allows further coordination to the nitrogen atoms, as desired.

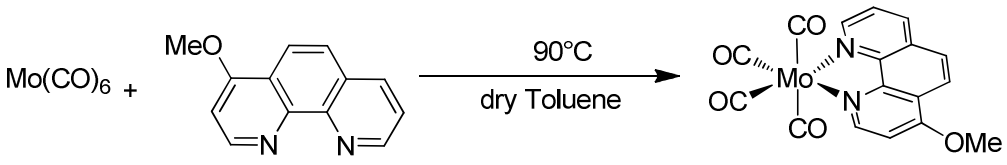

Scheme 12

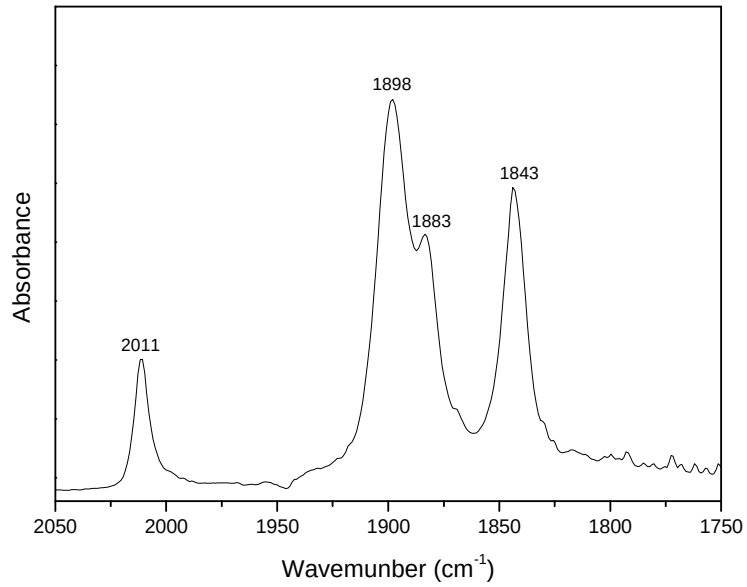

Figure 26: IR spectrum of the monomeric Mo carbonyl complex with 4-MeO-Phen in toluene.

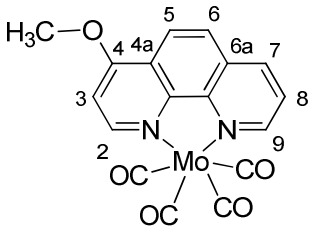

^{1}H NMR (300 MHz, $CDCl_3$) δ 9.44 (t, *J* = 8.7 Hz, 1H, H9), 9.24 (d, *J* = 5.7 Hz, 1H, H2), 8.39 (d, *J* = 8.0 Hz, 1H, H7), 8.29 (t, *J* = 12.3 Hz, 1H, H5), 7.88 (t, *J* = 11.9 Hz, 1H, H6), 7.70 (dd, *J* = 7.7, 5.0 Hz, 1H, H8), 7.12 (d, *J* = 5.7 Hz, 1H, H3), 4.20 (s, 3H, OCH_3) ppm. (figure 35)

^{13}C NMR (75 MHz, $CDCl_3$) δ 223.28 (C), 222.73 (C), 205.31 (C), 162.77 (C), 154.18 (CH), 152.77 (CH), 146.87 (C), 146.21 (C), 136.36 (CH), 129.91 (C), 125.68 (CH), 124.20 (CH), 122.17 (C), 121.19 (CH), 104.79 (CH), 56.95 (CH_3) ppm. (figure 36)

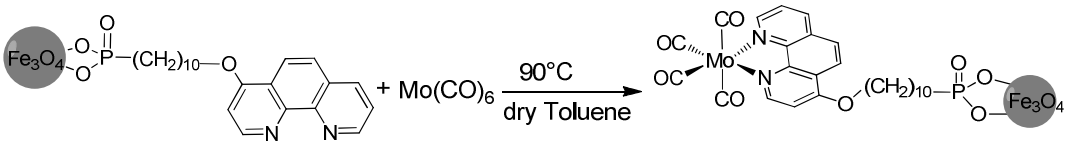

Scheme 13

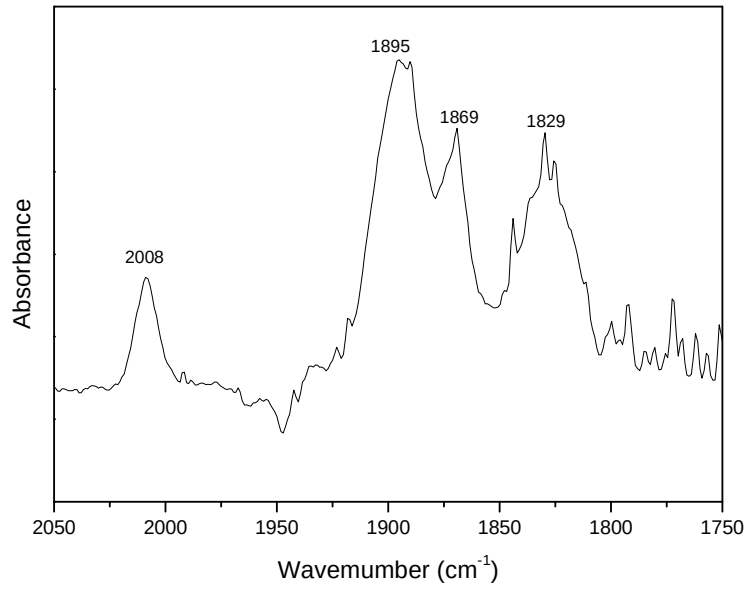

Figure 27: IR spectrum of the Mo carbonyl complex with the 4-OH-Phen on the protective layer of MNPs in toluene.

We also recorded the ATR spectrum of the Mo carbonyl complex on the protected MNPs (Scheme 13) to further prove the success of immobilization (Figure 28). The ATR spectrum showed signals at 2010 (w), 1895 (s), 1869 (m), and 1829 (m) cm^{-1}, which are very close to the values for the solution spectrum.

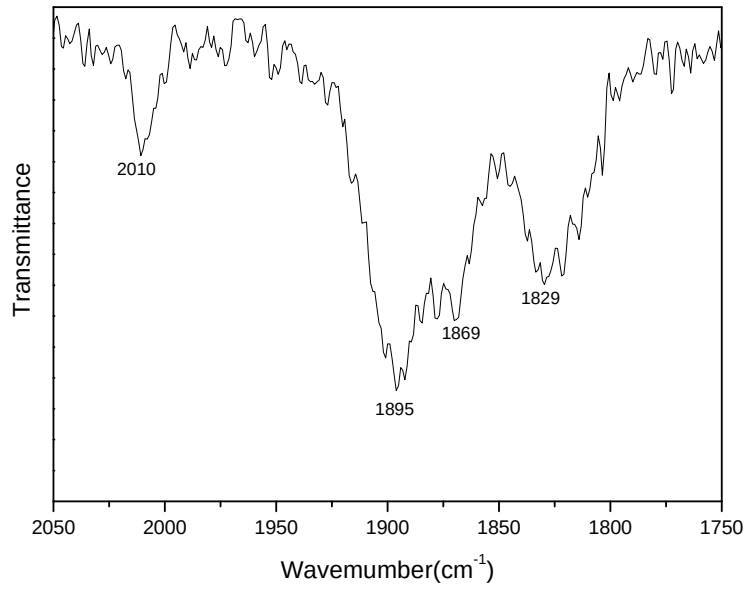

Figure 28: ATR spectrum of the Mo carbonyl complex 4-OH-Phen on the protective layer of MNPs.

We then used elemental analysis to compare the values predicted for complete substitution of all bromine atoms by phenanthroline with the experimental values.

Table 7. Attempts to immobilize 4-OH-Phen on the protective layer.

Synthesis		% C		% H		%N	
	Ligand	**Calculated**	**Found**	**Calculated**	**Found**	**Calculated**	**Found**
I	**4-OH-Phen[a]**	39.25	33.63	4.34	5.08	4.16	0.79
II	**4-OH-Phen[b]**	39.25	25.22	4.34	2.89	4.16	1.54
III	**4-OH-Phen[b]**	39.25	27.65	4.34	3.41	4.16	2.77
IV	**4-OH-Phen[b]**	39.25	36.50	4.34	4.35	4.16	3.72
V	**4-OH-Phen[b]**	39.25	37.57	4.34	4.45	4.16	3.95

a) In the syntheses I, a 1.5 excess of 4-OHPhen with respect to the estimated bromine content in the protective layer was used

b) a) In the syntheses II-V a 3.0 excess of 4-OHPhen with respect to the estimated bromine content in the protective layer was used.

2.6 Coordination of $Pd(OAc)_2$ to nanoparticles

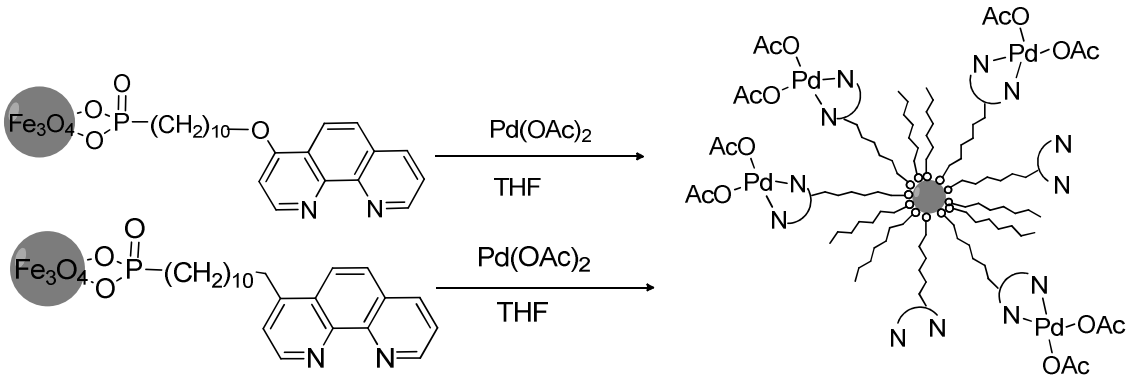

Scheme 14

We carried out various tests to examine palladium coordination to the functionalized nanoparticles (Scheme 14). Factors such as temperature, solvent, sonication time, and amount of palladium in excess to phenanthroline immobilized on the protective layer were examined. The best

results, as determined from the results of catalytic tests, were obtained when the coordination was carried out at RT using THF as the solvent and a four-fold excess of palladium with respect to phenanthroline immobilized on the protective layer. The same coordination procedure was used for both phenanthroline derivatives.

After coordination with palladium, the nanoparticles were separated and washed several times until the amount of extracted solid was less than 2 mg to ensure that the recorded catalytic activity is not due to excess amounts of palladium.

Experimental Section

2.7 Synthesis of 4-MePhen

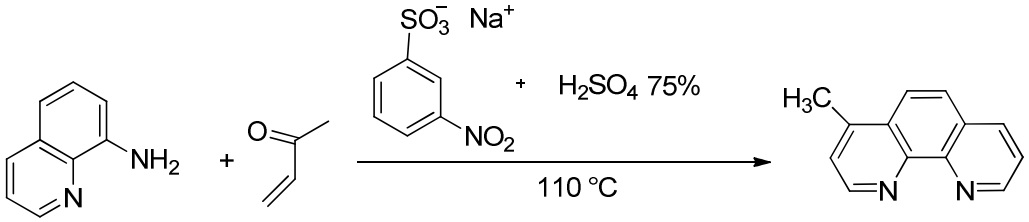

Reagent	M.W (g•mol^{-1})	g	mmol	Molar ratio	V [mL]	d[g/mL]
8-aminoquinoline (98%)	144.17	1.94	13.5	1		
1-Buten,3one (99%)	70.1		22.9	1.7	2.0[a]	0.842
3-nitrobenzenesulfonic acid (98%)	225.16	6.37	28.3	2.1		
H_2SO_4 (75%)					50	

[a] slight excess over the theoretical calculation.

Sulfuric acid, 8-aminoquinoline, and 3-nitrobenzenesulfonic acid were added under stirring to a 250 mL three-neck round bottom flask. The suspension was heated to 90 °C to help dissolve the reagents. Once the reagents were dissolved, the temperature was increased to 110 °C. At this temperature, 1-butene-3-one was slowly added over 6 h using a syringe pump. After the addition, the solution was stirred for a further hour and then neutralized with a 5 M NaOH solution. The solution was extracted with CH_2Cl_2 (4 × 200 mL) and re-extracted with 37% HCl (3 × 25 mL). The solution was returned to a basic pH with the addition of 65 mL of 9 M NaOH solution. The solution was then extracted with CH_2Cl_2 (3 × 70 mL), and the product was dried over Na_2SO_4. The solvent was evaporated under vacuum affording 1.88 g (9.68 mmol, 71.70%) of the crude product (see Figures 29 and 30 for the corresponding ^{1}H NMR spectrum).

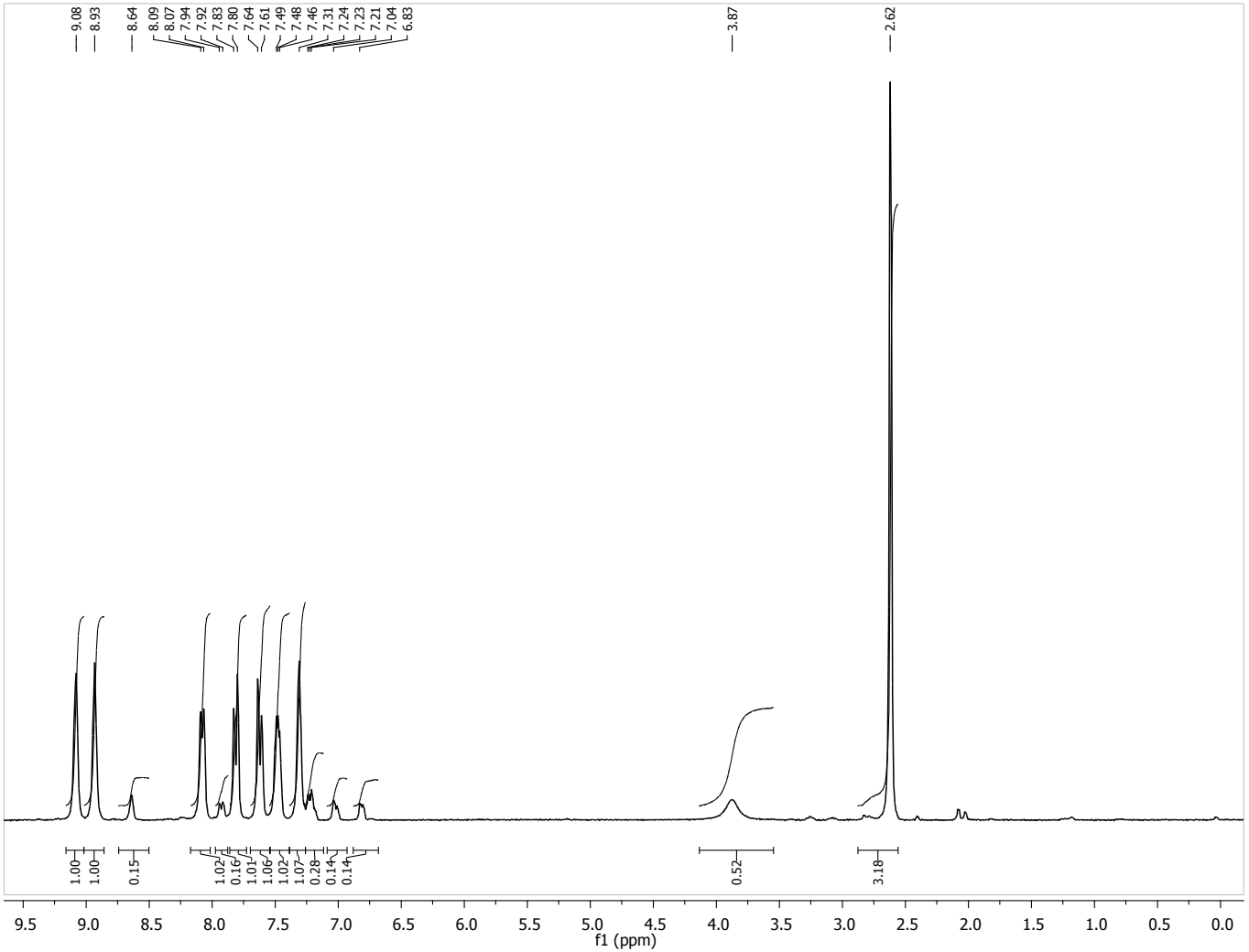

Figure 29: ^{1}H NMR (400 MHz, $CDCl_3$, 298 K) spectrum of impure 4-MePhen.

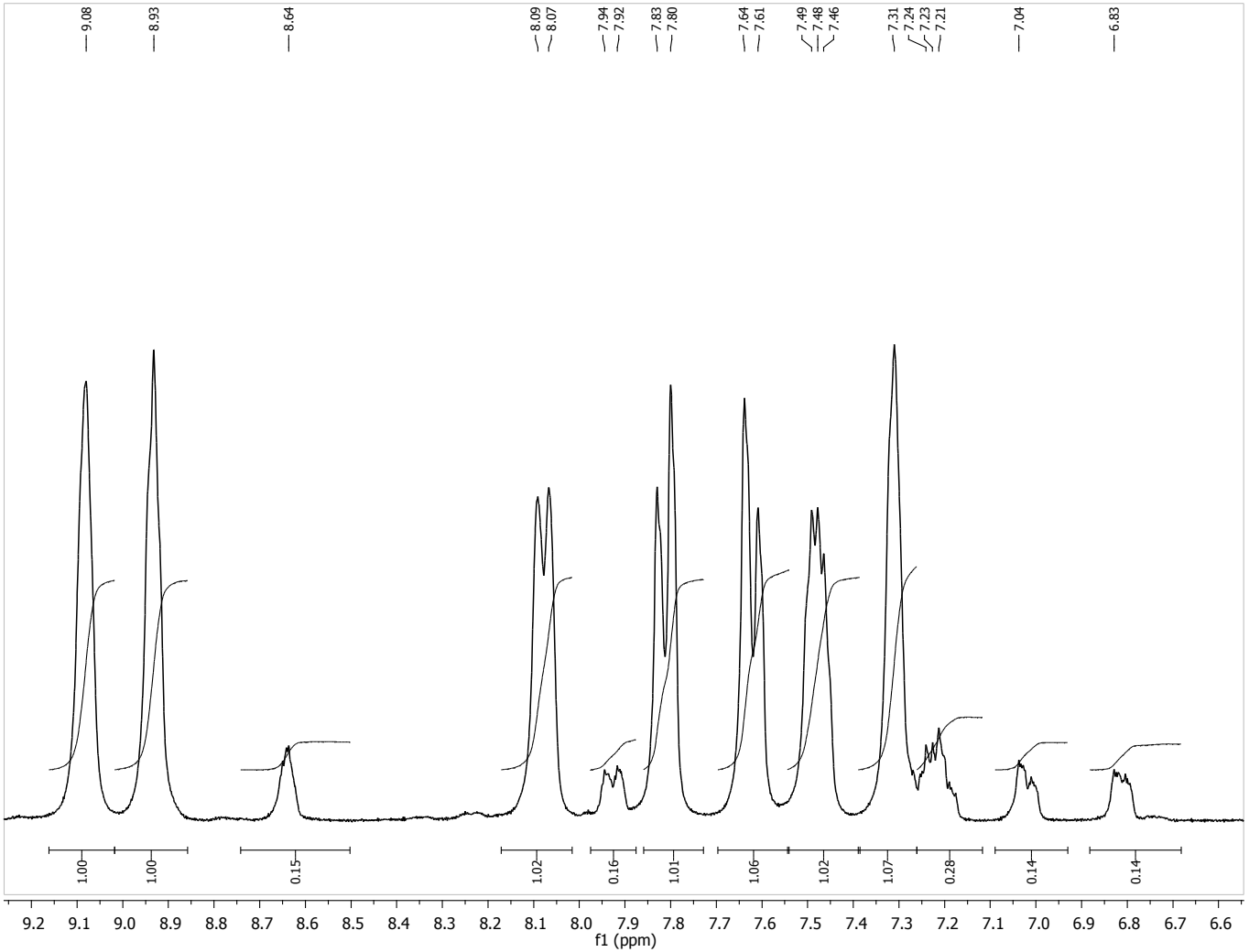

Figure 30: Expanded ^{1}H NMR (400 MHz, $CDCl_3$, 298 K) spectrum of impure 4-MePhen.

-

2.8 Purification of the 4-MePhen

2.8.1 Complexation

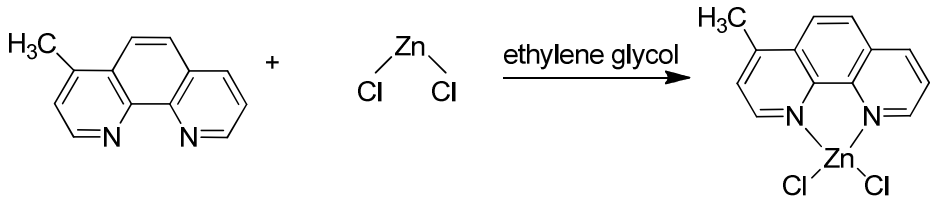

Reagent	M.W ($g \cdot mol^{-1}$)	g	mmol	Molar ratio	V [mL]	d[g/mL]
Raw Product [a]	194.24	1.88	9.68	1		
$ZnCl_2$	136.30	1.98	14.5	1.5		

[a] It was considered that the product obtained was only the phenanthroline.

The raw product and ethylene glycol (5 mL) were added to a 50 mL round bottom flask. The reaction mixture was heated at 55 °C for 1 h. In another 50 mL round bottom flask, $ZnCl_2$ was dissolved in ethylene glycol (5 mL). The second solution was then added to the first one under stirring. After the addition, the temperature was increased to 100 °C and the reaction mixture was maintained at this temperature for 1 h. Subsequently, the formed suspension was allowed to cool to RT under stirring. The obtained suspension was diluted with 5 mL of MeOH to decrease the viscosity and facilitate filtration. The final product was separated by filtration on a Buchner funnel and washed with ethyl ether (3 × 5 mL). The solvent was evaporated under vacuum affording 3.52 g of the zinc complex (10.6 mmol, 91.0%, assuming the starting material is perfectly pure, which is not the case).

2.8.2 Crystallization

Reagent	Complex (g)	Solvent (ml)	Yield (%)
1° Crystallization	3.5184	15	98.7
2° Crystallization	2.3622	10	68.0

Crystallization was performed by dissolving the complex in ethylene glycol at reflux for 3 h. Subsequently, the solution was allowed to cool to RT and 10 mL of MeOH was added. The solid was separated by filtration on a Buchner funnel, washing with a little ethyl ether. This procedure was repeated two times. The first crystallization yielded 3.47 g (10.50 mmol, 98.7%) of product, and the second 2.36 g (7.14 mmol, 68%).

2.8.3 Decomplexation

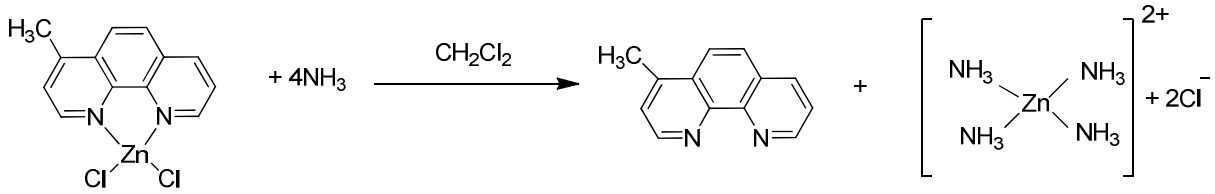

Reagent	M.W ($g \cdot mol^{-1}$)	g	mmol	Molar ratio	V [mL]	d[g/mL]
Complex	330.54	2.36	7.14			
NH_3 28%					23.6	
CH_2Cl_2					23.6	

To a flask containing the complex were added NH_3 and CH_2Cl_2, and the biphasic mixture was stirred for 16 h. During this time, zinc passed into the aqueous phase as its ammonia complex, whereas free 4-MePhen remained in the organic phase. After separation of the phases, the aqueous phase was further extracted with CH_2Cl_2 (3 × 15 ml). The combined organic extracts were dried over Na_2SO_4. The solvent was evaporated under vacuum affording 1.0769 g (5.55 mmol, 77.73%) of free purified ligand.

^{1}H NMR (300 MHz, $CDCl_3$) δ 9.22 (dd, $^3J_{H,H}$ = 4.3 Hz and $^4J_{H,H}$ = 1.7 Hz, 1H, H9), 9.09 (d, $^3J_{H,H}$ = 4.5 Hz, 1H, H2), 8.23 (dd, $^3J_{H,H}$ = 8.1 Hz and $^4J_{H,H}$ = 1.8 Hz, 1H, H7), 8.07 (d, $^3J_{H,H}$ = 9.1 Hz, 1H, H5), 7.83 (d, $^3J_{H,H}$ = 9.1 Hz, 1H, H6), 7.64 (dd, $^3J_{H,H}$ = 4.3 and 8.1 Hz, 1H, H8), 7.49 (d, $^3J_{H,H}$ = 4.5 Hz, 1H, H3), 2.81 (s, 3H, CH_3) ppm. (figure 31, 32)

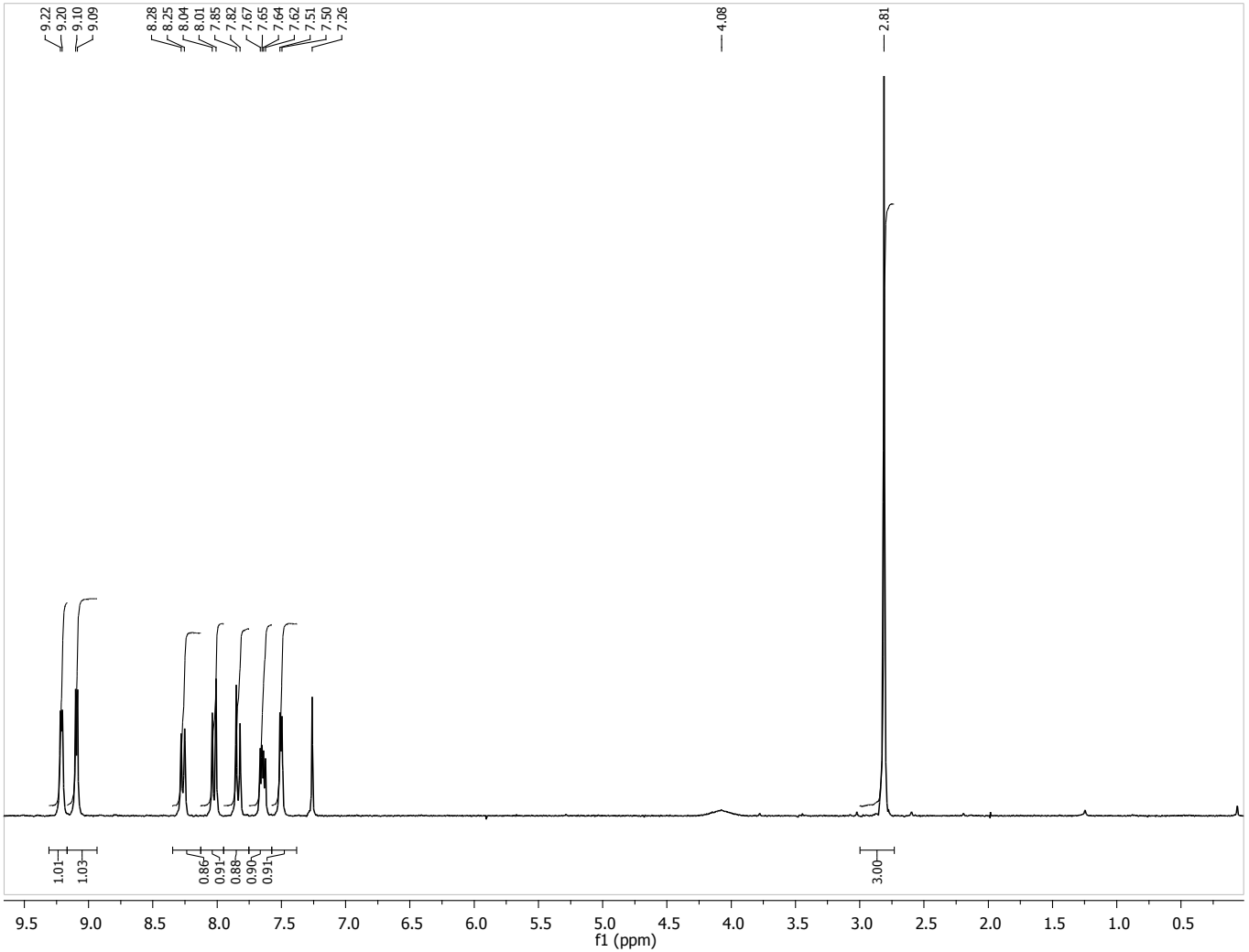

Figure 31: ^{1}H NMR (300 MHz, $CDCl_3$ 298 K) spectrum of purified 4-MePhen.

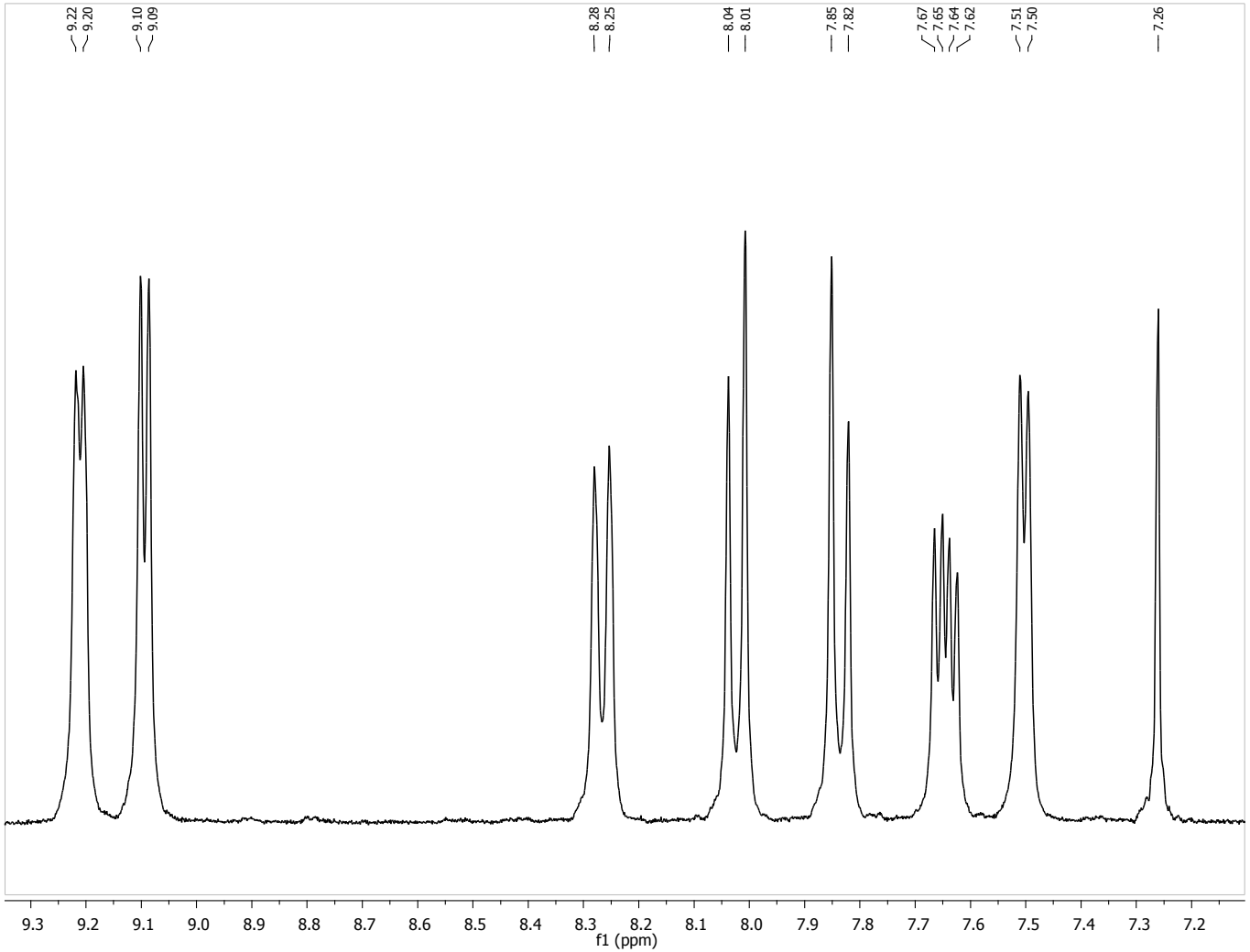

Figure 32: Expanded ^{1}H NMR (300 MHz, $CDCl_3$, 298 K) spectrum of purified 4-MePhen.

2.9 Immobilization of 4-MePhen on the protective layer

2.9.1 Test I

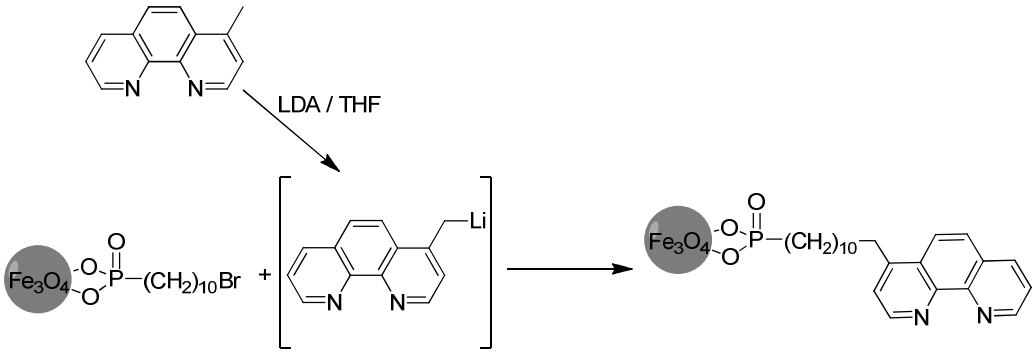

Reagent	M.W ($g \cdot mol^{-1}$)	mg	mmol	Molar ratio	V [mL]	d[g/mL]
4- MePhen	194.24	109.8	0.5653	1.5		
THF dry					16 + 5	
LDA (2M)	107.12		0.678	1.8	0.340	0.812
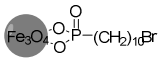	301.16	113.5[a]	0.3769	1		

[a] Amount of functionalized phosphonic acid bound to 200.8 mg of nanoparticles (protection level 56,54 %)

The reaction was performed under a N_2 atmosphere, and 4-MePhen used in the synthesis was dried. To a 50 mL Schlenk tube were added 200.8 mg of protected MNPs and 5 mL of THF, and the dispersion was sonicated for 4 h. To another 50 mL Schlenk tube were added 109.8 mg of 4-MePhen and 16 mL of THF. The latter solution was cooled with an acetone/dry ice bath. When the temperature reached -78 °C, 0.340 mL of LDA (2 M) were added in one shot to the 4-MePhen solution, after which the solution was left to stir at the same temperature for 1 h. Then, it was transferred to a dropping funnel using a Teflon cannula.

In this first immobilization attempt, lithiated 4-MePhen was added to the MNP dispersion. The dropwise addition lasted 3 h, and the temperature was maintained at -78 °C. After the addition, the temperature was increased to 0 °C and the solution was left at this temperature for 2 h under stirring. Then, the solution was allowed to reach RT overnight. The next morning, the reaction was stopped by adding 4 mL of Milli-Q water. Then, the obtained product was subjected to the washing

process. For such processes, magnetic separation with magnets could be used in addition to centrifugation. After the initial separation, the first wash was performed by adding 10 mL of Milli-Q water, stirring (10 min), sonicating (15 min), and finally separating. This same procedure was repeated with MeOH (3 × 10 mL), THF (10 mL), and CH_2Cl_2 (10 mL). After the washing process, the solid was dried in vacuo, affording 151.0 mg.

Elemental analysis was carried out to analyze the effectiveness of immobilization.
Calculated: C% 42.41, H% 4.81, N% 4.30.
Found: C% 25.44, H% 4.29, N% 0.13.

2.9.2 Test II

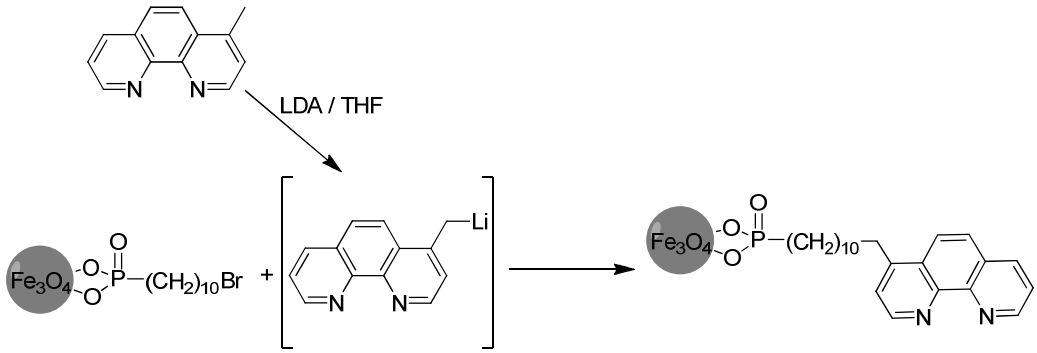

Reagent	M.W (g•mol^{-1})	mg	mmol	Molar ratio	V [mL]	d[g/mL]
4- MePhen	194.24	218.7	1.12	1.5		
THF dry					32+10	
LDA (2M)	107.12		1.35	1.8	0.680	0.812
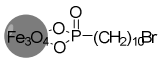	301.16	226.4[a]	0.75	1		

[a] Amount of functionalized phosphonic acid bound to 400.5 mg of nanoparticles (protection level 56,54 %)

The reaction was performed under a N_2 atmosphere, and 4-MePhen used in the synthesis was dried. In a 50 mL Schlenk tube, 400.5 mg of protected MNPs were put in a sonication bath for 6 h. In another 100 mL Schlenk tube, 218.7 mg of 4-MePhen was added to 32 mL of THF under agitation. When the temperature reached -78 °C, 0.680 mL of LDA (2 M) was added to 4-MePhen and the solution was maintained at this temperature under stirring for 1 h.

In this second immobilization attempt, the order of addition was inverted. In this case, the MNPs were added dropwise into the 4-MePhen/LDA solution over 2 h at -78 °C. Subsequently, the reaction mixture was allowed to reach RT overnight. The next morning, the reaction was refluxed for 2 h. After returning to RT, the reaction was stopped by adding 8 mL of Milli-Q water. Then, the obtained product was subjected to the washing process. For such processes, magnetic separation with magnets could be used in addition to centrifugation. After the initial separation, the first wash was performed by adding 20 mL of Milli-Q water, stirring (10 min), sonicating (15 min), and finally separating. This same procedure was repeated with MeOH (3 × 10 mL), THF (20 mL), and CH_2Cl_2 (20 mL). After the washing process, the solid was dried in vacuo, affording 290.4 mg.

Elemental analysis was carried out to analyze the effectiveness of immobilization.

Calculated: C% 42.41, H% 4.81, N% 4.30.

Found: C% 25.11, H% 4.33, N% 0.19.

2.9.3 Test III

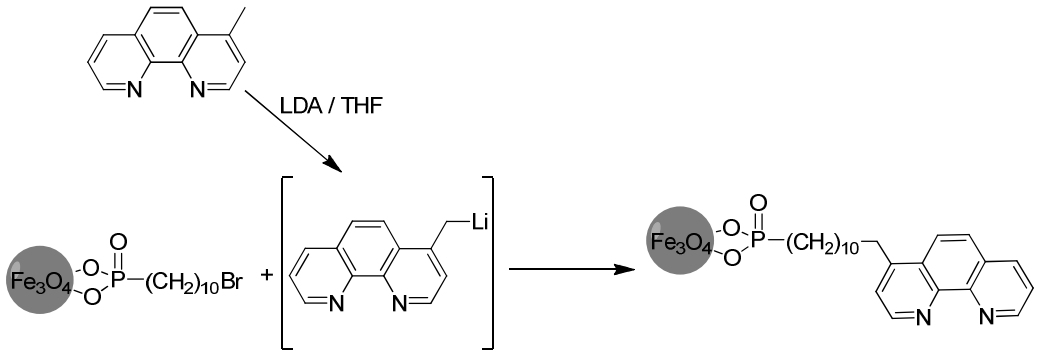

Reagent	M.W (g•mol^{-1})	mg	mmol	Molar ratio	V [mL]	d[g/mL]
4- MePhen	194.24	110.3	0.564	1.5		
THF dry					16+5	
LDA (2M)	107.12		0.675	1.8	0.340	0.812
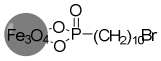	301.16	113.2[a]	0.375	1		

[a] Amount of functionalized phosphonic acid bound to 200.3 mg of nanoparticles (protection level 56,54 %)

The reaction was performed under a N_2 atmosphere, and 4-MePhen used in the synthesis was dried. In a 50 mL Schlenk tube, 200.3 mg of protected MNPs were put in a sonication bath for 8 h. In another 50 mL Schlenk tube, 110.3 mg of 4-MePhen was added to 16 mL of THF under agitation. When the temperature reached -78 °C, 0.340 mL of LDA (2 M) was added to 4-MePhen in one shot and the solution was maintained at this temperature under stirring for 1 h. The MNPs were then added dropwise into the 4-MePhen/LDA solution over 2 h at -78 °C. Subsequently, the temperature was allowed to reach RT overnight. The next morning, the reaction was refluxed for 2 h. After returning to RT, the reaction was stopped by adding 4 mL of Milli-Q water. Then, the obtained product was subjected to the washing process. For such processes, magnetic separation with magnets could be used in addition to centrifugation. After the initial separation, the first wash was performed by adding 10 mL of Milli-Q water, stirring (10 min), sonicating (15 min), and finally separating. This same procedure was repeated with MeOH (3 × 10 mL), THF (10 mL), and CH_2Cl_2 (10 mL). After the washing process, the solid was dried in vacuo, affording 153.4 mg.

Elemental analysis was carried out to analyze the effectiveness of immobilization.

Calculated: C% 42.41, H% 4.81, N% 4.30.

Found: C% 30.22, H% 4.44, N% 1.48.

2.9.4 Test IV

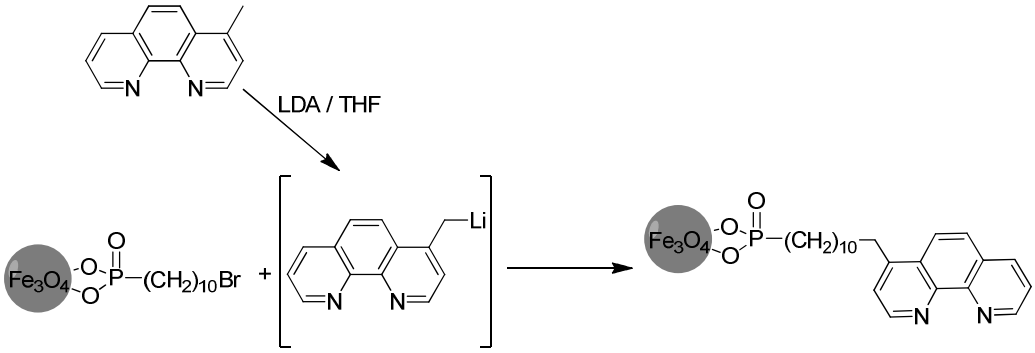

Reagent	M.W (g•mol^{-1})	mg	mmol	Molar ratio	V [mL]	d[g/mL]
4- MePhen	194.24	110.9	0.570	1.5		
THF dry					16+5	
LDA (2M)	107.12		0.676	1.8	0.340	0.812
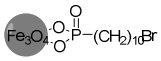	301.16	112.8[a]	0.375	1		

[a] Amount of functionalized phosphonic acid bound to 200.0 mg of nanoparticles (protection level 56,46 %)

The reaction was performed under a N_2 atmosphere, and 4-MePhen used in the synthesis was dried. In a 50 mL Schlenk tube, 200.0 mg of protected MNPs (freshly synthesized) was put in a sonication bath for 10 h. In another 50 mL Schlenk tube, 110.9 mg of 4-MePhen was added to 16 mL of THF under stirring. When the temperature reached -78 °C, 0.340 mL of LDA (2 M) was added to 4-MePhen in one shot and the solution was left at this temperature under stirring for 1 h. The MNPs were then added dropwise into the 4-MePhen/LDA solution over 2 h at -78 °C. Subsequently, the temperature was allowed to reach RT overnight. The next morning, the reaction was refluxed for 2 h. After returning to RT, the reaction was stopped by adding 4 mL of Milli-Q water. Then, the obtained product was subjected to the washing process. For such processes, magnetic separation with magnets could be used in addition to centrifugation. After the initial separation, the first wash was performed by adding 10 mL of Milli-Q water, stirring (10 min), sonicating (15 min), and finally separating. This same procedure was repeated with MeOH (3 × 10

mL), THF (10 mL), and CH_2Cl_2 (10 mL). After the washing process, the solid was dried in vacuo, affording 112.5 mg.

Elemental analysis was carried out to analyze the effectiveness of immobilization.
Calculated: C% 42.41, H% 4.81, N% 4.30.
Found: C% 32.89, H% 4.47, N% 2.26.

2.9.5 Test V

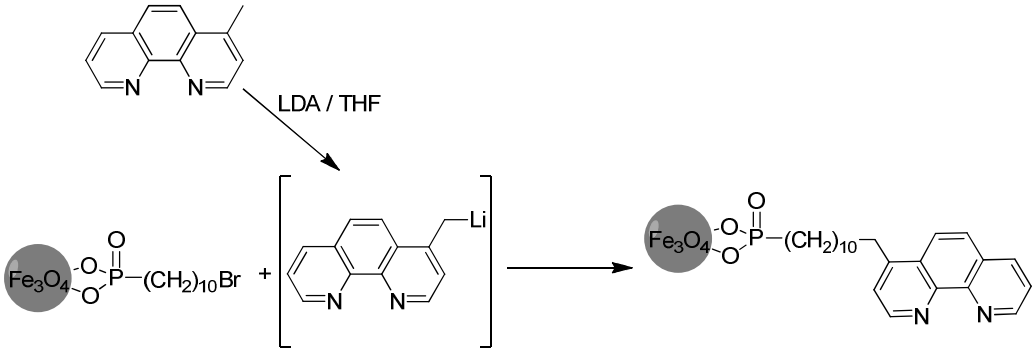

Reagent	M.W (g•mol^{-1})	mg	mmol	Molar ratio	V [mL]	d[g/mL]
4- MePhen	194.24	104.5	0.538	1.5		
THF dry					16+5	
LDA (2M)	107.12		0.646	1.8	0.330	0.812
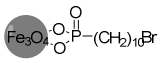	301.16	108.3[a]	0.359	1		

[a]Amount of functionalized phosphonic acid bound to 200.7 mg of nanoparticles (protection level 54%)

The reaction was performed under a N_2 atmosphere, and 4-MePhen used in the synthesis was dried. In a 50 mL Schlenk tube, 200.7 mg of protected MNPs (freshly synthesized) was put in a sonication bath for 14 h. In another 50 mL Schlenk tube, 104.5 mg of 4-MePhen was added to 16 mL of THF under stirring. When the temperature reached -78 °C, 0.330 mL of LDA (2 M) was added to 4-MePhen in one shot and the solution was left at this temperature under stirring for 1 h. The MNPs were then added dropwise into the 4-MePhen/LDA solution over 2 h at -78 °C. Subsequently, the temperature was allowed to reach RT overnight. The next morning, the reaction was refluxed for 2 h. After returning to RT, the reaction was stopped by adding 4 mL of Milli-Q water. Then, the obtained product was subjected to the washing process. For such processes, magnetic separation with magnets could be used in addition to centrifugation. After the initial separation, the first wash was performed by adding 10 mL of Milli-Q water, stirring (10 min), sonicating (15 min), and finally separating. This same procedure was repeated with MeOH (3 × 10

mL), THF (10 mL), and CH_2Cl_2 (10 mL). After the washing process, the solid was dried in vacuo, affording 114.6 mg.

Elemental analysis was carried out to analyze the effectiveness of immobilization.
Calculated: C% 42.41, H% 4.81, N% 4.30.
Found: C% 31.97, H% 4.40, N% 2.28.

2.9.6 Test VI

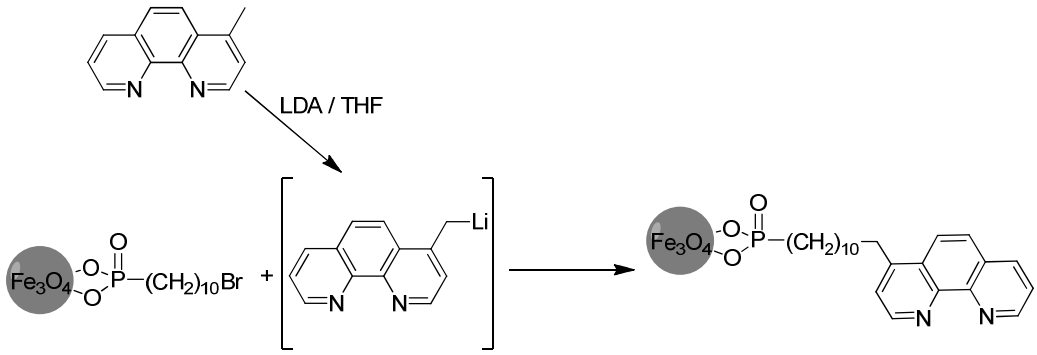

Reagent	M.W (g•mol^{-1})	mg	mmol	Molar ratio	V [mL]	d[g/mL]
4- MePhen	194.24	313.3	1.614	3.0[a]		
THF dry					46+7.5	
LDA (2M)	107.12		1.936	3.6	0.970	0.812
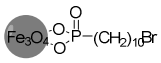	301.16	162.0[b]	0.538	1		

[a] The calculation was made considering the excess of (3 X) of the 4-MePhen in respect to the acid of the protective layer. [b]Amount of functionalized phosphonic acid bound to 300.1 mg of nanoparticles (protection level 54%)

The reaction was performed under a N_2 atmosphere, and 4-MePhen used in the synthesis was dried. In a 50 mL Schlenk tube, 300.1 mg of protected MNPs were put in a sonication bath for 14 h. In another 100 mL Schlenk tube, 313.3 mg of 4-MePhen was adding to 46 mL of THF under stirring. When the temperature reached -78 °C, 0.970 mL of LDA (2 M) was added to 4-MePhen in one shot and the solution was left at this temperature under stirring for 1 h. The MNPs were then added dropwise into the 4-MePhen/LDA solution over 2 h at -78 °C. Subsequently, the temperature was allowed to reach RT overnight. The next morning, the reaction was refluxed for 2 h. After returning to RT, the reaction was stopped by adding 10 mL of Milli-Q water. Then, the obtained product was subjected to the washing process. For such processes, magnetic separation with magnets could be used in addition to centrifugation. After the initial separation, the first washing was performed by adding 28 mL of Milli-Q water, stirring (10 min), sonicating (15 min), and finally separating. This same procedure was repeated with MeOH (3 × 28 mL), THF (28 mL), and CH_2Cl_2 (28 mL). After the washing process, the solid was dried in vacuo, affording 246.7 mg.

Elemental analysis was carried out to analyze the effectiveness of immobilization.

Calculated: C% 42.41, H% 4.81, N% 4.30.

Found: C% 31.39, H% 4.27, N% 2.04.

2.10 Synthesis of [Mo(CO)$_4$(4-MePhen)]

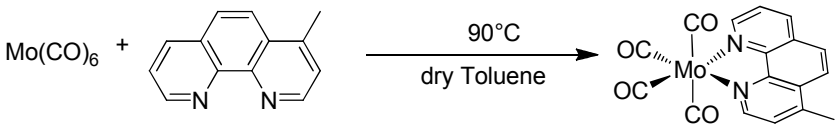

Reagent	M.W(g•mol^{-1})	mg	mmol	Molar ratio	V [ml]	d[g/mL]
4- MePhen	194.24	24.5	0.126	1.1		
Mo(CO)$_6$	264.0	30.2	0.114	1.0		
Toluene					4	

The reaction was performed under a N_2 atmosphere. In an oven-dried Schlenk flask, Mo(CO)$_6$ was dissolved in 2 mL of dry toluene. In another oven-dried Schlenk flask, 20.0 mg of 4-MePhen was dissolved in 2 mL of dry toluene. The molybdenum complex solution was added to the 4-MePhen solution, and then heated stepwise (30, 60, and 90 °C). After approximately 30 min, when temperature reached 90 °C, the solution was maintained at the same temperature for 3 h. Then, the solution was cooled and the solvent evaporated in vacuo. The obtained solid was dissolved in 1 mL of dry $CHCl_3$ and 1 mL of hexane with gentle warming (~30 °C), after which the solution was transferred in a centrifuge tube (still under N_2) and left to cool. A solid precipitated, which was separated by centrifugation and dried in vacuo, affording 39.2 mg (84.5% yield).

IR (toluene): 2011 (w), 1900 (s), 1886 (m), 1845 (m) cm^{-1}.

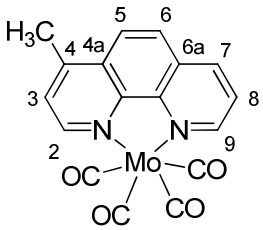

^{1}H NMR (300 MHz, $CDCl_3$) δ 9.48 (d, *J* = 4.6 Hz, 1H, H9), 9.31 (d, *J* = 5.1 Hz, 1H, H2), 8.41 (d, *J* = 8.1 Hz, 1H, H7), 8.13 (d, *J* = 9.0 Hz, 1H, H5), 7.97 (d, *J* = 9.1 Hz, 1H, H6), 7.73 (dd, *J* = 8.1, 5.0 Hz, 1H, H8), 7.57 (d, *J* = 5.1 Hz, 1H, H3), 2.90 (s, 3H, CH_3) ppm. Attribution of the ^{1}H NMR signals is based on the correspondence with those of the free ligand. (figure 33)

^{13}C NMR (75 MHz, $CDCl_3$) δ 223.34 (C), 205.46 (C), 153.29 (CH), 152.79 (CH), 146.27 (C), 136.57 (CH), 130.09 (C), 129.93 (C), 126.93 (CH), 125.73 (CH), 124.46 (CH), 123.77 (CH), 19.46 (CH_3) ppm. Signals corresponding to the carbonyl carbons could not be detected. (figure 34)

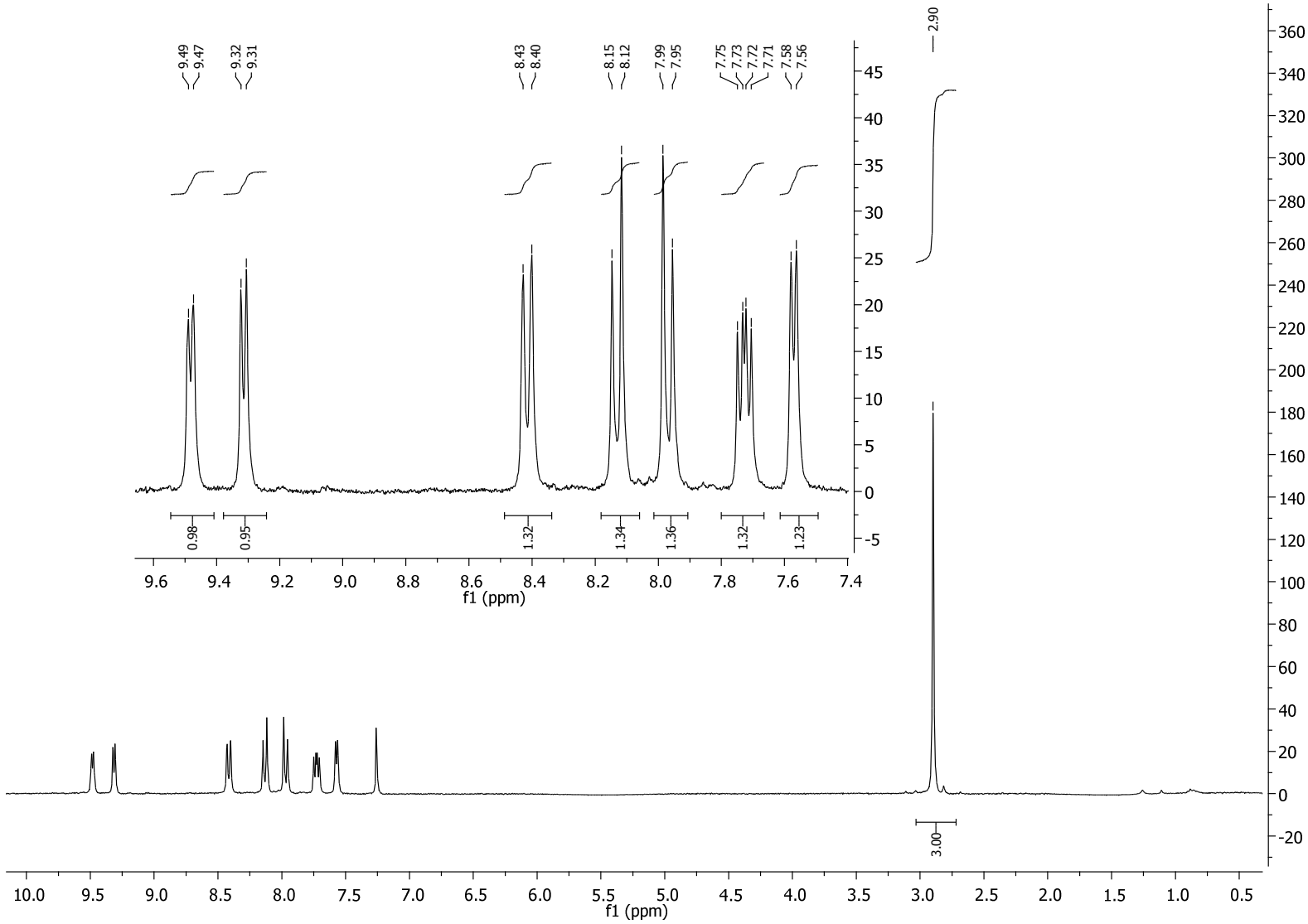

Figure 33: ^{1}H NMR (300 MHz, $CDCl_3$, 298 K) spectrum of $Mo(CO)_4$(4-MePhen) in $CDCl_3$.

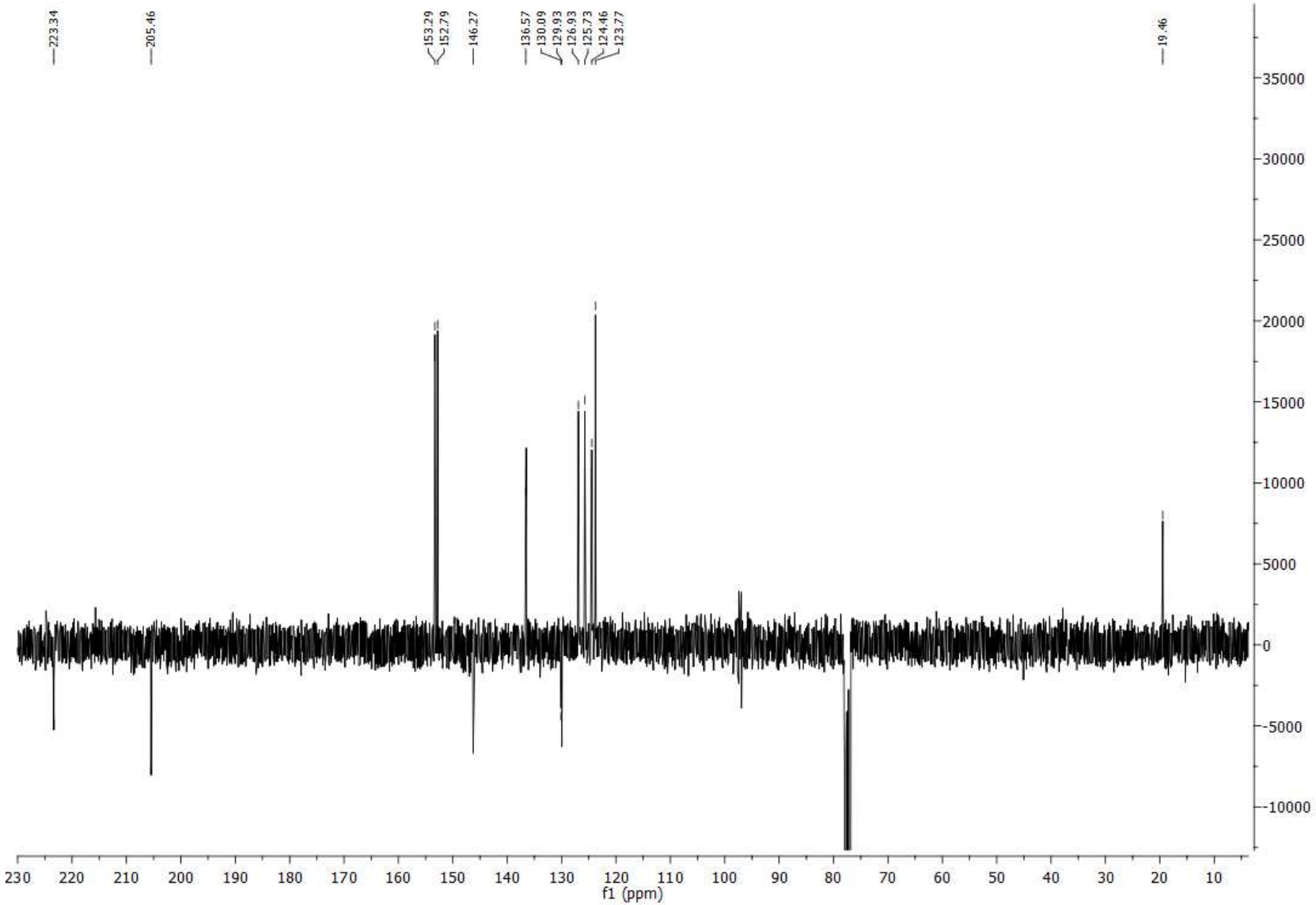

Figure 34: ^{13}C DEPT (75 MHz, $CDCl_3$, 298 K) spectrum of $Mo(CO)_4$(4-MePhen) in $CDCl_3$.

2.11 Reaction of $Mo(CO)_6$ with 4-MePhen immobilized on the protective layer

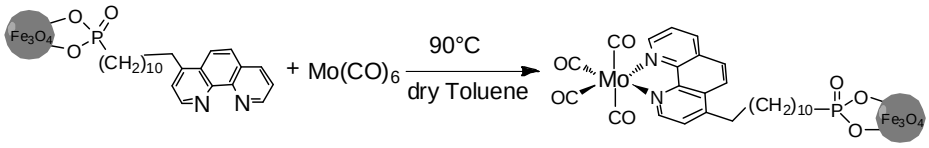

Reagent	M.W ($g \cdot mol^{-1}$)	mg	mmol	Molar ratio	V [ml]	d[g/mL]
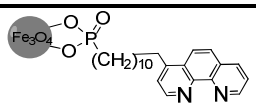	414.4	15.9[a]	0,038	1		
$Mo(CO)_6$	264.0	20.2	0,076	2		
Toluene					4	

[a]Amount of functionalized phosphonic acid bound to 28.2 mg of nanoparticles (protection level 56.54%)

The reaction was performed under a N_2 atmosphere. In an oven-dried Schlenk flask, $Mo(CO)_6$ was dissolved in 2 mL of dry toluene. In another over-dried Schlenk tube, 28.2 mg of immobilized nanoparticles was dispersed in 2 mL of dry toluene and then put in a sonication bath for 3 h. Following sonication, the molybdenum complex solution was added to the MNP dispersion and heated at 90 °C for 3 h. Then, 1 mL of the nanoparticle solution was evaporated and another 1 mL of dry toluene was added. Subsequently, the IR spectrum of the solution was recorded under a N_2 atmosphere: 2009 (w), 1889 (s), 1877 (m), and 1839(m) cm^{-1}. The ATR spectrum showed signals at 2013(w), 1899(s), 1868(m), and 1830 (m) cm^{-1}. The total amount of isolated solid was 27.0 mg.

2.12 Coordination of $Pd(OAc)_2$ to 4-MePhen immobilized on the protective layer

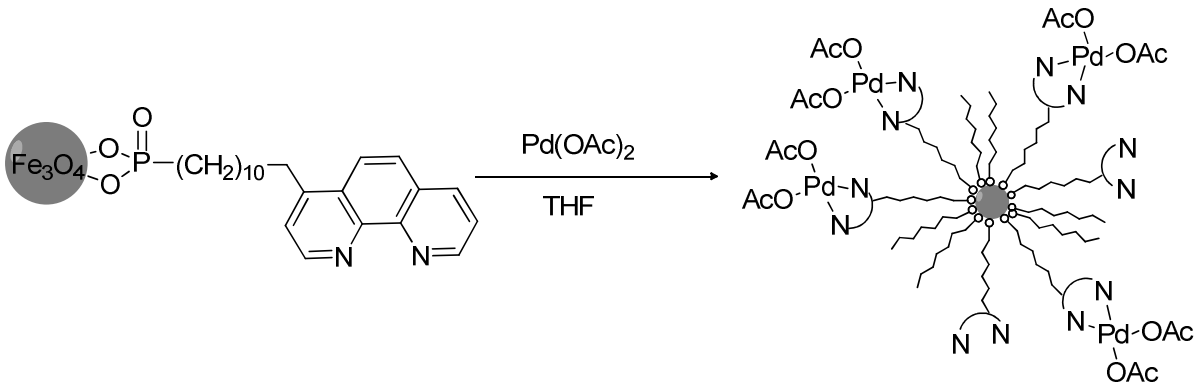

Reagent	M.W(g•mol^{-1})	mg	mmol	Molar ratio	V [ml]	d[g/mL]
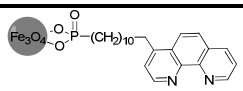	414.4	54.0[a]	0.13	1		
$Pd(OAc)_2$	224.51	116.8	0.52	4		
THF					12	

[a]Amount of functionalized phosphonic acid bound to 100.0 mg of nanoparticles (protection level 54%)

The reaction was performed under a N_2 atmosphere. In an oven-dried Schlenk flask, $Pd(OAc)_2$ was dissolved in 7 mL of dry THF. In another oven-dried Schlenk tube, 100.0 mg of phenanthroline-functionalized nanoparticles was dispersed in 5 mL of dry THF. To obtain a good dispersion, it was necessary to sonicate and stir for some hours. The palladium complex was then added to the nanoparticles, and the mixture was left to stir for 16 h at RT.

The nanoparticles can be separated magnetically or by centrifugation. In this case, we used centrifugation to optimize the process time and avoid loss of material, and washed the sample with dry THF (2 mL for each wash) several times. The washing procedure is the same as that used for washing nanoparticles, as described in Chapter 1, and consists of agitation, sonication, and separation. The washing procedure was repeated until the amount of solid extracted was less than 2 mg. The final yield was 75 mg.

2.13 Synthesis of 4-OH-Phen (first step)

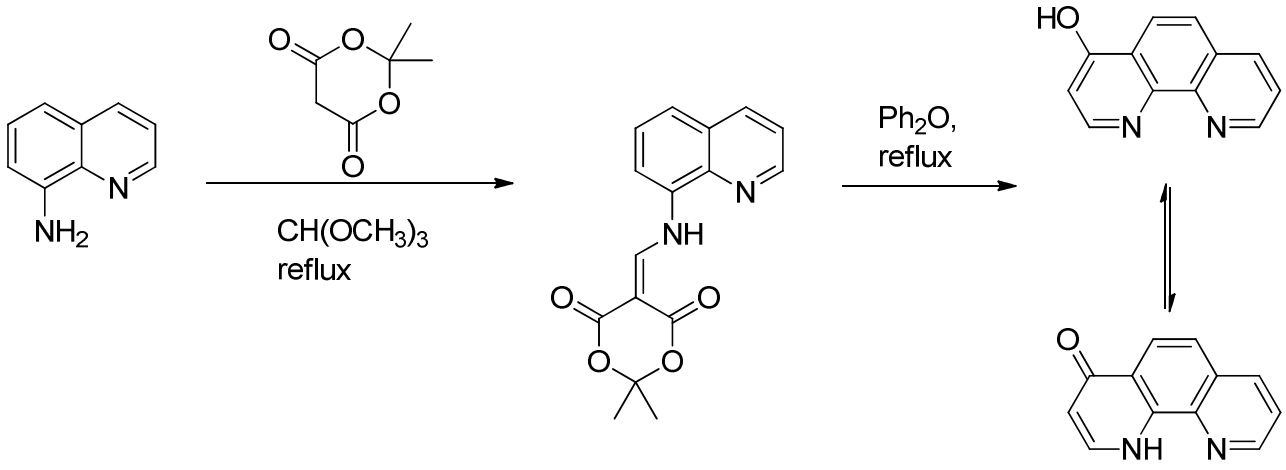

Reagent	M.W(g•mol^{-1})	g	mmol	Molar ratio	V [ml]	d[g/mL]
8-aminoquinoline	144.17	2.905	20.14	1		
Meldrum`s acid	114.13	3.501	24.29	1.2		
$CH(OCH_3)_3$	106.12		311	15.4	34	0.97

The synthesis was performed by adapting the literature procedure.[7] In an oven-dried Schlenk flask, a solution of Meldrum's acid in trimethyl orthoformate was refluxed for 2 h under N_2. The resulting yellow solution was allowed to cool (~60 °C). Aminoquinoline was then added, and the solution was heated to reflux for 1.5 h. The completion of the reaction was checked by TLC (alumina, 1:1 CH_2Cl_2/THF). After cooling to RT, an abundant yellow precipitate formed. The solvent was removed by rotary evaporation and the resulting solid was recrystallized from ethanol (40 mL). The yellow solid was separated by filtration on a Buchner funnel, washed with a small amount of cold ethanol, and dried in vacuo. The yield of the adduct was 4.6779 g (16.17 mmol, 80.3%).

^{1}H NMR (300 MHz, $CDCl_3$, 300 K) δ 12.86 (br d, $^3J_{H,H}$ = 14.9 Hz, 1H, NH), 9.02 (dd, $^3J_{H,H}$ = 4.2 Hz and $^4J_{H,H}$ = 1.6 Hz, 1H, H2), 8.94 (d, $^3J_{H,H}$ = 14.9 Hz, 1H, H-olefinic), 8.23 (dd, $^3J_{H,H}$ = 8.3 Hz and $^4J_{H,H}$ = 1.6 Hz 1H, H4), 7.73–7.69 (m, 2H, H5 and H7), 7.61 (ps t, $^3J_{H,H}$ = 7.8 Hz, 1H, H6), 7.56 (dd, $^3J_{H,H}$ = 8.3 and 4.2 Hz, 1H, H3), 1.80 (s, 6H, CH_3) ppm. (figure 35,36)

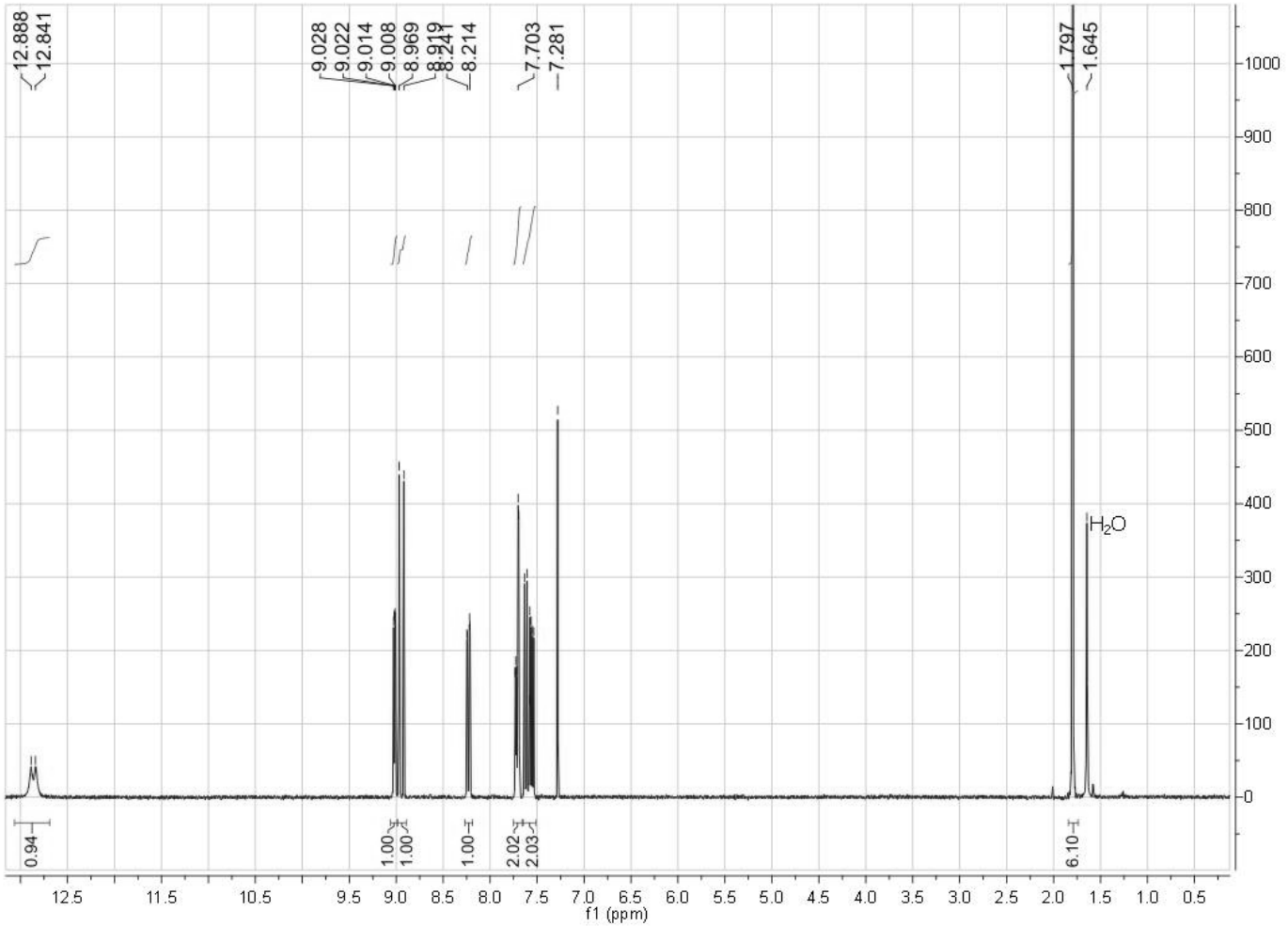

Figure 35: ^{1}H NMR (300 MHz, $CDCl_3$, 298 K) spectrum of after the first step in synthesizing 4-OH-Phen.

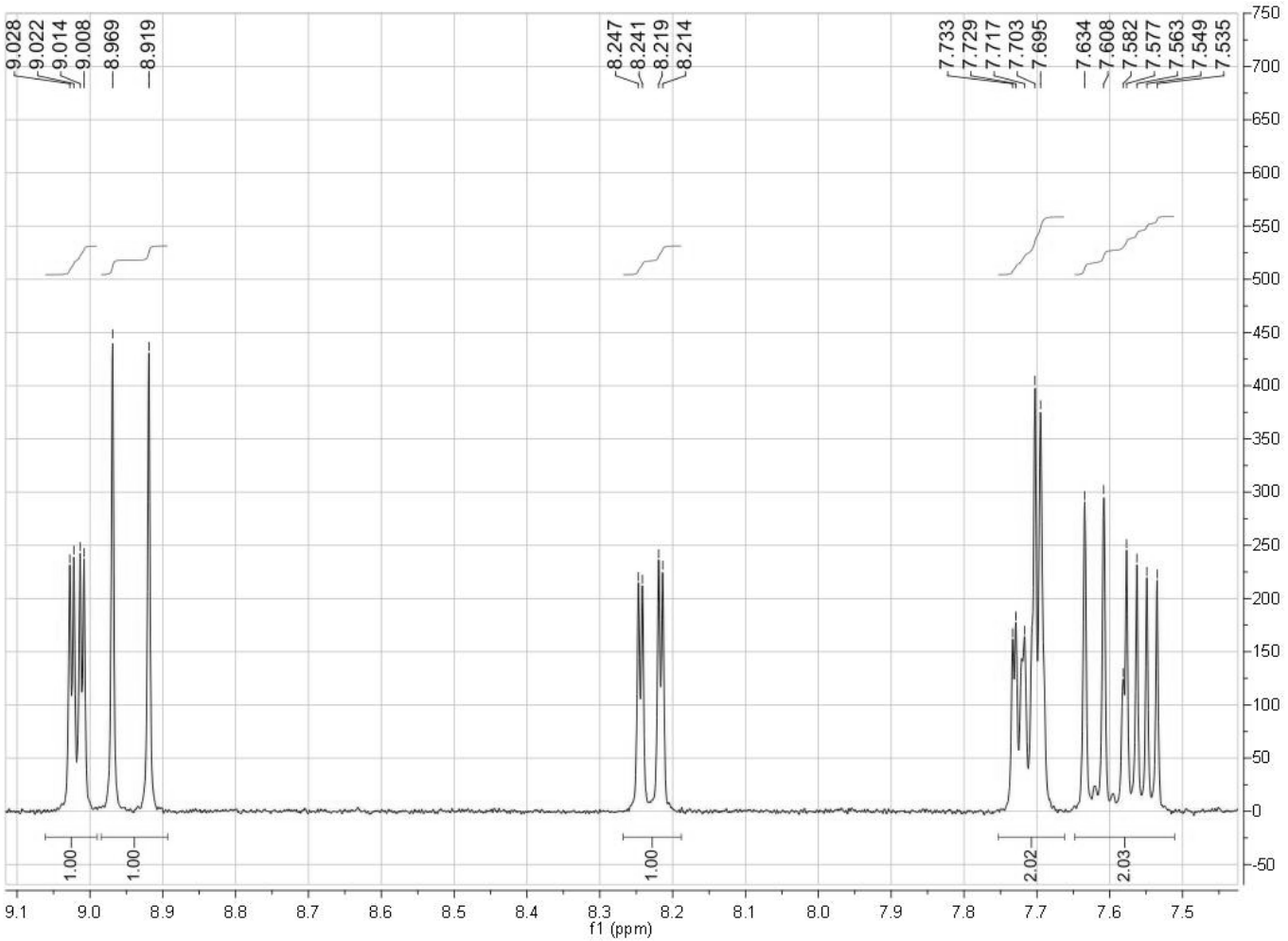

Figure 36: Expanded ^{1}H NMR (300 MHz, $CDCl_3$, 298 K) spectrum of after the first step in synthesizing 4-OH-Phen.

-

2.13.1 Synthesis of 4-OH-Phen (second step)

Reagent	M.W(g•mol^{-1})	g	mmol	Molar ratio	V [ml]	d[g/mL]
1	289.29	4.6779	16.17			
Diphenylether					200	

The synthesis was performed by adapting the literature procedure.[7] Adduct 1 was refluxed in diphenyl ether under vigorous stirring for 1 h. The mixture was allowed to cool and 100 mL of petroleum ether (40–60 °C fraction) was added. The brown precipitate that formed was vacuum filtered on a Buchner funnel, washed abundantly with petroleum ether, and dried under vacuum at ~70 °C, affording 2.4574 g of 2 (12.52 mmol, 77.42% yield).

Compound 2 is in tautomeric equilibrium with its ketonic form. Under the NMR experimental conditions, the equilibrium appears to be shifted towards the ketonic form.

^{1}H NMR (300 MHz, $CDCl_3$, 300 K) δ 10.47 (br, 1H, NH), 8.93 (dd, $^{3}J_{H,H}$ = 4.3 Hz and $^{4}J_{H,H}$ = 1.6 Hz, 1H, H9), 8.42 (d, $^{3}J_{H,H}$ = 8.9 Hz, 1H, H5), 8.28 (dd, $^{3}J_{H,H}$ = 8.2 Hz and $^{4}J_{H,H}$ = 1.6 Hz, 1H, H7), 7.85 (dd, $^{3}J_{H,H}$ = 7.5 and 5.8 Hz, 1H, H2), 7.67 (d, $^{3}J_{H,H}$ = 8.9 Hz, 1H, H6) overlapping with 7.64 (dd, $^{3}J_{H,H}$ = 8.2 and 4.3 Hz, 1H, H8), 6.57 (dd, $^{3}J_{H,H}$ = 7.5 Hz and $^{4}J_{H,H}$ = 1.6 Hz, 1H, H3) ppm. (figure 37,38)

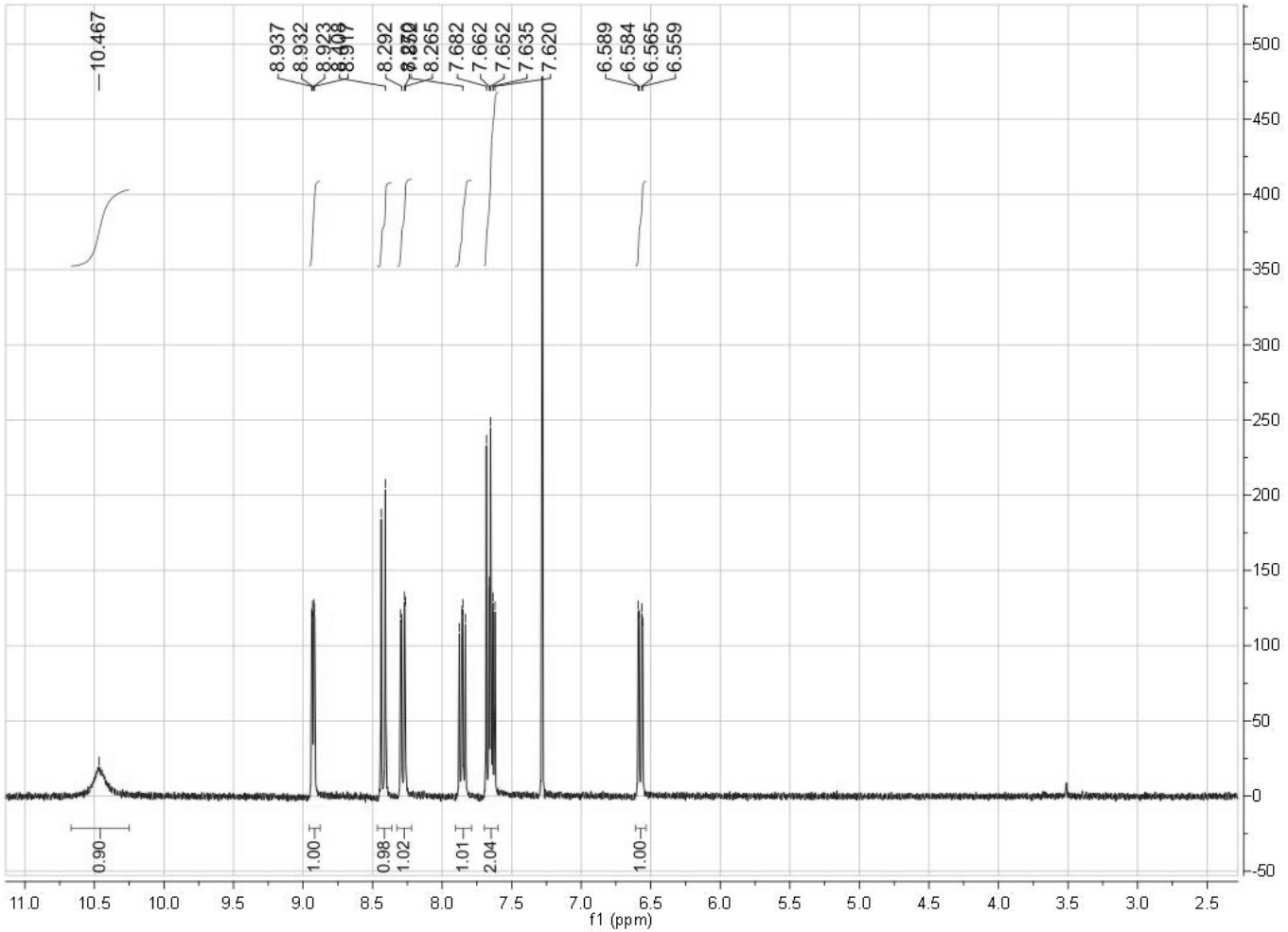

Figure 37: ^{1}H NMR (300 MHz, $CDCl_3$, 298 K) spectrum of 4-OH-Phen.

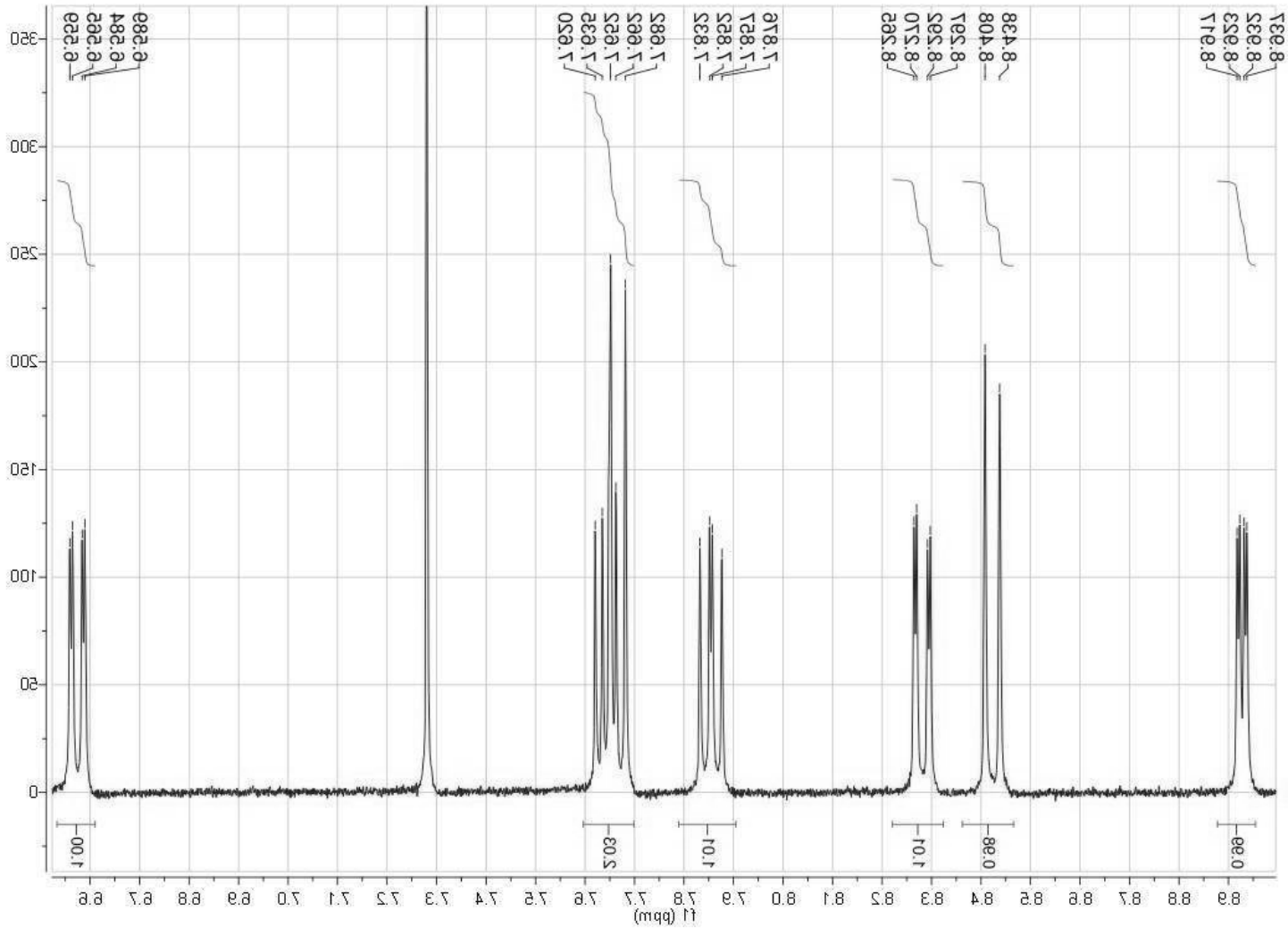

Figure 38: Expanded ^{1}H NMR (300 MHz, $CDCl_3$, 298 K) spectrum of 4-OH-Phen.

2.14 Immobilization of 4-OH-Phen on the protecting layer

2.14.1 Test I

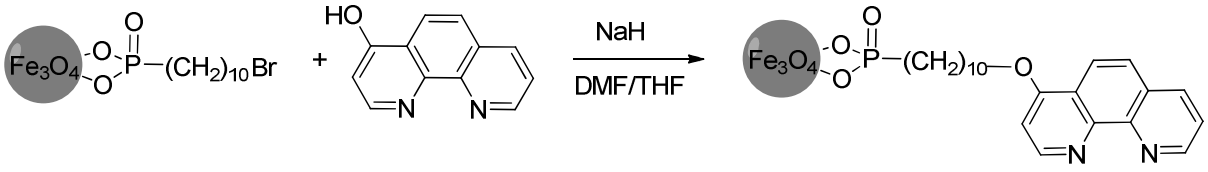

Reagent	M.W ($g \cdot mol^{-1}$)	mg	mmol	Molar ratio	V [ml]	d[g/mL]
4-OH-Phen	196.20	131.9	0.672	1.5		
NaH (60)%	24	28.7	0.718	1.6		
THF/DMF					6	
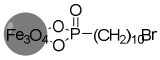	301.16	135.0[a]	0.448	1		
THF dry					5	

[a]Amount of functionalized phosphonic acid bound to 250.3 mg of nanoparticles (protection level 54%)

In a 50 mL Schlenk tube, 250.3 mg of protected MNPs were put in a sonication bath for 8 h. The dispersion of MNPs was transferred to a dropping funnel using a Teflon cannula just before adding it dropwise into the 4-OH-Phen solution.

In another 50 mL Schlenk tube, NaH was added to 3 mL of THF and 3 mL of DMF under stirring. The suspension was cooled and when the temperature reached 0 °C, the 4-OH-Phen solution was added. The suspension was maintained at this temperature under stirring for 30 min.

The MNP solution was added dropwise into the 4-OH-Phen/NaH solution at 0 °C, and after the addition, the solution was allowed to reach RT overnight. The next morning, the reaction was refluxed for 1 h. After returning to RT, the reaction was stopped by adding 5 mL of Milli-Q water. Then, the obtained product was subjected to the washing process. For such processes, magnetic separation with magnets could be used in addition to centrifugation. After the initial separation, the first wash was performed by adding 10 mL of Milli-Q water, stirring (10 min), sonicating (15 min), and finally separating. This same procedure was repeated with MeOH (4 × 10 mL), THF (10 mL), and CH_2Cl_2 (10 mL). After the washing process, the solid was dried in vacuo, affording 125.2 mg.

Elemental analysis was carried out to analyze the effectiveness of immobilization.

Calculated: C% 39.25, H% 4.34, N% 4.16.

Found: C% 33.63, H% 5.08, N% 0.79.

2.14.2 Test II

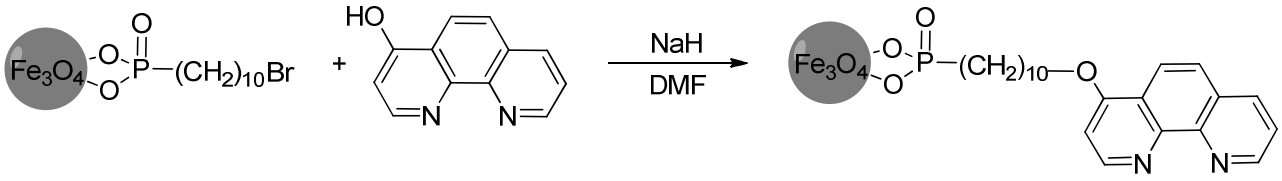

Reagent	M.W ($g \cdot mol^{-1}$)	mg	mmol	Molar ratio	V [ml]	d[g/mL]
4-OH-Phen	196.20	210.4	1.075	3		
NaH (60)%	24	57.5	1.4344	4		
DMF					6	
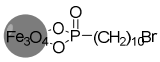	301.16	108.2[a]	0.3586	1		
THF[a] dry					5	

[a]Amount of functionalized phosphonic acid bound to 200.4 mg of nanoparticles (protection level 54%)

In a 50 mL Schlenk tube, 200.4 mg of protected MNPs were put in a sonication bath for 8 h. The dispersion of MNPs was transferred to a dropping funnel using a Teflon cannula just before adding it dropwise into the 4-OH-Phen solution.

In another 50 mL Schlenk tube, NaH was added to 6 mL of DMF under stirring. The suspension was cooled and when the temperature reached 0 °C, the 4-OH-Phen solution was added. The suspension was maintained at this temperature under stirring for 30 min.

The MNP solution was added dropwise into the 4-OH-Phen/NaH solution at 0 °C, and after the addition, the solution was allowed to reach RT overnight. The next morning, the reaction was heated to 120 °C (bath temperature) for 1 h. After returning to RT, the reaction was stopped by adding 5 mL of Milli-Q water. Then, the obtained product was subjected to the washing process. For such processes, magnetic separation with magnets could be used in addition to centrifugation. After the initial separation, the first wash was performed by adding 10 mL of Milli-Q water, stirring (10 min), sonicating (15 min), and finally separating. This same procedure was repeated with MeOH (4 × 10 mL), THF (10 mL), and CH_2Cl_2 (10 mL). After the washing process, the solid was dried in vacuo, affording 100.7 mg.

Elemental analysis was carried out to analyze the effectiveness of immobilization.
Calculated: C% 39.25. H% 4.34, N% 4.16.
Found: C% 25.22, H% 2.89, N% 1.54.

Note: To determine the reaction conditions to be used in this attempt, a test was performed using fast GC in the absence of nanoparticles. The same procedure was followed as described above using 1-bromohexadecane. At time = 0, before heating, GC showed the presence of a peak at about 4 min. After 6 h at 120 °C, the peak was no longer present, suggesting that all 1-bromohexadecane was consumed. For this reason, we used this temperature in this attempt.

2.14.3 Test III

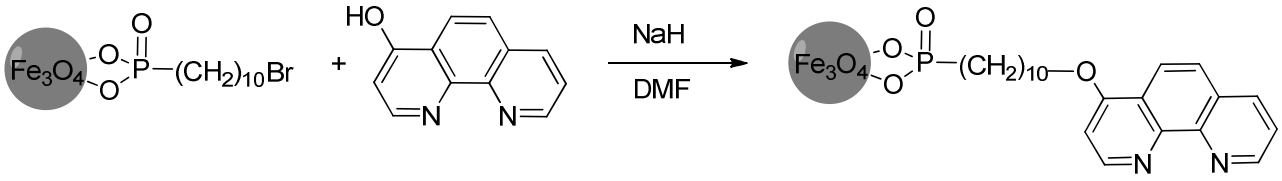

Reagent	M.W ($g \cdot mol^{-1}$)	mg	mmol	Molar ratio	V [ml]	d[g/mL]
4-OH-Phen	196.20	1055.2	5.373	3		
NaH (60)%	24	286.3	7.165	4		
DMF					30	
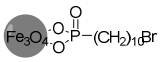	301.16	540.0[a]	1.791	1		
THF[a] dry					20	

[a]Amount of functionalized phosphonic acid bound to 1000.3mg of nanoparticles (protection level 54%)

In a 50 mL Schlenk tube, 1000.3 mg of protected MNPs were put in a sonication bath for 10 h. The dispersion of MNPs was transferred to a dropping funnel using a Teflon cannula just before adding it dropwise into the 4-OH-Phen solution.

In another 100 mL Schlenk tube, NaH was added to 30 mL DMF under stirring. The suspension was cooled and when the temperature reached 0 °C, the 4-OH-Phen solution was added. The suspension was maintained at this temperature under stirring for 30 min.

The MNP solution was added dropwise into the 4-OH-Phen/NaH one at 0 °C, and after the addition, the solution was allowed to reach RT overnight. The next morning, the reaction was stopped by adding 20 mL of Milli-Q water. Then, the obtained product was subjected to the washing process. For such processes, magnetic separation with magnets could be used in addition to centrifugation. After the initial separation, the first wash was performed by adding 30 mL of Milli-Q water, stirring (10 min), sonicating (15 min), and finally separating. This same procedure was repeated with MeOH (4 × 30 mL), THF (30 mL), and CH_2Cl_2 (30 mL). After the washing process, the solid was dried in vacuo, affording 361.9 mg.

Elemental analysis was carried out to analyze the effectiveness of immobilization.

Calculated: C% 39.25, H% 4.34, N% 4.16.

Found: C% 27.65, H% 3.41, N% 2.77.

2.14.4 Test IV

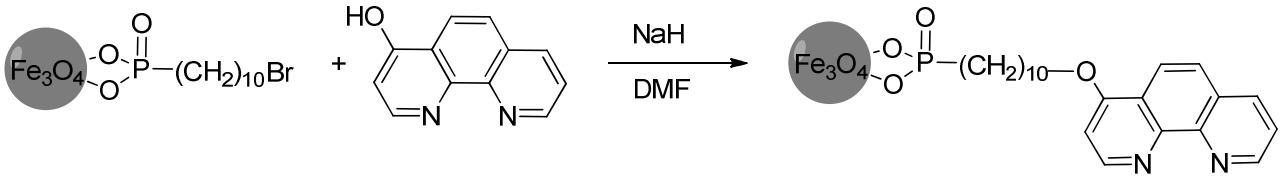

Reagent	M.W ($g \cdot mol^{-1}$)	mg	mmol	Molar ratio	V [ml]	d[g/mL]
4-OH-Phen	196.20	210.4	1.075	3		
NaH (60)%	24	57.5	1.4344	4		
DMF					6	
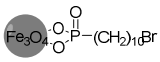	301.16	108.2[a]	0.3586	1		
THF dry					5	

[a]Amount of functionalized phosphonic acid bound to 200.2 mg of nanoparticles (protection level 54%)

In a 50 mL Schlenk tube, 200.2 mg of protected MNPs were put in a sonication bath for 14 h. The dispersion of MNPs was transferred to a dropping funnel using a Teflon cannula just before adding it dropwise into the 4-OH-Phen solution.

In another 50 mL Schlenk tube, NaH was added to 6 mL of DMF under stirring. The suspension was cooled and when the temperature reached 0 °C, the 4-OH-Phen solution was added. The suspension was maintained at this temperature under stirring for 30 min.

The MNP solution was added dropwise into the 4-OH-Phen/NaH one at 0 °C, and after the addition, the solution was allowed to reach RT. In this attempt, the solution was left in the sonication bath overnight. According to the elemental analysis, this procedure afforded better results than that in Test III. The next morning, the reaction was stopped by adding 5 mL of Milli-Q water. Then, the obtained product was subjected to the washing process. For such processes, magnetic separation with magnets could be used in addition to centrifugation. After the initial separation, the first wash was performed by adding 10 mL of Milli-Q water, stirring (10 min), sonicating (15 min), and finally separating. This same procedure was repeated with MeOH (4 × 10 mL), THF (10 mL), and CH_2Cl_2 (10 mL). After the washing process, the solid was dried in vacuo, affording 72.3 mg.

Elemental analysis was carried out to analyze the effectiveness of immobilization.

Calculated: C% 39.25, H% 4.34, N% 4.16.

Found: C% 36.50, H% 4.35, N% 3.72.

2.14.5 Test V

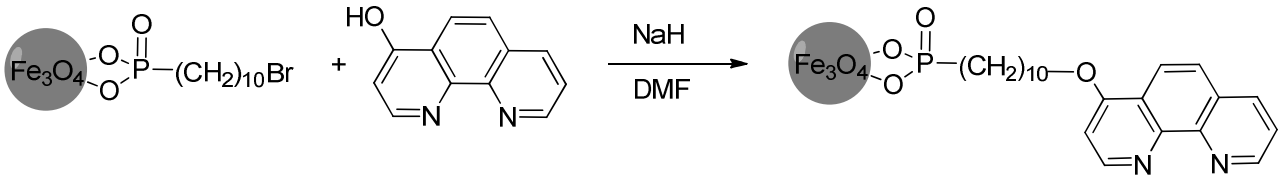

Reagent	M.W ($g \cdot mol^{-1}$)	mg	mmol	Molar ratio	V [ml]	d[g/mL]
4-OH-Phen	196.20	209.6	1.079	3		
NaH (60)%	24	57.0	1.4344	4		
DMF					6	
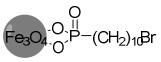	301.16	108.2	0.3586	1		
THF dry					5	

[a]Amount of functionalized phosphonic acid bound to 200.8 mg of nanoparticles (protection level 54%)

In a 50 mL Schlenk tube, 200.8 mg of protected MNPs were put in a sonication bath for 14 h. The dispersion of MNPs was transferred to a dropping funnel using a Teflon cannula just before adding it dropwise into the 4-OH-Phen solution.

In another 50 mL Schlenk tube, NaH was added to 6 mL of DMF under stirring. The suspension was cooled and when the temperature reached 0 °C, the 4-OH-Phen solution was added. The suspension was maintained at this temperature under stirring for 30 min.

The MNP solution was added dropwise into the 4-OH-Phen/NaH one at 0 °C, and after the addition, the solution was allowed to reach RT. In this attempt, the solution was left in the sonication bath overnight, as in Test IV. The next morning, the reaction was stopped by adding 5 mL of Milli-Q water. Then, the obtained product was subjected to the washing process. For such processes, magnetic separation with magnets could be used in addition to centrifugation. After the initial separation, the first wash was performed by adding 10 mL of Milli-Q water, stirring (10 min), sonicating (15 min), and finally separating. This same procedure was repeated with MeOH (4 × 10 mL), THF (10 mL), and CH_2Cl_2 (10 mL). After the washing process, the solid was dried in vacuo, affording 75.9 mg.

Elemental analysis was carried out to analyze the effectiveness of immobilization.

Calculated: C% 39.25, H% 4.34, N% 4.16.

Found: C% 37.57, H% 4.45, N% 3.95.

2.15 Synthesis of [$Mo(CO)_4$(4-MeO-Phen)]

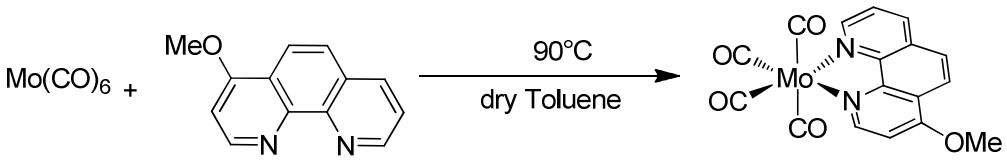

Reagent	M.W(g•mol^{-1})	mg	mmol	Molar ratio	V [ml]	d[g/mL]
4-MeO-Phen	210.23	25.7	0.128	1.1		
$Mo(CO)_6$	264.0	30.7	0.116	1.0		
Toluene					4	

The reaction was performed under a N_2 atmosphere. In an oven-dried Schlenk flask, $Mo(CO)_6$ was dissolved in 2 mL of dry toluene. In another oven-dried Schlenk flask, 25.7 mg of 4-MeO-Phen was dissolved in 2 mL of dry toluene. The molybdenum complex solution was added to the 4-MeO-Phen solution, and the heated stepwise (30, 60, and 90 °C). After approximately 30 min, when the temperature reached 90 °C, the solution was maintained at the same temperature for 3 h. Subsequently, the solution was cooled and hexane (4 mL) was added. The precipitate was separated by centrifugation. The resulting solid (which contained some toluene) was redissolved in $CHCl_3$ and the solvent was evaporated again to afford 40.7 mg (83.0% yield).

IR (toluene): 2011(w), 1898 (s), 1883 (m), 1843 (m) cm^{-1}.

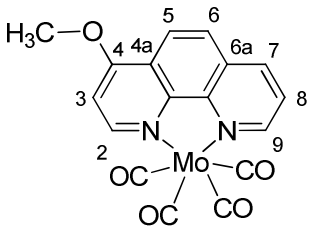

^{1}H NMR (300 MHz, $CDCl_3$) δ 9.44 (t, *J* = 8.7 Hz, 1H, H9), 9.24 (d, *J* = 5.7 Hz, 1H, H2), 8.39 (d, *J* = 8.0 Hz, 1H, H7), 8.29 (t, *J* = 12.3 Hz, 1H, H5), 7.88 (t, *J* = 11.9 Hz, 1H, H6), 7.70 (dd, *J* = 7.7, 5.0 Hz, 1H, H8), 7.12 (d, *J* = 5.7 Hz, 1H, H3), 4.20 (s, 3H, OCH_3) ppm. (figure 39)

^{13}C NMR (75 MHz, $CDCl_3$) δ 223.28 (C), 222.73 (C), 205.31 (C), 162.77 (C), 154.18 (CH), 152.77 (CH), 146.87 (C), 146.21 (C), 136.36 (CH), 129.91 (C), 125.68 (CH), 124.20 (CH), 122.17 (C), 121.19 (CH), 104.79 (CH), 56.95 (CH_3) ppm. (figure 40)

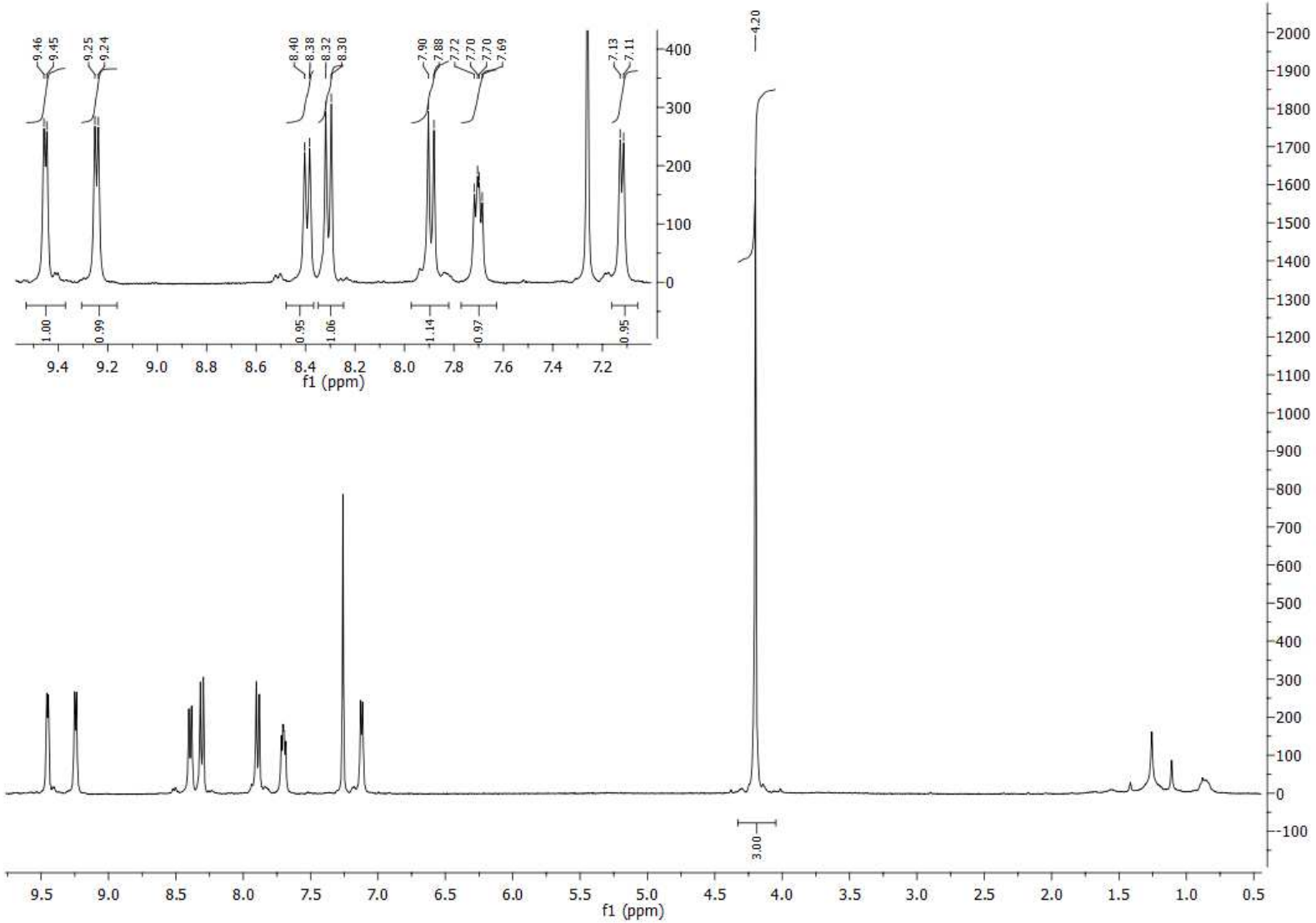

Figure 39: ^{1}H NMR (300 MHz, $CDCl_3$, 298 K) spectrum of $Mo(CO)_4$(4-MeO-Phen).

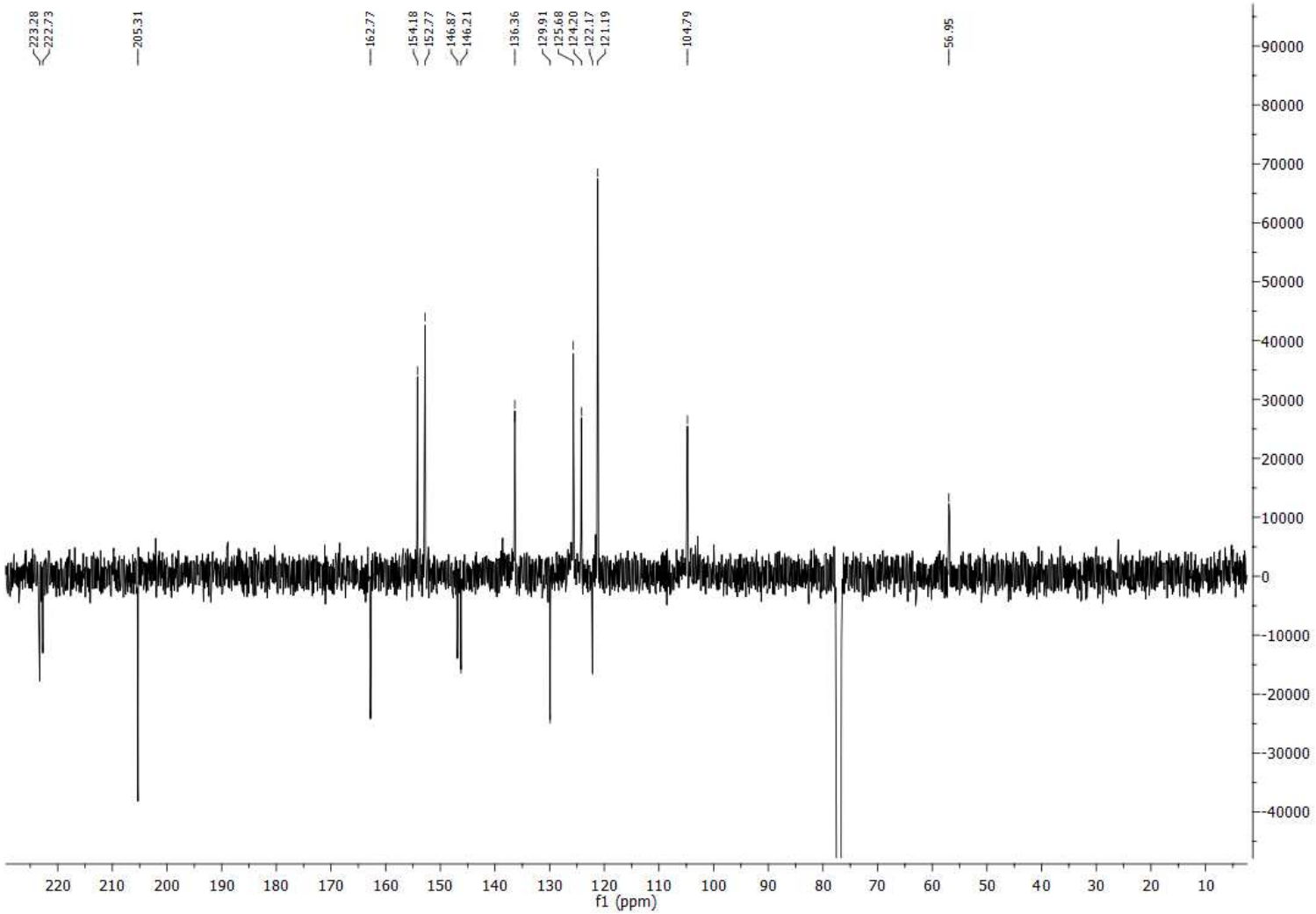

Figure 40: ^{13}C DEPT (75 MHz, $CDCl_3$, 298 K) spectrum of $Mo(CO)_4$(4-MeO-Phen).

2.16 Reaction of $Mo(CO)_6$ and 4-OH-Phen immobilized on the protective layer

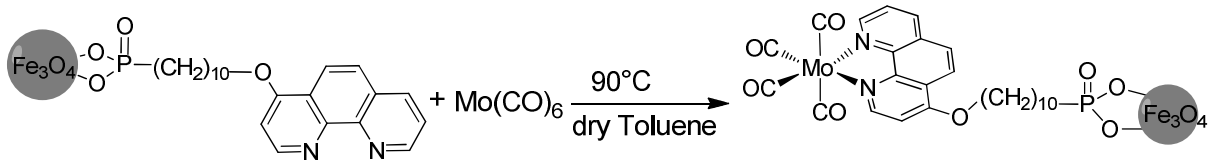

Reagent	M.W(g•mol^{-1})	mg	mmol	Molar ratio	V [ml]	d[g/mL]
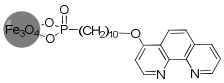	-	21.2[a]	0.050 Phen[a]	1		
$Mo(CO)_6$	264.0	26.5	039.101	2		
Toluene					4	

[a] Extimated amount based on the amount of phosphonic acid (54% by weight) bound to the nanoparticles

The reaction was performed under a N_2 atmosphere. In an oven-dried Schlenk flask, $Mo(CO)_6$ was dissolved in 2 mL of dry toluene. In another over-dried Schlenk tube, 39.2 mg of OH-Phen-functionalized nanoparticles were dispersed in 2 mL of dry toluene and placed in a sonication bath for 3 h. Following sonication, the molybdenum complex solution was added to the nanoparticle dispersion and heated at 90 °C for 3 h. Subsequently, 1 mL of the nanoparticle solution was evaporated and other 1 mL of dry toluene was added. Then, the IR spectrum of the solution was recorded under a N_2 atmosphere: 2008(w), 1895 (s), 1869(m), and 1829(m) cm^{-1}. The ATR spectrum showed signals at 2010 (w), 1895(s), 1869(m), and 1829 (m) cm^{-1}. The total amount of isolated solid was 42.4 mg.

2.17 Coordination of $Pd(OAc)_2$ to 4-OH-Phen immobilized on the protective layer

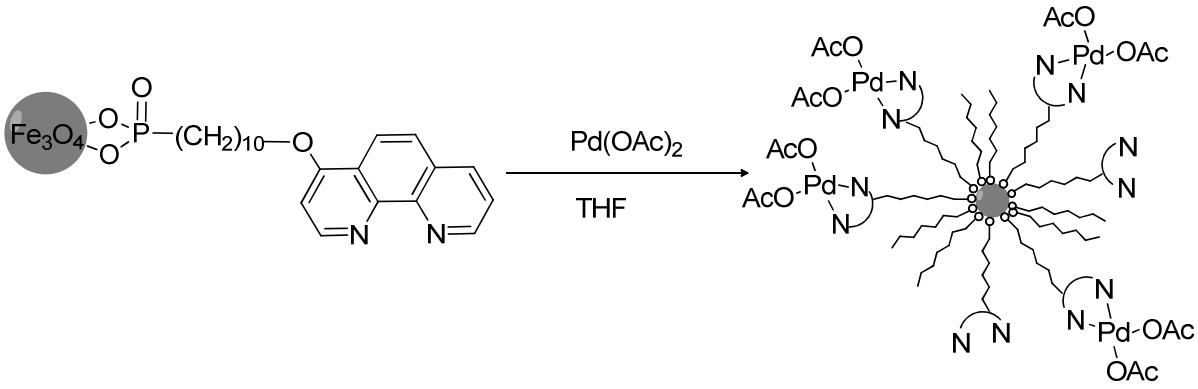

Reagent	M.W(g•mol^{-1})	mg	mmol	Molar ratio	V [ml]	d[g/mL]
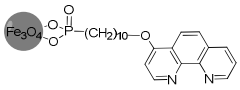	-	37.8[a]	0.091 Phen[a]	1		
$Pd(OAc)_2$	224.51	81.6[a]	0.364	4		
THF					12	

[a] Extimated amount based on the amount of phosphonic acid (54% by weight) bound to the nanoparticles

The reaction was performed under a N_2 atmosphere. In an oven-dried Schlenk flask, $Pd(OAc)_2$ was dissolved in 7 mL of dry THF. In another oven-dried Schlenk tube, 70.0 mg of OH-Phen-functionalized nanoparticles were dispersed in 5 mL of dry THF. To obtain a good dispersion, it was necessary to sonicate and stir the solution for some hours. The palladium complex was then added to the nanoparticles, and the mixture was stirred for 16 h at RT.

The nanoparticles can be separated magnetically or by centrifugation. In this case, we used centrifugation to optimize the process time and avoid loss of material. In was necessary to repeat the washing procedure until the amount of solid extracted was less than 2 mg. The solid was dried in vacuo, affording 51.7 mg.

References

[1] Z. H. Skraup, G. Vortmann, *Monatshefte Fur Chemie*, **1882**, 3, 570-602.

[2] F. Blau, *Monatshefte Fur Chemie*, **1898**, 19, 647-689.

[3] C. J. Moody, C. W. Rees, R. Thomas, *Tetrahedron Letters*, **1990**, 31 (30), 4375-4376.

[4] F. H. Case, *J. Amer. Chem. Soc*. **1948**, 70, 3994.

[5] P. Belser, S. Bemhard, U. Guerig, *Tetrahedron*, **1996**, 52, 2937.

[6] C. O. Murchu, *Synthesis*, **1989**, 880.

[7] G. I. Graf, D. Hastreiter, L. Everson ASilva, R. A. Rebelo, A. G. Montalban, A. McKillop, *Tetrahedron*, **2002**, 58, 9095-9100.

[8] F. M. Menger and Jeng-Jong Lee, *J. Org. Chem*, **1993**, 58(7), 1909-1916.

[9] Sjogren. M. P. T., H. Frisell, B. Åkermark, P. Norrby, L. Eriksson, A. Vitagliano, *Organometallics*, **1997,** 16, 942-950

[10] X. Liu, X. Li, Y. Chen,Y. Hu,Y. Kishi, *J. Am. Chem. Soc*, **2012**,134,6136-6139.

Chapter 3

Catalytic Applications

Introduction

3.1 Catalysis

From the scientific and industrial points of the view, catalysis is a very interesting field. Therefore, this study focuses on the preparation of novel catalysts. A catalyst is usually defined as a substance that participates in a reaction without being consumed in the process, increasing the speed of the reaction by creating an alternative path. In this new reaction pathway, all the steps have lower activation energies in comparison with those of the original path, as shown in Figure 41.

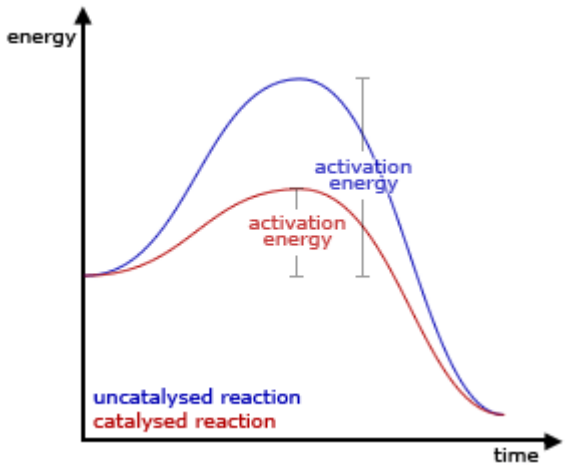

Figure 41: Changes in activation energy in the presence of a catalyst.[1]

Nowadays, successful catalysis requires the realization of several features, such as low preparation cost, high activity, great selectivity, efficient recovery, and recyclability. Conventional catalysts can be divided into two categories: homogeneous and heterogeneous. In homogeneous catalysis, the catalyst is in the same phase as the reactants, whereas in heterogeneous catalysis, the catalyst is in the solid phase with the reaction occurring on the surface.[2] However, difficulties in separating homogeneous catalysts from the reaction medium restrict their employment in industrial applications, especially in the manufacture of drugs and pharmaceuticals in the case of metal-

catalyzed synthesis owing to the issue of metal contamination. In heterogeneous catalysis, the reaction rate is restricted owing to the limited surface area of the catalyst.

A strategy that implements the advantages of both catalyst types involves the heterogenization of active molecules on a solid support, such as nanoparticles. As discussed previously, the use of MNPs for heterogenization requires the system to have various properties, such as stability, high surface area, a tendency to not form aggregates, and the possibility of functionalizing the capping agent.

3.2 Heterocyclic compounds

Heterocyclic compounds are present in biological and synthetic drugs. Various currently marketed drugs have heterocycles as their core structure, as shown in Scheme 15.

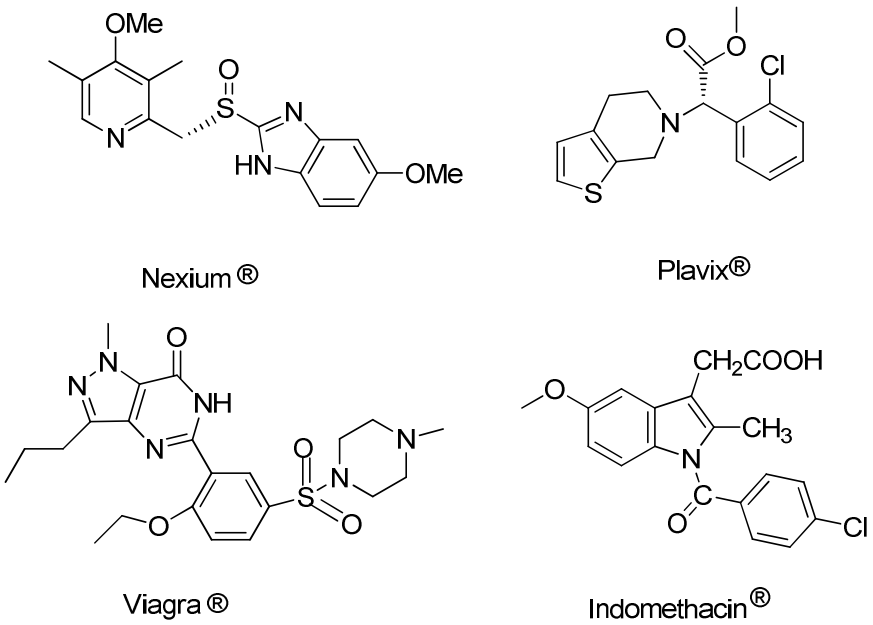

Scheme 15

Indoles are probably the most widely distributed heterocyclic compounds in nature with medicinal importance (Scheme 16). Tryptophan is an essential amino acid and, as such, is a constituent of most proteins; it also serves as a biosynthetic precursor for a wide variety of secondary metabolites. Serotonin or 5-hydroxytryptamine (5-HT) is a monoamine neurotransmitter in the central nervous system, and also in the cardiovascular and gastrointestinal systems, which

regulates mood, sleep, appetite, and the emotional perception of pain. The structurally similar hormone melatonin is thought to control the diurnal rhythm of physiological functions.

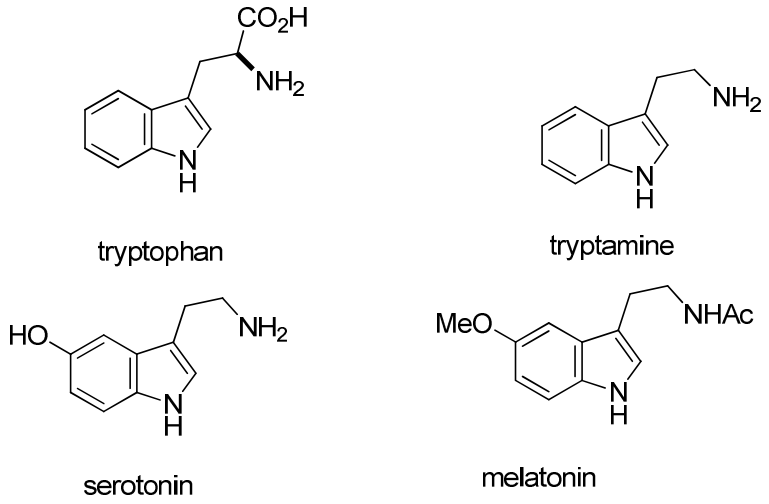

Scheme 16

In pharmaceutical drugs, the indole skeleton is present as a basic molecular structure, as demonstrated in Table 8. However, in general, high cost and complicated synthesis operations are required to obtain indoles. Syntheses of indoles have been performed by Fischer, Madelung, Bischler, Reissert, Nenitzescu, Leimgruber-Batcho, etc. In various methods, transition metals have been used as catalysts, especially palladium complexes. Palladium is tolerant to a wide range of functionalities and has many applications in organic synthesis. Both palladium(II) and palladium(0) can be used for the synthesis of indoles. Palladium(II), which is very electrophilic and tends to react with electron-rich alkenes and arenes, presents the best results in a number of studies.

Table 8. Indole-ring-containing drug molecules.[3]

Drug	*Application*	*Drug*	*Application*	*Drug*	*Application*
Vincristine	Anticancer	**Vincamine**	Vasodilator	**Roxindole**	Schizophrenia
Vinblastine	Anticancer	**Reserpine**	Antihypertensive	**Delavirdine**	Anti-HIV
Vinorelbine	Anticancer	**Peridopril**	Antihypertensive	**Atevirdine**	Anti-HIV
Vindesine	Anticancer	**Pindolol**	Antihypertensive	**Arbidol**	Antiviral
Mitraphylline	Anticancer	**Binedaline**	Antidepressant	**Zafirlukast**	Anti-Asthmatic
Cediranib	Anticancer	**Amedalin**	Antidepressant	**Bucindolol**	β-Blockers
Panobinostat	Anti-leukamic	**Oxypertine**	Antipsychotic	**Pericine**	Opioid agonist
Apaziquone	Anticancer	**Siramesine**	Antidepressant	**Mitragynine**	Opioid agonist
Tropisetron	Antiemetic	**Indalpine**	Antidepressant	**Pravadoline**	Analgesic
Doleasetron	Antiemetic	**Yohimbine**	Sexual Disorder	**Bufotenidine**	Toxin
Oglufanide	Immunomodulatory	**Indomethacin**	Anti-inflammatory	**Proamanullin**	Toxin

The reductive cyclization of *o*-nitrostyrenes has been known since 1965 when Sundberg[4] developed a reductive cyclization of *o*-nitrostyrenes to indoles using trivalent phosphorus as a ligand. In 1986, Cenini and coworkers[5] employed the same substrates to obtain catalytic deoxygenation of the nitro group using carbon monoxide and transition metal carbonyls under harsh conditions, as shown in Scheme 17.

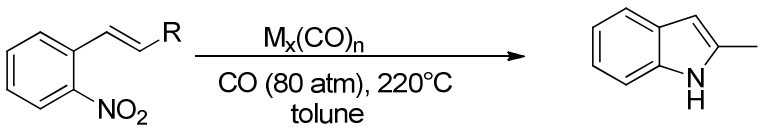

Scheme 17

In 1997 and 1999, Soderberg[6a,b] demonstrated that it is possible to synthesize indole compounds by reductive N-heteroannulation of 2-nitrostyrenes using carbon monoxide as a reductive agent and Pd/phosphine, as shown in Scheme 18. In general, the mechanism involves reductive deoxygenation of a nitro group and the use of palladium as a catalyst.

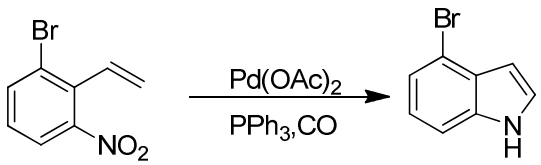

Scheme 18

Depending on the basicity of the phosphine, the catalytic activity may be improved or worsened and, in general, phosphine ligands are good σ-donors.

In 2005, Davies and coworkers[7] showed that is possible to improve the efficiency of the catalytic system for reactions of *o*-nitrostyrenes affording indoles. Conditions similar to those used by Soderberg were tested for the Pd/phosphine-catalyzed reductive cyclization of *o*-nitrostyrenes. The results showed that reducing the ligand and catalyst loading resulted in decreased yields owing to lower conversion. Taking into account this result, the authors searched for another efficient catalyst system. Catalytic reactions with palladium(II) salts and bidentate nitrogen ligands are highly reactive systems, and the use of bidentate nitrogen ligands has been demonstrated to be very efficient for the reductive carbonylation of nitroarenes to give isocyanates and carbamates. Moreover, this system had already been employed to reduce nitrostyrene, but at high temperature

and pressure. Using these arguments, Davies decided to replace the phosphine ligand with a phenanthroline ligand. The initial results with Phen demonstrated that is possible to use this catalytic system at lower pressures and temperatures.

In 2009, Ragaini and coworkers[8] showed that is possible to synthesize indoles by intermolecular cyclization (Scheme 19).

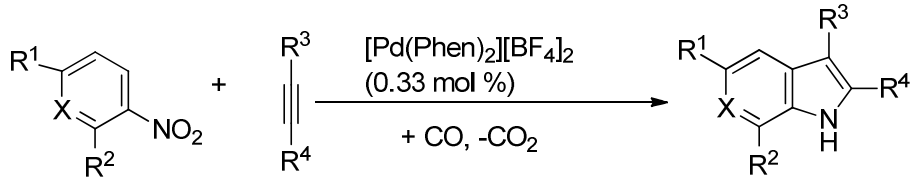

Scheme 19

In this study, a Pd/phenanthroline complex was chosen as an active catalyst for the reduction of nitroarenes. Several nitroarenes and alkynes were studied, and the reaction was found to be completely regioselective. Further, the Pd/phenanthroline catalyst proved to be very efficient.

3.3 Oxidative Heck reactions

The first example of an oxidative Heck reaction was reported by Heck[9] using arylmercuric chlorides, but owing to the employment of toxic organomercury compounds, the reaction was not widely accepted in the scientific community (Scheme 20).

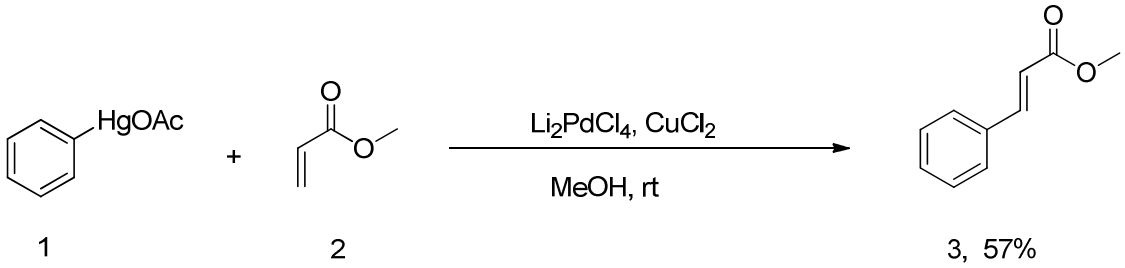

Scheme 20

Several years later, in 1994, Uemura et al.[10] demonstrated that the reaction could be carried out equally well with arylboronic acids (Scheme 21).

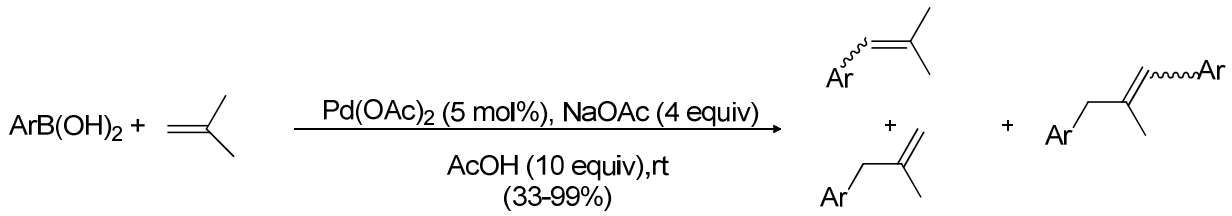

Scheme 21

Jung and coworkers[11] reported the first example of an aerobic oxidative Heck reaction. In this work, molecular oxygen was investigated as an effective oxidant for the reaction (Scheme 22).

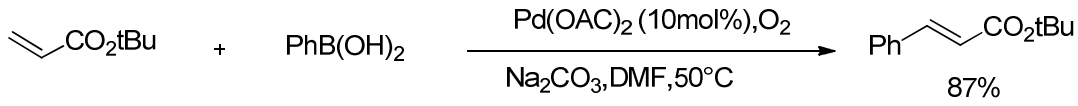

Scheme 22

Larhed and coworkers[12,13] studied the influence of an added ligand on this reaction. They found 2,9-dimethyl-1,10-phenanthroline (dmphen) to be a highly effective ligand for this reaction, when carried out in the presence of *N*-methylmorpholine as a base. In comparison, the use of phosphines was found to be ineffective owing to their oxidation under the same conditions (Scheme 23).

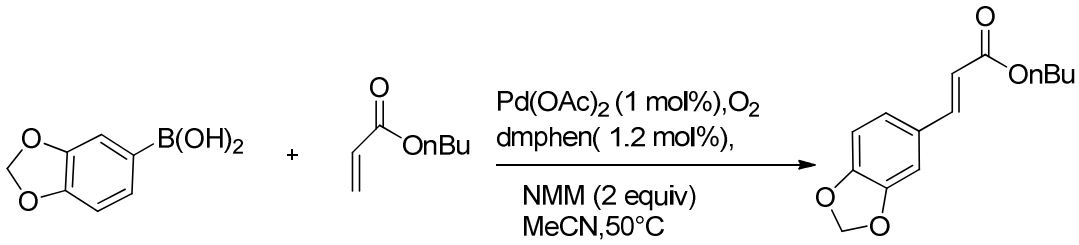

Scheme 23

The same group investigated the very important feature of regioselectivity in the arylation of enamides, revealing that it is influenced by the electronic properties of boronic acid. These results demonstrated that higher selectivity is obtained in the reaction in the presence of electron-rich boronic acids; consequently, the use of electron-poor boronic acids led to poor selectivity. Other

studies performed by the same group and Jung and coworkers demonstrated that it is possible to use this catalyst, even in the absence of a base, when the product is an enone. The effectiveness of dmphen was attributed to the methyl groups at the 2 and 9 positions, which prevent the formation of inactive palladium dimers. The same steric effect is important for other reactions, such as the oxidation of alcohols. It should be noted that the use of a supported ligand may be advantageous in such situations, as dimerization may become impossible for geometric reasons, which would eliminate the need for *ortho*-substituents. This would be an advantage because the presence of such substituents may retard individual steps of the catalytic cycle and add synthetic complexity during ligand synthesis.

Results and Discussion

3.4 Synthesis of substrate for catalytic applications

The coordination of $Pd(OAc)_2$ to the $–CH_2$-Phen and –O-Phen moieties immobilized on the nanoparticles cannot be assessed spectroscopically because of the lack of characteristic IR absorption bands and the impossibility of using ^1H NMR spectroscopy owing to the superparamagnetic nature of the nanoparticle core. Thus, the most straightforward evidence for coordination is the successful use of the prepared substrates in catalysis. Consequently, we synthesized various substituted *o*-nitrostyrenes to form indoles using CO as a reductant (Scheme 24). The catalytic cycle involves the reaction of a nitro compound in the presence of a Pd catalyst and CO. The initial *o*-nitrostyrene gives an *o*-nitrososty rene by elimination of CO_2, which undergoes further reaction to give a nitrone. A subsequent 1,5-hydrogen shift and isomerization affords a *N*-hydroxyindole that reacts with a second equivalent of CO to finally afford the indole.

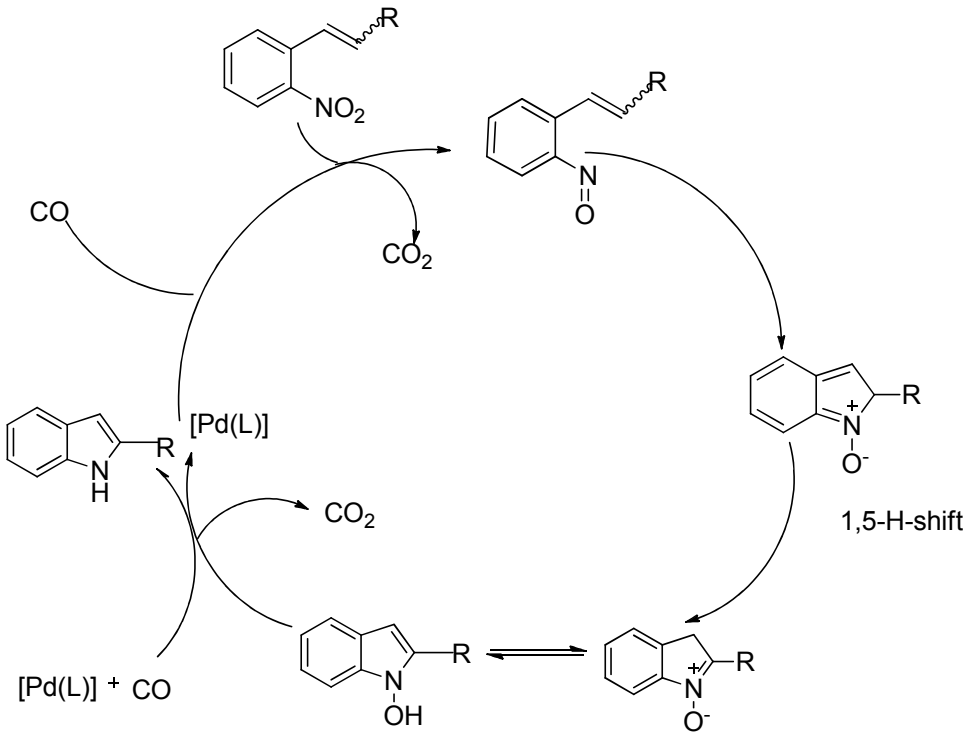

Scheme 24

3.4.1 Synthesis of (*E*)-2-(2-nitrostyril)pyridine

This starting material (Schemne 25) was prepared by the reaction of *o*-nitrobenzaldehyde, 2-picoline, and acetic anhydride for 28 h at reflux. The product was obtained as a yellow solid (69% yield).

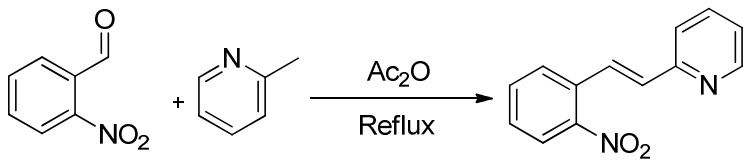

Scheme 25

^{1}H NMR: (400 MHz, $CDCl_3$) δ 8.66 (d, *J* = 4.1 Hz, 1H), 8.06 (d, *J* = 16.0 Hz, 1H), 8.00 (dd, *J* = 8.0, 1.2 Hz, 1H), 7.81 (d, *J* = 7.8 Hz, 1H), 7.73 (td, *J* = 7.71, 1.7 Hz, 1H), 7.65 (t, *J* = 7.5 Hz, 1H), 7.51 (d, *J* = 7.9 Hz, 1H), 7.49 (t, *J* = 7.8 Hz, 1H), 7.26 (d, 1H, overlaps with $CDCl_3$), 7.17 (d, *J* = 16.1 Hz, 1H) ppm. (figure 46,47)

3.4.2 Synthesis of 2-(pyridine-2-yl)-1*H*-indole

In this synthesis (Scheme 26), (*E*)-2-(2-nitrostyril)pyridine was employed as the substrate and the catalyst was the palladium complex of 4-MePhen immobilized on the protective layer of MNPs, as discussed in Chapter 2. The experimental conditions for the catalytic tests were adapted from a procedure reported by Davies et al.[7]

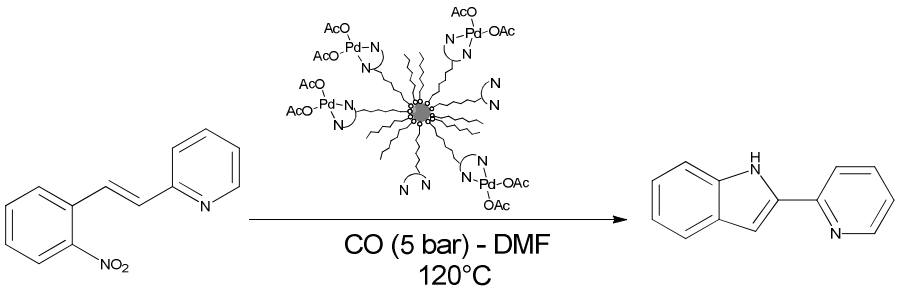

Scheme 26

The approximate amount of palladium bound to the nanoparticles employed as catalysts was estimated based on the amount of bound phenanthroline, which in turn was calculated by elemental analysis, as detailed in Chapter 2. The data for synthesis V (Table 6, Chapter 2) were employed, as this sample was used for the following tests. The initial tests with MNPs were carried out employing 12 mg of MNPs (corresponding to 0.043 mmol of Pd) and a CO pressure of 2 bar, but this attempt was not successful, as shown in Table 9. In the second attempt, the time and amount of MNPs was doubled, but again the results were poor. Thus, we increased the CO pressure to 20 bar, which is significantly higher than the pressure employed in the Davies study. Although improved results were observed at this pressure, the selectivity decreased if the temperature was also increased to 120 °C (entry V, Table 9). After some optimization, we found that the best conditions for this reaction system were 5 bar and 120 °C in DMF (entry VIII, Table 9).

Table 9. Catalytic results for the conversion of (*E*)-2-(2-nitrostyril)pyridine to 2-(pyridine-2-yl)-1*H*-indole.

Entry	Pressure (CO)/ bar	Solvent	Temp. (°C)	Time (h)	Conv. (%)	Selec. (%)
I[a]	2	DMF	80	8	0	0
II[a]	2	DMF	80	15	0	0
III[b]	20	DMF	80	7	6	81
IV[b]	20	DMF	80	14	9	76
V[b]	20	DMF	120	21	36	64
VI[b]	5	DMF	150	3	0	0
VII[b]	5	CH_3CN	120	7	23	54
VIII[b]	5	DMF	120	7	62	79
Recycle*VIII[b]	5	DMF	120	7	13	52

Experimental conditions: [a] 0.5 mmol nitro compound,12 mg, MNP(N^N), corresponding to 0.043 mmol Pd. 5 mL DMF. [b] 0.5 mmol nitro compound, 24 mg MNP(N^N), corresponding to 0.086 mmol Pd. 5 mL DMF; * a recycle of reaction VIII.

Using the results in entry VIII, we tested the recyclability of this catalyst system. These tests were performed as shown in Figure 42 (recycle* VIII) by employing magnetic bars. The separation process was very fast (taking about 5 min overall), easy, and very attractive from the point of view of experimental conditions. As shown in Table 9, it was only possible to recycle the catalyst once. This recycling issue may be attributed the coordinating ability of the pyridine moiety in the substrate, which may favor loss of palladium from the nanoparticle. For this reason, we synthesized another substrate.

(a) (b)

Figure 42: Process for recycling the MNPs: (a) before and (b) after separation using magnetic bars.

3.4.3 Synthesis of methyl-2-nitrocinnamate

The synthesis was performed by reacting 2-nitrocinnamic acid, sulfuric acid, and MeOH at reflux for 21 h. The product was obtained as a yellow solid (57% yield).

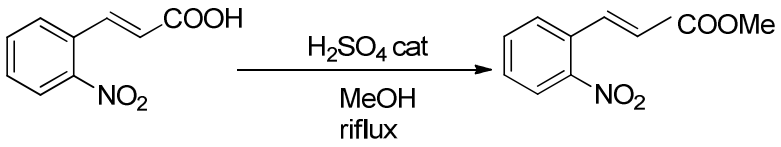

Scheme 27

^{1}H NMR (400 MHz, $CDCl_3$) δ 8.16 (d, ^{3}J = 15.8 Hz, 1H, H^e), 8.06 (d, ^{3}J = 7.9 Hz, 1H, H^d), 7.70–7.65 (m, 2H, H^a and H^b), 7.57 (dd, 1H, H^c), 6.37 (d, ^{3}J = 15.8 Hz, 1H, H^f), 3.86 (s, 3H, CH_3) ppm. (figure 48,49)

3.4.4 Synthesis of methyl-1*H*-indole-2-carboxylate

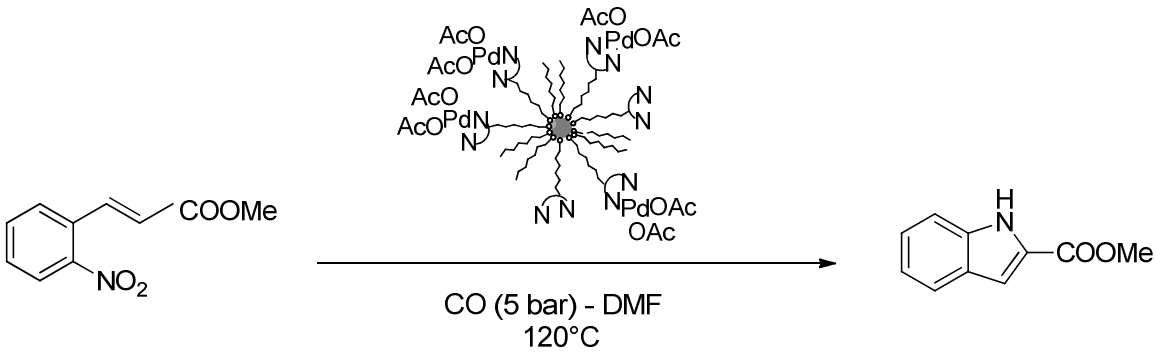

Scheme 28

In this synthesis, we employed methyl-2-nitrocinnamate as the substrate and the palladium complex of the –O-Phen-functionalized nanoparticles as the catalyst. Nanoparticles functionalized under the best immobilization conditions for 4-OH-Phen (entry V, Table 7, Chapter 2) were employed, using the best catalytic conditions for solvent, pressure, and temperature, as identified in section 3.4.2. The results of this catalytic reaction are shown in Table 10, entry I.

The catalyst was recycled by following the procedure described above. In this case, the recycling results were better than when (*E*)-2-(2-nitrostyril)pyridine was employed as the substrate. However,

even in this case, the conversion decreased after the first recycle. Thus, the coordinating ability of the pyridine moiety of the substrate is only part of the problem. In general, it is clear that some palladium is lost during the catalytic reaction.

Table 10. Catalytic results for the conversion of methyl-2-nitrocinnamate to methyl-1*H*-indole-2-carboxylate.

Entry	Pressure (CO)/ bar	Solvent	Temp.	Time (h)	Conv. (%)	Selec. (%)
I	5	DMF	120°C	7	79	72
Recycle* I	5	DMF	120°C	7	31	88

Experimental conditions: 0.5 mmol nitro compound, 24 mg MNP(N^N), corresponding to 0.172 mmol Pd. 5 mL DMF; * a recycle of reaction I

3.5 Oxidative Heck reactions

As discussed in the general introduction, Oxidative Heck reactions were used as a second strategy to test our system. The conditions for such reactions are milder than those used in the synthesis of indoles. In this case, we employed commercially available phenylboronic acid and styrene as substrates (Scheme 29). Initially, we tested the reaction by employing a homogeneous catalyst to determine the analytical procedure and optimize the experimental conditions (Table 11). As a starting point, we used the conditions reported by Larhed and coworkers.[13]

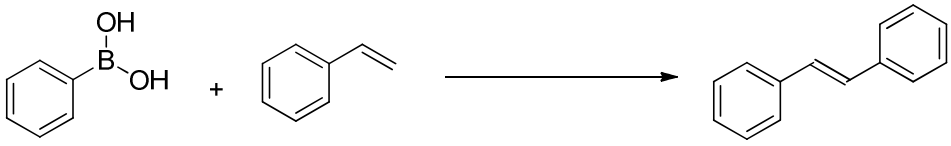

Scheme 29

The original study employed 2 mmol of phenylboronic acid and 1 mmol of styrene. As phenylboronic acid is more expensive than styrene, we initially tried to employ a lower amount of the former reagent. We conducted a series of tests (Table 11). A batch of phenylboronic acid already available in the laboratory was used in the initial tests (entries 1–8), but the purity of this batch was apparently compromised, and subsequent tests were conducted with a newly purchased batch. In the first five attempts, we performed the reaction at 80 °C for 3 h without the addition of a base. To mimic the process in our system employing 4-OH-Phen-functionalized nanoparticles, we

tested 4-MeO-Phen as a ligand (entry 5). Even though the results showed a low activity, we decided to start testing our system with MNPs using the same conditions (entry 6). However, the results were disappointing. More tests were then carried out in the homogeneous phase. In entry 8, we carried out a control experiment without palladium, which demonstrated that catalysis does not occur, as expected.

Suspecting that the catalyst was easily deactivated at 80 °C, from entry 11 onwards, we performed the reaction at RT. Among the various results, entry 13 indicates the importance of preformation of the catalyst in the process. Initially (entries 1–12), the reagents were added in the following order: phenylboronic acid, styrene, solution with ligand (1 mL), solution with palladium acetate (2 mL), and finally base (if applicable). In the original study, palladium acetate and the bidentate ligand were dissolved together in MeCN and then added to the reaction mixture. We ascribed the better results in entry 13 to the adoption of this procedure, which allows catalyst preformation. Following these tests in the homogeneous phase, we decided to use the same amounts of reagents as reported in the reference article, abandoning our attempt to employ a lower amount of phenylboronic acid. In this case (entry 15), the results were indeed similar to those reported in the original article. We decided to test 4-MeO-Phen again to mimic the reaction with our system containing nanoparticles, now at RT and using a preformed catalyst (entry 16). As this result was better than that in entry 5, we decided to test the (4-OH-Phen)-MNP system again (entry 17), but the results were again below expectations. We performed a test without the ligand and found that the catalytic reaction does not proceed in the presence of only palladium (entry 18). We then tested our MNP system with 4-MePhen as a ligand using the same conditions as listed previously, but increasing the reaction time by performing the test over a weekend (entry 21). We also performed one recycling test for this entry, as shown in entry 21-R, but the results were poorer than expected.

At this point, we decided to carry out atomic absorption spectroscopy measurements on the palladium coordination systems to check the amount of palladium present in both systems, that is, MNPs functionalized with 4-OH-Phen and 4-MePhen. The atomic absorption analysis was performed following the procedure for destruction of the nanoparticles; however, in this case, we employed a mixture of nitric acid and hydrochloric acid, known as "aqua regia", and for analysis of the recycling test, we employed the solution remaining after separation with magnetic bars (entry 21-R). We found that the amount of palladium measured by atomic absorption, assuming all bound phenanthrolines coordinate one palladium atom, was lower than expected by eight times for 4-OH-Phen-MNPs (entry 26) and six times for 4-MePhen-MNPs (entry 27). In the case of indole synthesis

using CO as a reductant, although we encountered problems in the recycling of the catalyst, the catalytic reactions proceeded, even if the amount of palladium was lower than expected. Clearly, the catalytic system is very active for this reaction. However, in the case of oxidative Heck reactions, the amount of MNPs (24 mg) seems to be insufficient. It is important to note that the results for the recycling solution confirmed the loss of palladium to be about 27%.

The reaction in entry 22 was performed by withdrawing six aliquots of the solution at 3 h intervals to monitor the changes in conversion and selectivity for a reaction performed in the homogeneous phase using Neoc as a ligand. The results of this text are shown in Figures 43–45. In Figure 43, it is interesting to observe that the conversion does not change appreciably after the first 9 h, suggesting that either the catalyst has been deactivated or one of the reagents has been completely consumed. The available data are insufficient to draw clear-cut conclusions, but some tentative explanations for the observed results can be given, which should be considered as provisional for the moment.

a) The fact that the amount of *trans*-stilbene continues to increase, even after no further styrene is consumed, indicates that some long-lived intermediate is formed that is slowly converted to the final product.
b) *cis*-Stilbene is not formed initially, but appears at a later stage, which may be associated with a slower decay of the long-lived intermediate for this product or with the fact that it is only produced by isomerization of initially formed *trans*-stilbene. Further, *cis*-stilbene is a very minor product, with the reaction being selective for the *trans* isomer.
c) The fact that the selectivity for both *trans*- and *cis*-stilbene is much lower than expected in all cases in which an excess of boronic acid is not present and that, in the case of reaction 22, the selectivity increases with time up to a certain point and then decreases is puzzling. The only explanation we can advance for both these observations is that styrene is consumed by polymerization, a reaction known to be catalyzed by palladium complexes. This would also explain the otherwise difficult to rationalize decrease of selectivity at the end of the reaction for both *trans*- and *cis*-stilbene. If we assume that polymerization of styrene occurs, inclusion of stilbene in the polymer chain is highly likely. As stilbene is still formed, its rate of formation may be higher than that of inclusion in the polymer, resulting in an increase in the amount in solution. However, once most styrene has been consumed, stilbene consumption becomes faster, and the amount in solution decreases. Although not stated in the literature, polymerization of styrene may be the reason why most authors perform the

reaction in the presence of an excess of the boronic acid instead of working with an excess of the cheaper and more easily separable olefin.

d) The above supposition was experimentally confirmed by running a reaction under the conditions of entry 15 in the absence of phenylboronic acid (entry 28). A 60% styrene conversion was observed, but no product could be detected by GC, which is in accordance with the high molecular weight of the products and their polymeric nature.

The reaction in entry 23 was run using THF as the solvent, and the results demonstrated that this solvent can be used as an alternative to MeCN. To simulate the amount of palladium that was found to be present on the nanoparticles by atomic adsorption spectroscopy in the system with 4-MePhen, the experiment in entry 24 was performed using a 6-fold lower amount of palladium than usually employed The obtained conversion, as expected, was about 6 times lower than that for the best result (entry 15). We also tested the 4-OH-Phen-functionalized MNPs with 2.0 mmol of phenylboronic acid (entry 25). This result confirmed once again the observed problem regarding selectivity.

To simplify Table 11, we have employed the following numbers to identify the reagents:

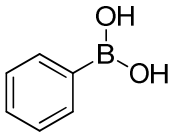

Phenylboronic acid

1

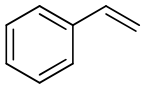

Styrene

2

For the ligands, we employed the following numbers:

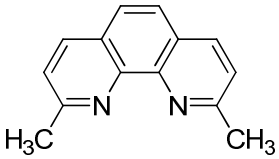

Neocuproine

3

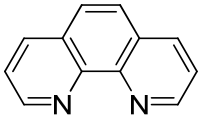

1,10-phenanthroline

4

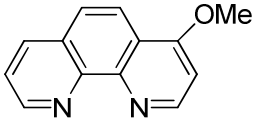

4-Methoxy-1,10-phenanthroline

5

For the MNPs (coordinated to $Pd(OAc)_2$, although only the ligand is shown), we employed the following numbers:

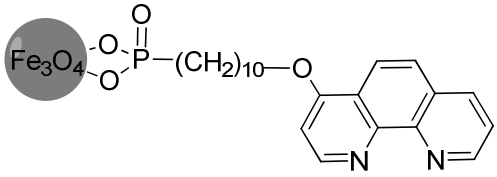

4-OH-Phen

6

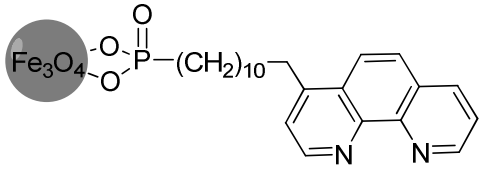

4-MePhen

7

For the base, we employed the following number:

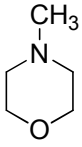

4-Methylmorpholine

8

Table 11. Catalytic results for oxidative Heck reactions.

Entry	Reagent 1 [mmol]	Reagent 2 [mmol]	Ligand	Base	$Pd(OAc)_2$ [mmol]	T(°C)	Time (h)	cis-stilbene	Conv. (%)	Selec. (%)
1	1.5[a]	1	3	-	0.02l	80	3	-	21	27
2	1.1[a]	1	3	-	0.02	80	3	-	13	25
3	1.1[a]	1	3	-	0.02	80	3	9	53	45
4	1.1[a]	1	4	-	0.02	80	3	-	46	12
5	1.1[a]	1	5	-	0.02	80	3	-	35	7
6	1.1[a]	1	**6**	-		80	3	-	35	1
7	1.1[a]	1	3	8	0.02	80	3		13	57
8	1.1[a]	1	5	-	-	80	3	-	0	0
9	1.1	1	3	-	0.02	80	3	11	29	57
10	1.1	1	5	-	0.02	80	3	3	59	54
11	1.1	1	3	-	0.02	RT	24	5	99	32
12	1.1	1	3	8	0.02	RT	24	11	58	55
13	1.1	1	3	8	0.02	RT	24	11	61	64
14	1.1	1	3	-	0.02	RT	24	5	83	34
15	2.0	1	3	8	0.02	RT	24	3	95	92
16	1.1	1	5	8	0.02	RT	24	-	54	53
17	1.1	1	**6**	8		RT	24	-	0	0
18	1.1	1	5	8		RT	24	-	0	0
19	1.1	1	3	8	0.02	RT	48	7	55	70
20	1.1	1		8	0.02	RT	24	-	0	0

21	1.1	1	**7**	8		RT	64	-	39	14
21-R	1.1	1	**7**	8		RT	61	-	49	4
22-1P	2.2	2	3	8	0.04	RT	24	-	89	3
22-2P	2.2	2	3	8	0.04	RT	24	-	91	5
22-3P	2.2	2	3	8	0.04	RT	24	-	92	6
22-4P	2.2	2	3	8	0.04	RT	24	1	90	14
22-5P	2.2	2	3	8	0.04	RT	24	2	92	24
22-6P	2.2	2	3	8	0.04	RT	24	1	92	14
23	1.1	1	3	8	0.04	RT	24	28	42	71
24	2.0	1	3	8	0.02/6	RT	24	-	16	33
25	2.0	1	**6**	8		RT	24	-	18	7
26	1.1	1	**6**	8	8x	RT	24	-	73	12
27	1.1	1	**7**	8	6x	RT	24	-	65	8
28	-	1	3	8	0.02	RT	24	-	60	-

Experimental conditions: Open vessel charged with phenylboronic acid [(1.1= 2-14,16-21-23) – 1.5(1) and 2.0 (15)mmol], (olefin -2.0 mmol), N- methylmorpholine (2.0 mmol), $Pd(OAc)_2$ (0.02 mmol), Neoc (0.024 mmol) and acetonitrile (3 mL) employed under homogeneous catalysis conditions. [a] old phenylboronic acid. Undistilled acetonitrile was employed in entries 1 and 2 . All other other reactions were performed in dried and distilles acetonitrile, except for entry 10, where DMF was used as a solvent and entry 23, where THF was used as a solvent. 24 mg of nanoparticles was employed in the case of the system with MNP(N^N) entries 6,17,21 and 21R. The reaction in entry 22 was performed employing a double amount of the substrate, base, catalyst and solvent (6 mL). The reaction in entry 28 was performed employing in absence of phenylboronic acid.

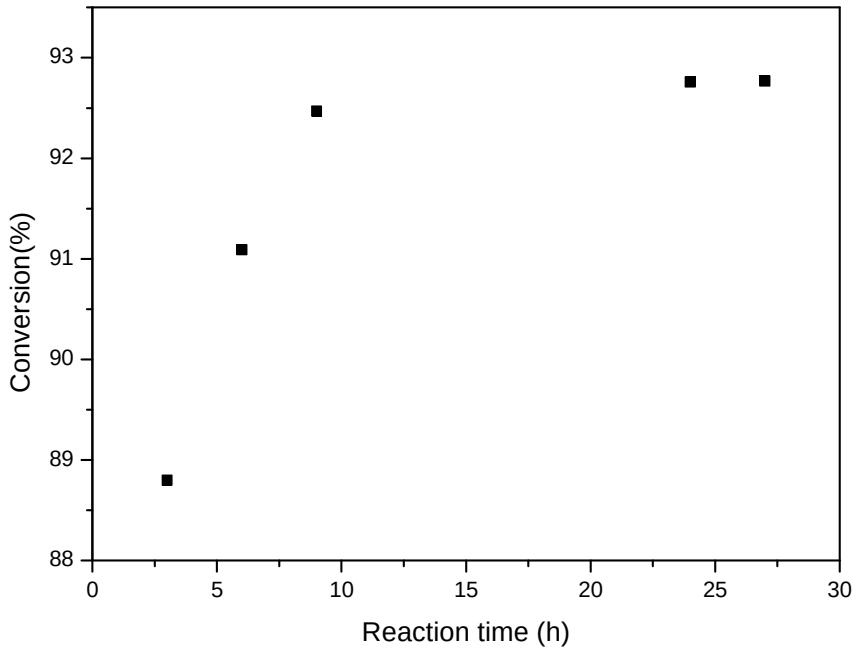

Figure 43: Conversion of styrene (results of entry 22).

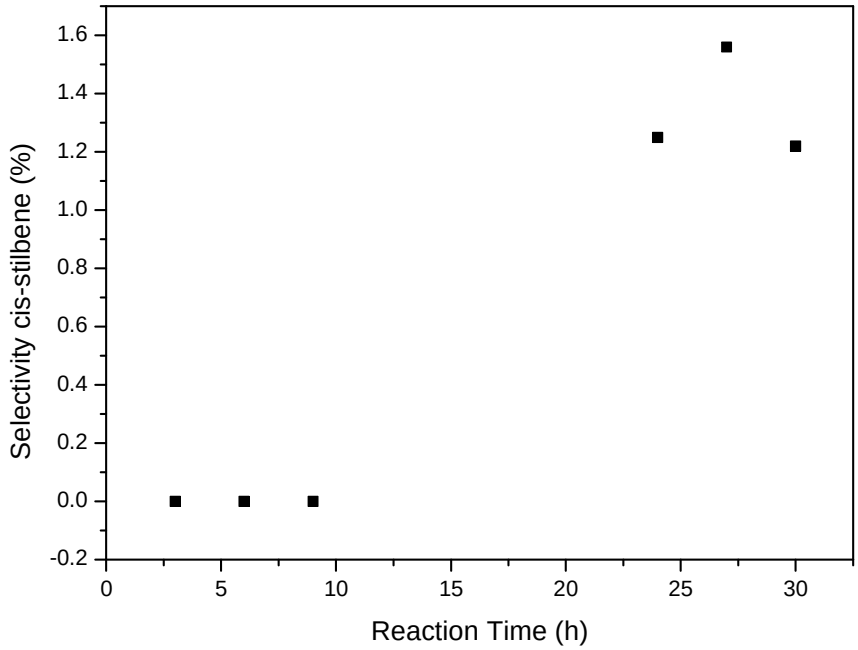

Figure 44: Selectivity for *cis*-stilbene (results of entry 22).

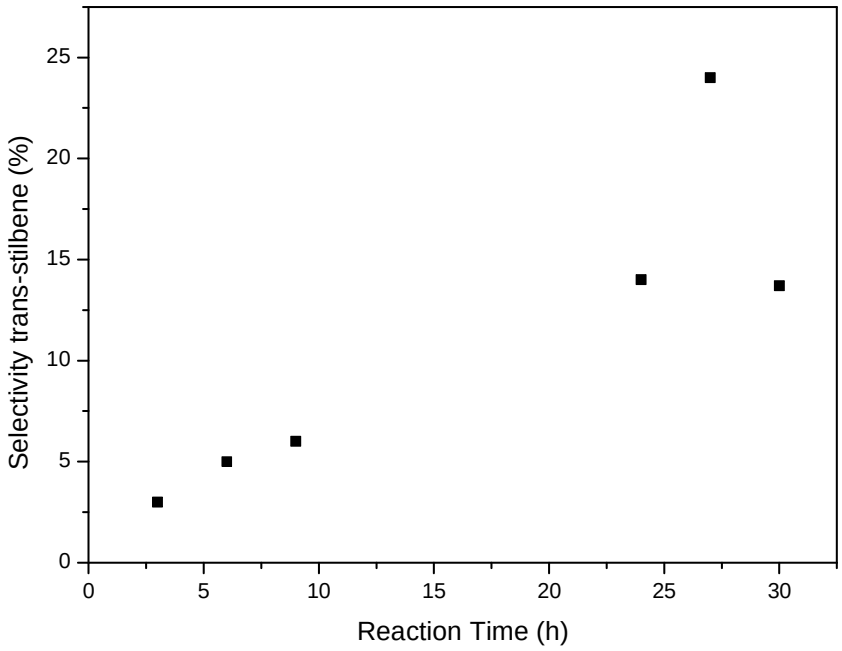

Figure 45: Selectivity for *trans*-stilbene (results of entry 22).

Experimental Section

3.6 Synthesis of (*E*)-2-(2-nitrostyril)pyridine

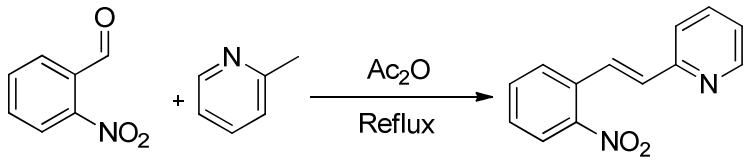

Reagent	M.W(g•mol^{-1})	mg	mmol	Molar ratio	V [ml]	d[g/mL]
o-nitrobenzaldehyde	151.12	1.7054	11.26	1		
2-picoline	93.13	1.369	14.70	1.31	1.45	0.944
Acetic anhydride					3	

A 25 mL Schlenk round-bottom flask was charged with *o*-nitrobenzaldehyde, 2-picoline, and acetic anhydride. A reflux condenser was attached and the solution was heated to reflux for 28 h (reaction conversion was monitored by TLC on silica using AcOEt:hexane = 7:3 as the eluent). The color of the solution gradually turned dark. At the end of the reaction, 5 mL of water was added and the reaction mixture was maintained at RT for 90 min under stirring. The formed dark solution was filtered on a Buchner funnel and washed with a little cold water. A TLC (AcOEt:hexane = 8:2 as the eluent) showed that the product is present, but there was also a dark spot at the bottom of the TLC plate. To isolate the product, a filtration over silica gel was performed (AcOEt:hexane = 8:2 as the eluent). After drying over Na_2SO_4 and evaporation of the solvent in vacuo, the product was obtained as a yellow solid (1.7587 g, 69.09% yield). The ^{1}H NMR spectrum revealed the presence of only the *E* isomer (Figures 46, 47).

^{1}H NMR: (400 MHz, $CDCl_3$, 298 K) δ 8.66 (d, *J* = 4.1 Hz, 1H), 8.06 (d, *J* = 16.0 Hz, 1H), 8.00 (dd, *J* = 8.0, 1.2 Hz, 1H), 7.81 (d, *J* = 7.8 Hz, 1H), 7.73 (td, *J* = 7.71, 1.7 Hz, 1H), 7.65 (t, *J* = 7.5 Hz, 1H), 7.51 (d, *J* = 7.9 Hz, 1H), 7.49 (t, *J* = 7.8 Hz, 1H), 7.26 (d, 1H, overlapped with $CDCl_3$), 7.17 (d, *J* = 16.1 Hz, 1H) ppm.

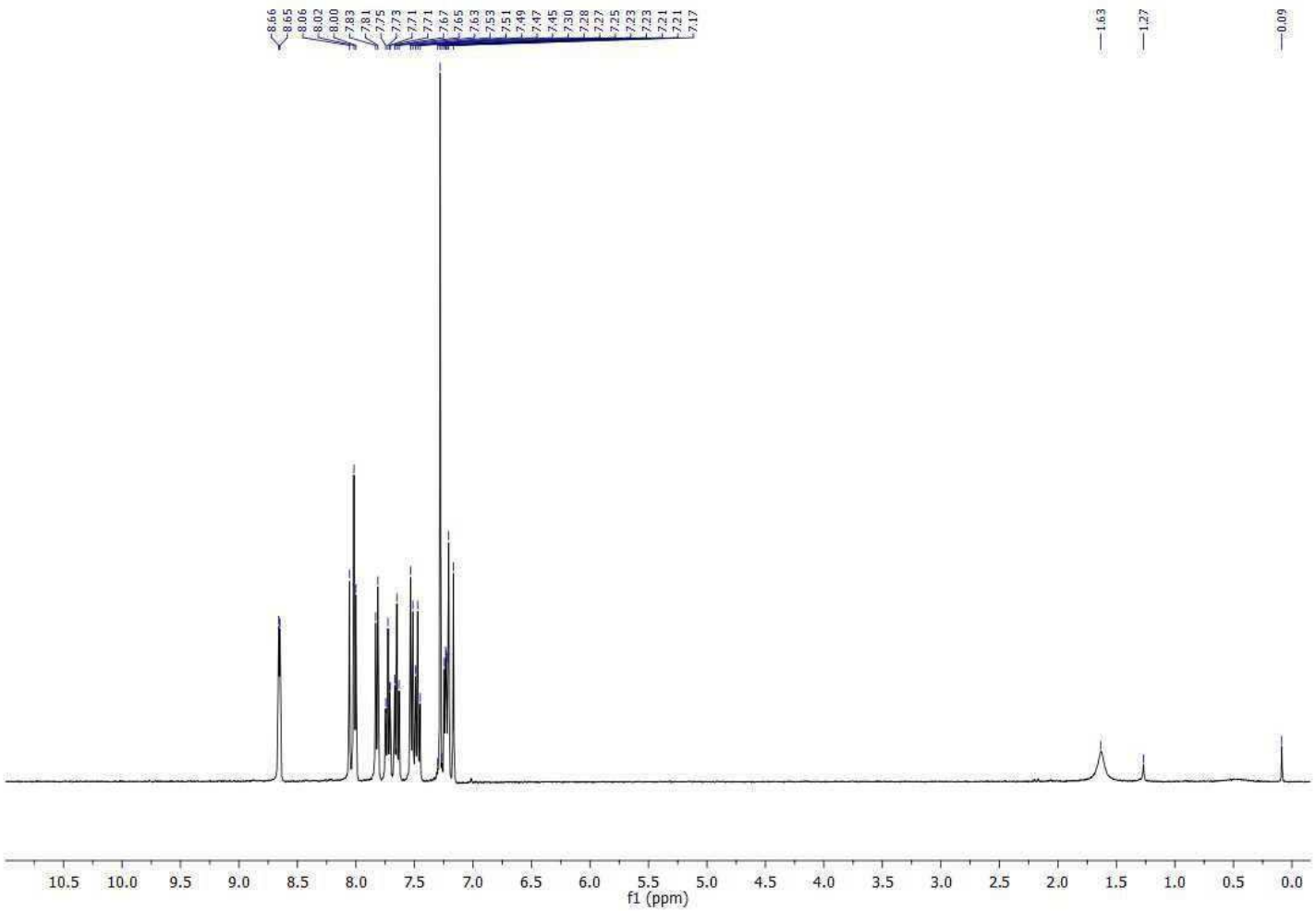

Figure 46: ^{1}H NMR (400 MHz, $CDCl_3$, 298 K) spectrum of (*E*)-2-(2-nitrostyril)pyridine.

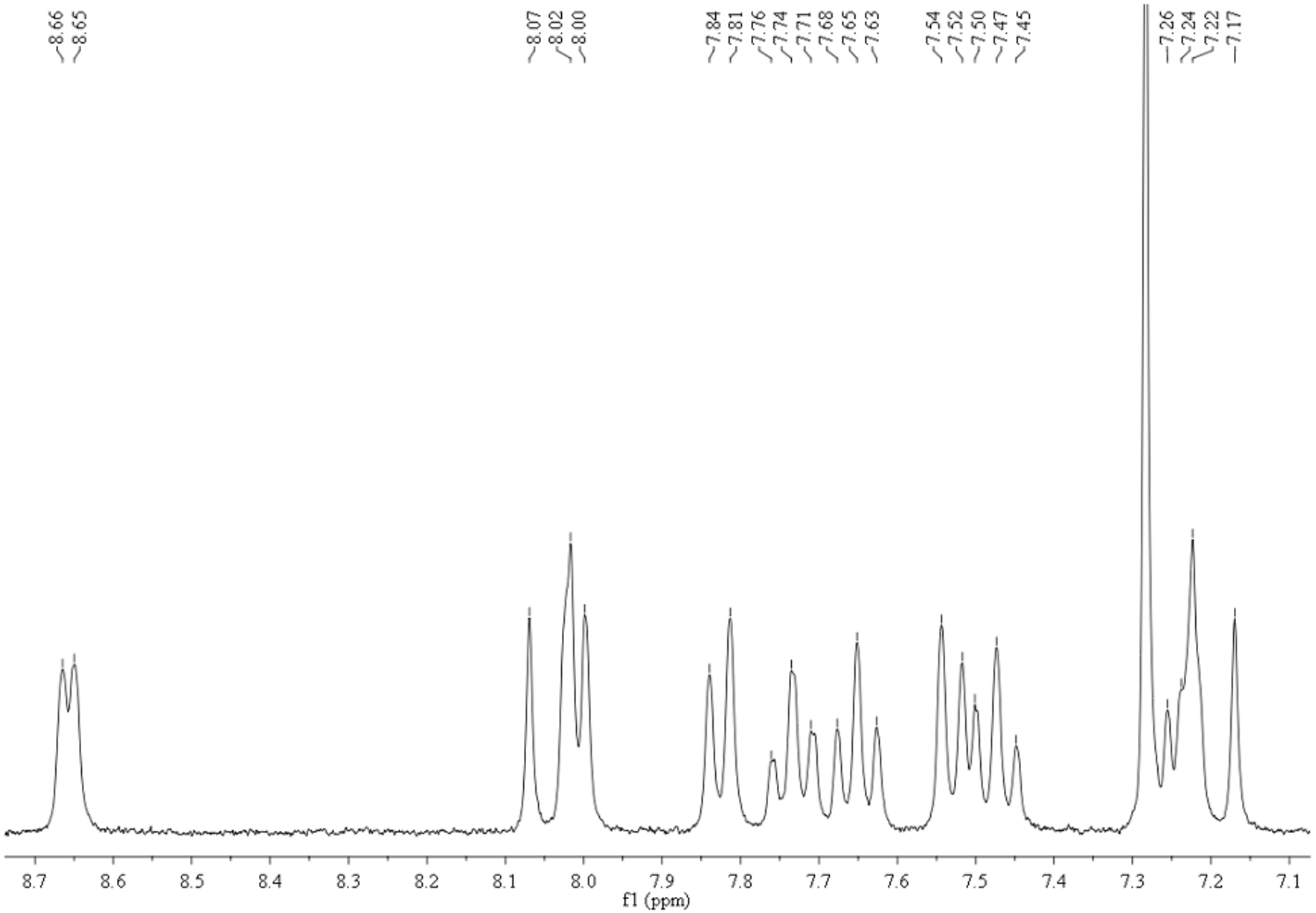

Figure 47: Expanded ^{1}H NMR (400 MHz, $CDCl_3$, 298 K) spectrum of (*E*)-2-(2-nitrostyril)pyridine.

3.7 Synthesis of 2-(pyridine-2-yl)-1*H*-indole

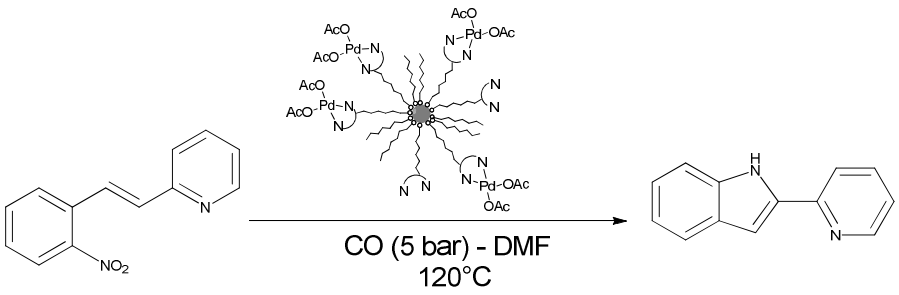

Reagent	M.W(g•mol^{-1})	mg	mmol	Molar ratio	V [ml]	d[g/mL]
(E)-2-(2-nitrostyril)pyridine	226.03	126.6	0.5601	15		
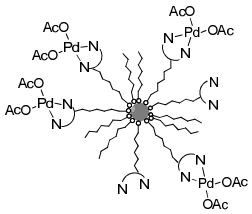	638.71	24[a]	0.0375	1		
DMF					5	

[a]The value found was approximate considering the best immobilization (entry V) table 6 chapter 2.
In this attempt we used the catalyst derived from the immobilization of 4-Me-Phen onto MNPs.

All manipulations of the reagents involved in the catalytic reactions were conducted under a N_2 atmosphere. All glassware and magnetic stirring bars used in the catalytic reactions were kept in an oven at 120 °C for at least 2 h and allowed to cool under vacuum before use. Reactions were performed in a glass liner closed with a screw cap with a glass-wool-filled open mouth to allow exchange of gaseous reagents. The substrate ((*E*)-2-(2-nitrostyril)pyridine) was weighed in the liner, which was then placed inside a Schlenk tube with a wide opening and placed under a N_2 atmosphere. The MNPs were dispersed in DMF and added under stirring, and then the liner was transferred to the autoclave. The autoclave was closed, filled with CO, and then evacuated three times, after which, it was filled with CO at the desired pressure. The autoclave was placed into a preheated oil bath and heated at the desired temperature for the desired time. We performed several trials following the same procedure, but changing the solvent, temperature, and pressure of CO, as summarized in Table 9. At the end of the reaction, the autoclave was cooled in an ice bath and vented. An internal standard was added for the GC analysis and the catalyst was magnetically

separated before performing the analysis. For the recycling test, we added fresh reagent and solvent to the same MNPs and repeated the reaction following the same procedure. Attention was paid not to allow the solution to be exposed to air between reactions.

For quantification by GC, we added biphenyl as an internal standard. The amount of added internal standard was calculated as one quarter of the mass of the substrate. After adding the internal standard, we made a diluted solution with an internal standard concentration of 0.1 mg/mL.

3.8 Synthesis of methyl-2-nitrocinnamate

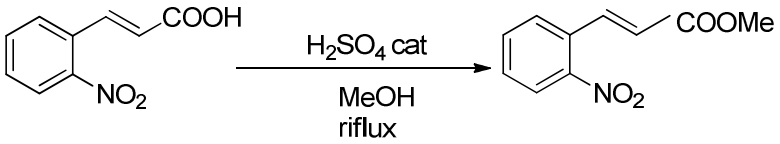

Reagent	M.W(g•mol^{-1})	g	mol	Molar ratio	V [ml]	d[g/mL]
2-nitrocinnamic acid	193.16	4.0406	2.09	3		
H_2SO_4	98.08		7.02	1	0.374	1.840
MeOH dry					120	

To a 100 mL Schlenk flask was added 2-nitrocinnamic acid. The flask was evacuated by three vacuum–nitrogen cycles. In a nitrogen stream, MeOH and sulfuric acid were added. The reaction was refluxed for a total of 21 h and checked by TLC (hexane:AcOEt = 8:2 as the eluent). MeOH was then evaporate in vacuo and the product was suspended in 30 mL of a saturated $NaHCO_3$ solution to neutralize excess H_2SO_4. The reaction mixture was extracted with CH_2Cl_2 (3 × 50 mL). The organic phase was washed with 30 mL of a saturated $NaHCO_3$ solution and twice with 30 mL of water. The product was dried over Na_2SO_4, filtered, and the solvent removed under vacuum. A yellow solid was obtained (2.63 g, 56.7%).

^{1}H NMR (400 MHz, $CDCl_3$, 298 K) δ 8.16, (d, ^3J = 15.8 Hz, 1H, H^e), 8.06 (d, ^3J = 7.9 Hz, 1H, H^d), 7.70–7.65 (m, 2H, H^a and H^b), 7.57 (dd, 1H, H^c), 6.37 (d, ^3J = 15.8 Hz, 1H, H^f), 3.86 (s, 3H, CH_3) ppm.

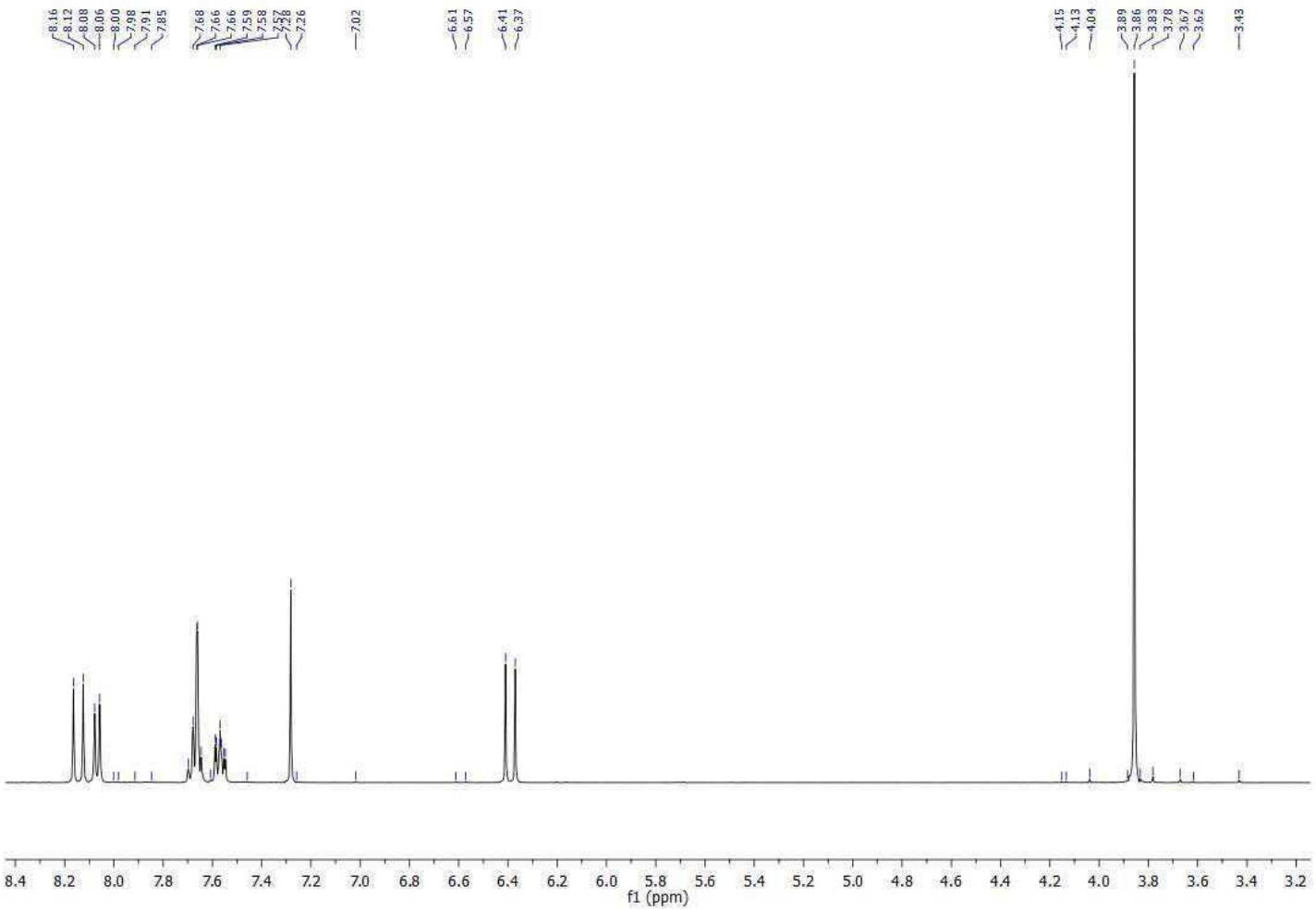

Figure 48: ^{1}H NMR (400 MHz, $CDCl_3$, 298 K) spectrum of methyl-2-nitrocinnamate.

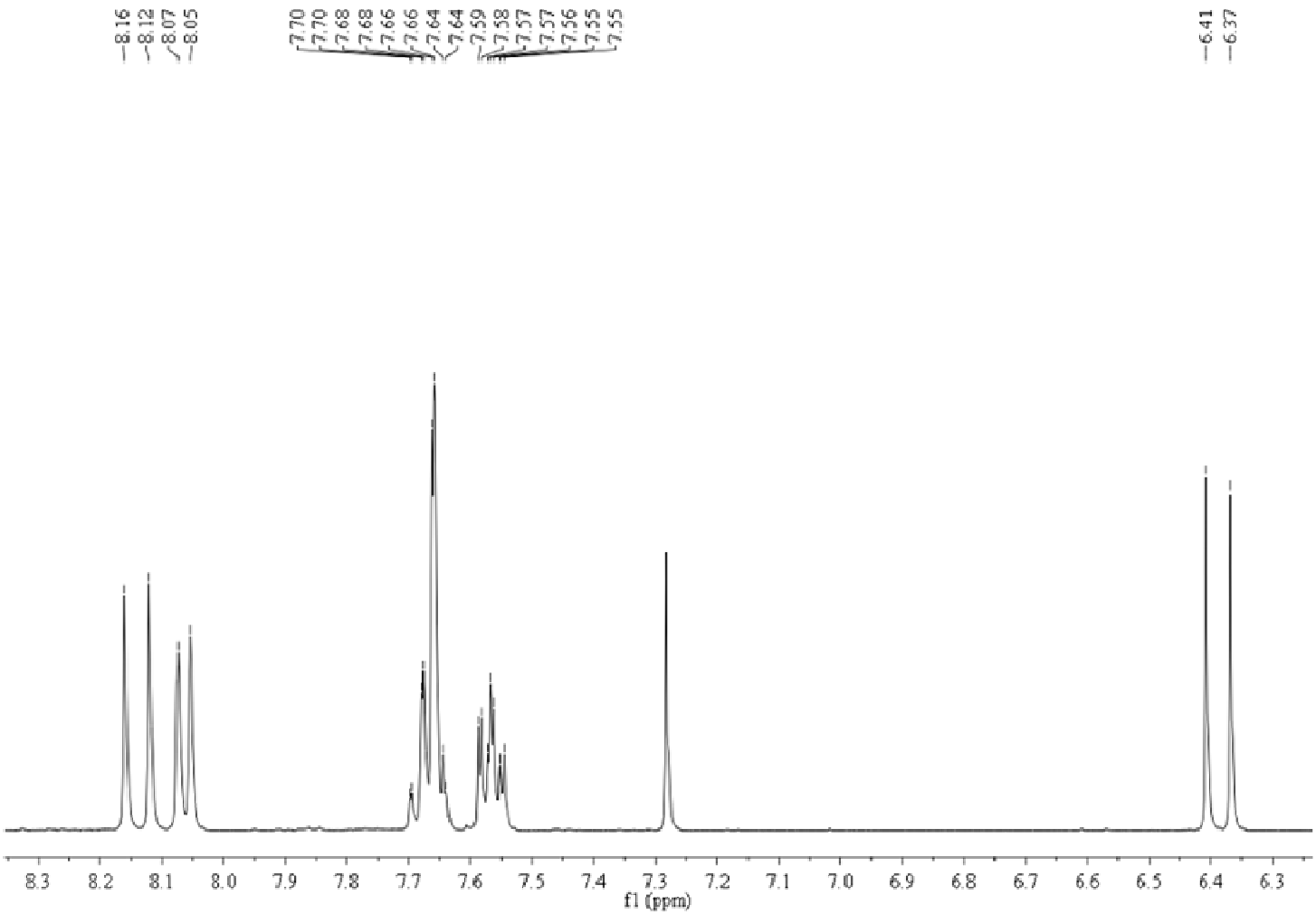

Figure 49: Expanded ^{1}H NMR (400 MHz, $CDCl_3$, 298 K) spectrum of methyl-2-nitrocinnamate.

3.9 Synthesis of methyl-1*H*-indole-2-carboxylate

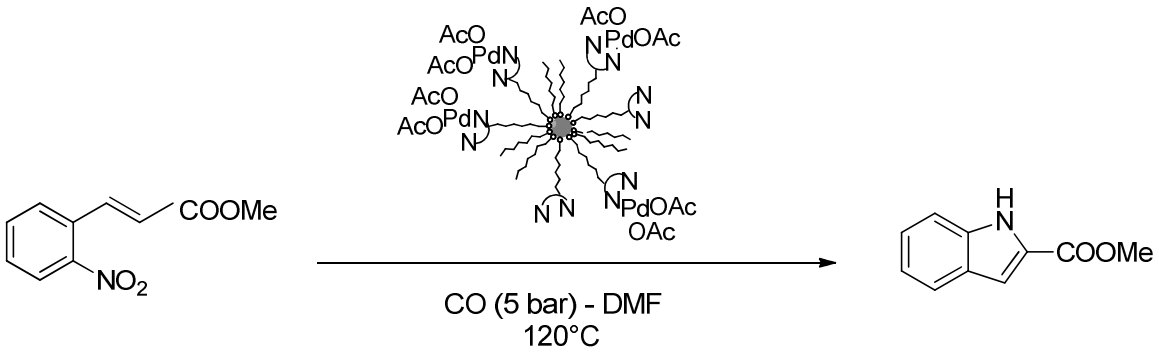

Reagent	M.W(g•mol^{-1})	mg	mmol	Molar ratio	V [ml]	d[g/mL]
Methyl-2 Nitrocinnamate	222.22	124.5	0.5601	15		
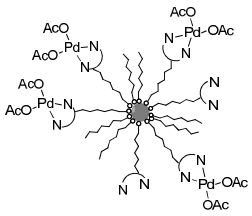	640.87	24[a]	0.0375	1		
DMF					5	

[a]The value found was approximate considering the best immobilization (entry V) table 7chapter 2.
In this attempt, we used the catalyst derived from the immobilization of 4-OH-Phen onto MNPs.

All manipulations of the reagents involved in the catalytic reactions were conducted under a N_2 atmosphere. All glassware and magnetic stirring bars used in the catalytic reactions were kept in an oven at 120 °C for at least 2 h and allowed to cool under vacuum before use. Reactions were performed in a glass liner closed with a screw cap with a glass-wool-filled open mouth to allow exchange of gaseous reagents. The substrate (methyl-2-nitrocinnamate) was weighed in the liner, which was then placed inside a Schlenk tube with a wide opening under a N_2 atmosphere. The MNPs were dispersed in DMF and then added under stirring, and then the liner was transferred to the autoclave. The autoclave was closed, filled with CO, and then evacuated three times, after which, it was filled with CO at the desired pressure. The autoclave was placed into a preheated oil bath and heated at the desired temperature for the desired time. We performed several trials following the same procedure, but changing the solvent, temperature, and pressure of CO, as

summarized in Table 10. At the end of the reaction, the autoclave was cooled in an ice bath and vented. An internal standard was added for the GC analysis and the catalyst was magnetically separated before performing the analysis. For the recycling test, we added fresh reagent and solvent to the same MNPs and repeated the reaction following the same procedure. Attention was paid not to allow the solution to be exposed to air between reactions.

For quantification by GC, we added biphenyl as an internal standard. The amount of added internal standard was calculated as one quarter of the mass of the substrate. After adding the internal standard, we made a diluted solution with an internal standard concentration of 0.1 mg/mL.

3.10 Synthesis of *trans*-stilbene

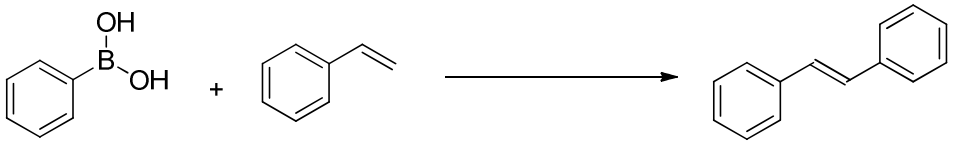

Reagent	M.W ($g \bullet mol^{-1}$)	mg	mmol	Molar ratio	V [mL]	d[g/mL]
Phenylboronic acid	121.93	134.4	1.10	1.1		
Styrene	104.15	104.0	1.0	1		0,909
Ligand*	208.26	5	0.024	0.024		
$Pd(OAc)_2$	224.51	4.5	0.02	0.02		
4-NMM	101.15	202.3	2	2		0.920
CH_3CN					3	

The reactions were performed in dried and distilled acetonitrile, except for entry 10 in Table 11, where DMF was used as a solvent and entry 23, where THF was used as a solvent.

Initial tests (entries 1–12 in Table 11):

To an open vessel were added phenylboronic acid, styrene, the ligand solution (0.024 mmol in 1 mL of MeCN), the palladium acetate solution (0.02 mmol in 2 mL of MeCN), and finally the base (if applicable). The vessel was immersed in a preheated oil bath and heated at 80 °C for 3 h. At the end of the reaction, the vessel was cooled on an ice bath and a GC analysis of the reaction mixture was immediately performed. We used and added internal standard (naphthalene) of all analyses. The amount of internal standard added was equivalent to one quarter of the mass of styrene. After adding the internal standard, we made a diluted solution with an internal standard concentration of 0.1 mg/mL. In all analyses, the conversion and selectivity refer to styrene.

From entry 13 onward in Table 11, we used the following procedure:

To an open vessel were added phenylboronic acid, styrene, base, and 1 mL of MeCN under stirring. In a separate flask, a solution containing the ligand and palladium acetate in 2 mL of MeCN was prepared. After preformation of the catalyst, the latter solution was added to the former in an open vessel. The reaction was performed at RT, and immediately after the end of the reaction, a GC analysis was performed. This procedure provided the best results and for this reason, all

homogenous catalysis trials from Entry 13 onward were performed by preforming the catalyst. For quantification by GC (Shimadzu GC-2010, Column SUPELCO EQUITY^{TM}-5ms, 10 m × 0.1 nm × 0.1 μm film thickness capillary column), naphthalene was added as an internal standard. The amount of added naphthalene was calculated as one quarter of the mass of the substrate (styrene). After adding the internal standard, we made a final solution containing 0.1 mg/mL of the internal standard using CH_2Cl_2 as a diluent.

Procedure using MNPs:

The procedure for trials using the MNPs is analogous to the one described above, but a solution of palladium-functionalized nanoparticles in MeCN (2 mL) was employed instead of the palladium complex. At the end of the reaction, we removed the catalyst by magnetic separation. In the recycling test, we used the same MNPs with fresh substrate and solvent.

GC method for oxidative Heck reactions

	Rate	Temperature	Hold Time
	-	100°C	1 min
PTV1	50	200°C	3 min
100°C	50	270°C	2 min
	-	90°C	0 min
Column	4.00	140°C	0 min
90°C	80.00	225°C	0 mim
	80.00	280°C	1.50 min

3.11 Atomic absorption spectroscopy

Reagent	M.W(g•mol^{-1})	mg	V [mL]	d[g/mL]
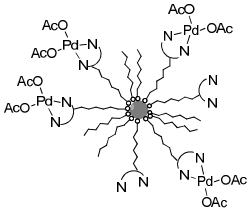	-	24.3		
HNO_3	63.01		1	1.51
HCl	36.46		3	1.19

[a] **In this analysis was used the 4-Me-Phen immobilized onto MNPs.**
Only Milli-Q water was used during the process.

We performed atomic absorption spectroscopy to analyze the quantity of palladium in our system. In an open vessel, we added 24.3 mg of the MNPs and a mixture of HNO_3 and HCl ("aqua regia"). The solution stirred vigorously, and when the nanoparticles were completely solubilized, 1 mL of the resulting solution was transferred to a test tube and diluted with a solution of 5% nitric acid in Milli-Q water.

We constructed a calibration curve (0.1–6 ppm) using a certified standard. The obtained coefficient of correlation was 0.99984. To analyze the palladium content in the recycled solution, we removed the nanoparticles by magnetic separation after the catalytic reaction and analyzed the remaining solution.

Results:

Theoretical palladium (calculated assuming each anchored phenanthroline binds one palladium atom): 4-OH-Phen-MNPs: 0.1575 mg Pd/mg 4-OH-Phen-MNPs.

PdAAS: 1.967×10^{-2} mg = 1.85×10^{-4} mmol Pd/mg 4-OH-Phen-MNPs (1/8 of the calculated amount).

Theoretical palladium (calculated assuming each anchored phenanthroline binds one palladium atom): 4-MePhen-MNPs: 0.1650 mg Pd/mg 4-MePhen-MNPs.

PdAAS: 2.75×10^{-2} mg = 2.58×10^{-4} mmol Pd/mg 4-MePhen-MNPs (1/6 of the calculated amount).

References

[1] Figure adapted from: http://ch302.cm.utexas.edu/kinetics/catalysts/catalysts-all.php.

[2] Govan J. and Gun'ko Y. K, *Nanomaterials*, **2014**, *4*, 222-241.

[3] Kaushik N. K, Kaushik N, Attri. P, Kumar. N, Verma A. K and Choi E. H, *Molecules* **2013**, 18, 6620-6662.

[4] R. J. Sundberg, *J. Org. Chem*, **1965**, 30, 3604-3610.

[5] C. Crotti, S. Cenini, B. Rindone, S. Tollari, F. Demartin, *J. Chem.Soc, Chem.Commun*, **1986**, 784-786.

[6] [a]Soderberg J. Org. Chem., 1999, Vol. 64, 64, 9731. [b]Soderberg. B. C and Shriver J. A, *Org. Chem.* **1997,** *62*, 5838-5845.

[7] I. W. Davies, J. H. Simitrovich, R. Qu. Sidler, R. V. Gresham, C. Bazaral, *Tetrahedron*, **2005**, 61, (26), 6425-6437.

[8] F. Ragaini, F. Ventriglia, M. Hagar, S. Fantauzzi, and S. Cenini, *Eur. J. Org. Chem*. 2009, 2185-2189.

[9] Heck, R. F, *J. Am. Chem. Soc*. **1968**, 90, 5518.

[10] Cho, C. S.; Uemura, S. *J. Organomet. Chem*. **1994**, 465, 85.

[11] Jung, Y. C.; Mishra, R. K.; Yoon, C. H.; Jung, K. W. *Org. Lett*, **2003**, 5, 2231.

[12] J. Lindh, P. A. Enquist A. Pilotti, P. Nilsson, M. J. Larhed,. *Org. Chem.* **2007**, 72, 7957.

[13] P. A. Enquist, J. Lindh, P. Nilsson and M. J. Larhed, *Green Chem*, **2006**, 8, 338-343.

Conclusions

- MNPs were synthesized and protected with 10-bromodecylphosphonic acid, and the procedure was found to be reproducible.
- The synthesis and characterization of 4-MePhen and 4-OH-Phen were in accordance with the literature, and the corresponding $Mo(CO)_4$ complexes were prepared and characterized.
- 4-MePhen and 4-OH-Phen were also attached to the nanoparticles, and the success of this procedure was proven by coordination with molybdenum.
- Elemental analyses supported the presence of nitrogen ligands, and it was possible to quantify the amount of immobilized phenanthroline derivatives.
- Palladium was successfully attached to the phenanthroline-functionalized nanoparticles.
- The heterogenized complex successfully catalyzed the formation of indoles, but the recycled catalyst rapidly lost activity.
- In the case of oxidative Heck reactions, we first optimized the conditions in the homogeneous phase.
- Employing the MNP complexes, we observed low selectivity that was attributed to the polymerization of styrene. This issue needs to be investigated further.

List of Figures

List of Tables

Index

Lilian Marcia Silva Ansaloni - Curriculum Vitae

Personal Details

Lilian Marcia Silva Ansaloni was born on January 18, 1979 in Belo Horizonte, Brazil.

Academic Background

- January 2014: starts the **Ph.D. program in Chemistry**, with a fellowship from the Brazilian program Science Without Borders at Università degli Studi di Milano, under the supervision of Prof. Fabio Ragaini.

- 2006/2008: **Master's degree in Materials Science**, Center of Nuclear Technology Development (CDTN), Brazil. Thesis: "Boron Nitride Nanostructured: Synthesis, Characterization and Potential Use in Cosmetics. Advisor: Prof. Edesia Martins Barros de Sousa.

- A.A 2001/2005: **Degree in Pharmacy**, Federal University of Minas Gerais (UFMG), Brazil.

Research experience

From A.A 2004/2005: **Grant from the Chemistry department (UFMG)**: Development of methods for the determination of toxic metals by neutron activation analysis and atomic absorption spectrometry in a graphite furnace employing permanent modifiers for quality control of drugs handled and industrialized in prolonged use. Advisor: Prof. José Bento Borba da Silva.

From A.A 2006 to A.A 2008: **Master's Degree**: Boron Nitride Nanostructured: Synthesis, Characterization and Potential Use in Cosmetics. Advisor: Prof. Edesia Martins Barros de Sousa.

Research interests

Chemistry of organometallic compounds, organic compounds, catalysis, synthesis and applications of nanomaterials, composites, templates, surfactants, determination of drugs and contaminants, use of permanent modifiers in atomic absorption spectrometry.

Publications

Papers

Lilian Marcia Silva Ansaloni and Edesia Martins Barros de Sousa, Boron Nitride Nanostructured: Synthesis, Characterization and Potential use in Cosmetics. *Materials Sciences and Applications*, 4, **2013**, 22–28.

Lilian Marcia Silva Ansaloni, Rey, U. V.; Pinto, F. G.; Andrada, D.; silva, J. B. B. Employment of Ruthenium as Permanent Modifier for the Determination of Copper in Serum Samples by Electrothermal Atomic Absorption Spectrometry. *Analytical Letters*, 39, **2006**, 2441–2451.

Lilian Marcia Silva Ansaloni; Pinto, F. G.; Rey, U. V.; Andrada, D.; Silva, J. B. B. Determination of the Cadmium in Human Serum and Urine by Electrothermal Atomic Absorption Spectrometry. *Ecletica Chemistry*, 30, **2005, 59-65.**

Congresses

Lilian Marcia Silva Ansaloni; Francesco Ferretti; Fabio Ragaini. Synthesis of organic compounds using homogeneous catalysts anchored on magnetic nanoparticles. In: XII Congresso del Gruppo Interdivisionale di Chimica Organometallica (Co.G.I.C.O.) della Società Chimica Italiana, 2016, Genova, Italy.

Francesco Ferretti; **Lílian Márcia Silva Ansaloni**; Fabio Ragaini. Ferrite Magnetic Nanoparticle for the Recycle of Palladium/Phenanthroline Catalytic Systems. In: XLIII Congresso Nazionale di Chimica Inorganica, 2015, Camerino, Italy.

Líliam Márcia Silva Ansaloni; Francesco Ferretti; Fabio Ragaini. Functionalization of ferrite nanoparticles by phenanthroline/palladium complexes and their use as catalysts in pharmaceutical syntheses. In: International School of Organometallic Chemistry, 2015, Camerino, Italy.

Lilian M. Silva Ansaloni; Andrea Pichmeo; Francesco Ferretti; Fabio Ragaini. Synthesis of magnetic nanoparticles functionalized with transition metals: Surface effects on coordination geometry. In: Co.G.I.C.O., 2014, Milan, Italy.

Lilian Marcia Silva Ansaloni, Sousa, E. M. B. Synthesis of Mesoporous Boron Nitride Using SBA-15 as a Template for Cosmetic Application. In: First International Conference on Multifunctional, Hybrid and Nanomaterials, 2009, Tours, France.

Lilian Marcia Silva Ansaloni, Sousa, E. M. B. Synthesis of Boron Nitride Nanotubes from Melamine Diborate for Application in Cosmetics. In: 51º Brazilian Congress Ceramics, 2007, Salvador, Brazil.

Lilian Marcia Silva Ansaloni; Sousa, E. M. B. Synthesis of boron nitride using mesoporous silica SBA-15 as template. In: Conference International Ceramics, 2007, Natal, Brazil.

Lilian Marcia Silva Ansaloni, Pinto, F. G.; Silva, J. B. B.; Amorim, L.; Niccacio, J.; Fernandez, E. F. Determination of manganese in urine and blood for atomic absorption spectrometry graphite furnace, ET AAS. In: XVI Latin American Congress of Chemistry, 2004, Salvador, Brazil.

Lilian Marcia Silva Ansaloni, Pinto, F. G.; Silva, J. B. B.; Rey, U. V. Employment of Ruthenium as Permanent Modifier for Copper Determination in Serum Samples by EETAAS. In: Rio Symposium Atomic Spectroscopy, 2004, Parati, Brazil.

Lilian Marcia Silva Ansaloni, Niccacio, J.; Demicheli, c.; Silva, J. B. B. Determination of lead content in an antihypertensive drug by EETAAS. Study of chemical modifiers. In: Rio Symposium Atomic Spectroscopy, 2004, Parati, Brazil.

Lilian Marcia Silva Ansaloni, Pinto, F. G.; Rey, U. V.; d, m.; silva, j. B. B. Direct determination of cadmium in human serum for ET AAS with iridium use of permanent modifier. In: XII National Meeting of Analytical Chemistry, 2003, São Luiz, Brazil.

Complete works published in conference proceedings

Lilian M. Silva Ansaloni; Sousa, E. M. B. Synthesis of Boron Nitride Nanotubes from Melamine Diborate for Applications in Cosmetics. *51º Brazilian Congress Ceramics*, **2007**, Salvador, Brazil.

Technical skills

- Synthesis of nanomaterials.
- Synthesis of organic compounds, in particular, phenanthroline and nitrogen-heterocyclic compounds.
- Use of autoclaves and high-pressure equipment.
- Use of the Schlenk technique to operate under an inert atmosphere.
- Use of instruments and methods for spectroscopic and chromatographic analysis: IR, GC, GC/MS, ET AAS.
- Use of tubular furnaces in materials science.